



Universidade de  
Aveiro  
2010

Departamento de Química

**Nuno Pedro  
Domingues Loureiro**

**FURFURYL-FUNCTIONALIZED SOYBEAN OIL  
DERIVATIVES: SYNTHESIS AND POLYMERIZATION**





**Nuno Pedro  
Domingues Loureiro**

## **FURFURYL-FUNCTIONALIZED SOYBEAN OIL DERIVATIVES: SYNTHESIS AND POLYMERIZATION**

Dissertação apresentada à Universidade de Aveiro para cumprimento dos requisitos necessários à obtenção do grau de Mestre em Materiais Derivados de Recursos Renováveis, realizada sob a orientação científica do Professor Doutor Armando Silvestre, Professor Associado com Agregação, e co-orientação científica do Investigador Coordenador *Emeritus* Alessandro Gandini, ambos membros do Departamento de Química da Universidade de Aveiro.

Apoio financeiro da FCT, e da UE,  
através do Projecto ERA-NOEL  
(ERA-IB/BIO/0001/2008), no âmbito do  
FP6.



**FCT**

Fundação para a Ciência e a Tecnologia  
MINISTÉRIO DA CIÊNCIA, TECNOLOGIA E ENSINO SUPERIOR



SIXTH FRAMEWORK  
PROGRAMME



## **o júri**

### **Presidente**

Prof. Doutor Dmitry Evtyugin

Prof. Associado com Agregação do Departamento de Química da Universidade de Aveiro

### **Vogal – Arguente Principal**

Prof. Doutor Jorge Coelho

Prof. da Faculdade de Ciências e Tecnologia da Universidade de Coimbra

### **Vogal - Orientador**

Prof. Doutor Armando Silvestre

Professor Associado com Agregação do Departamento de Química da Universidade de Aveiro

### **Vogal – Co-Orientador**

Prof. Doutor Alessandro Gandini

Investigador Coordenador *Emeritus* do Departamento de Química da Universidade de Aveiro



## Acknowledgements

I warmly acknowledge my supervisor, Professor Armando Silvestre and my co-supervisor, Professor Alessandro Gandini, for entrusting me with this challenging project and for their always constructive and supportive comments. To Andrea Figueiredo, my “lab coach”, as I called her, for her guidance, support and friendship. You’re an incredible human being and an excellent professional. I was very fortunate to be your first novice (the first of many, I truly hope!) and I’m really thankful for all that you’ve taught me. We’ll meet again, surely...

To Juanjo Villaverde, who we affectionately nicknamed “Espanholito”, for his “kick off” push, patience and fellowship as well as for our incomprehensible but joyful conversations...

To my laboratory colleagues for having welcomed me so warmly into the LignoMacro Research group and particularly to Belinda, Marina and Carla for their help, advice and funny moments shared together.

To Ana Margarida, for her friendship, support (we both were paddling in the same boat!), and for sharing the lab bench with me...

Last but not least to mum, dad, my beloved sister and closest friends. Thank you for being so supportive right from the start. I couldn’t have made it without you. You mean the world to me. I love you dearly.

And to all of you who have helped me to come this far and couldn’t be mentioned on this brief acknowledgements letter, my apologies and thank you.

Sincerely,  
Nuno





## Palavras-Chave

**Aducto; Funcionalização; Reticulação; Diels-Alder; Furano; Maleimidas; Polimerização; Recursos Renováveis; Retro-Diels-Alder; Auto-reparável; Reversibilidade Térmica; Óleos Vegetais**

## Resumo

O interesse em polímeros de origem renovável tem crescido incessantemente nos últimos anos, não só quer por razões ambientais mas também devido à preocupante diminuição das reservas petrolíferas que se reflecte no aumento dos preços dos intermediários petroquímicos utilizados para sintetizar a maioria dos materiais e produtos químicos do dia-a-dia. Os óleos vegetais são utilizados há décadas na síntese de polímeros e são considerados um dos recursos renováveis mais promissores para o desenvolvimento de materiais inovadores.

Neste âmbito, o nosso grupo de pesquisa tem-se dedicado ao desenvolvimento de novos materiais poliméricos derivados de óleos vegetais assim como a uma nova geração de biopolímeros com propriedades únicas, tais como reciclabilidade e capacidade de se auto-reparar, tirando partido da reversibilidade térmica da reacção de Diels-Alder entre furanos e maleimidas.

Neste trabalho apresentamos a funcionalização assistida por micro-ondas do óleo de soja com grupos substituintes furfurilamina, catalisada pelo líquido iónico  $[C_1Im][BF_4]$ . As condições reaccionais foram ajustadas com base nas utilizadas na síntese optimizada do derivado monofuncional a partir do oleato de metilo, levada a cabo propositadamente. A caracterização estrutural de ambos os compostos será discutida.

Os resultados dos estudos de polimerização realizados com os agentes de reticulação 1,6-bismaleimido-hexano e a N-tris(etil)maleimida, com base na reacção de Diels-Alder serão também apresentados.



## **Keywords**

**Adduct; Cross-linking; Diels-Alder; Furan; Maleimides; Polymerization; Renewable Resources; Retro-Diels-Alder; Self-healing; Thermoreversibility; Vegetable oils**

## **Abstract**

Interest in polymers from renewable resources has been growing at a fast pace due to the ever-increasing environmental concerns as well as the decline of crude oil reserves and the rising cost of the evermore dominant petroleum-based purveyors for chemical commodities. Vegetable oils have been explored for decades for polymer synthesis and are among the most promising renewable resources for the development of innovative materials.

Within this realm, we have been working on the development of new oil-based polymers as well as on a new generation of biopolymers with unique properties, including self-mendability and recyclability, based on the thermoreversible Diels-Alder reaction between furans and maleimides.

Here we report the microwave-assisted functionalization of epoxidized soybean oil with furfurylamine moieties catalysed by the ionic liquid  $[C_1Im][BF_4]$ . Reaction conditions were tuned using epoxidized methyl oleate as model compound. The structural characterization of both compounds will be discussed.

Results on the thermoreversible polymerization studies with 1,6-bismaleimidoheptane and N-tris(ethyl)maleimide using the Diels-Alder reaction will be presented as well.



# CONTENTS

<b>1. Introduction .....</b>	<b>1</b>
1.1 Contextualization .....	1
1.2 Chemistry Contribution to Sustainable Development .....	3
1.3 Renewable Feedstocks – Vegetable Oils .....	6
1.4 Vegetable Oils: Composition and Chemistry.....	8
1.5.1 Chemical Modification and Polymerization.....	14
1.6 Self-Healing Polymeric Materials.....	15
1.6.1 Design Strategies .....	16
1.6.2 Diels-Alder based Crosslinked Polymers .....	19
1.7 Scope.....	32
<b>2. Experimental Procedures.....</b>	<b>33</b>
2.1. Materials.....	33
2.2. Instrumentation .....	34
2.3. Syntheses.....	35
2.3.1. Epoxidation of Methyl Oleate (MO) .....	35
2.3.2. Synthesis of Furfuryl-MO.....	35
2.3.3. Synthesis of Furfuryl-SBO .....	38
2.3.4. DA-based Polymer Synthesis .....	40
<b>3. Results and Discussion.....</b>	<b>41</b>
3.1. Epoxidized Methyl Oleate (EMO).....	41
3.1.1. Synthesis of EMO.....	41
3.1.2. Structural Characterization of EMO .....	41
3.2 Furfuryl-Functionalized Methyl Oleate (Furfuryl-MO) .....	44
3.2.1 Synthesis of the Furfuryl-MO Derivative.....	44
3.2.2 Structural Characterization of Furfuryl-MO Derivative.....	49

3.3	Furfuryl-Functionalized Soybean Oil (Furfuryl-SBO) .....	59
3.3.1	Synthesis of the Furfuryl-SBO derivative .....	59
3.3.2	Furfuryl-SBO Synthesis Reproducibility & Feasibility .....	60
3.3.3	Structural Characterization of the Furfuryl-SBO Derivative .....	64
3.4	Polymeric Materials Based on the Diels-Alder Reversible Reaction .....	69
<b>4.</b>	<b>Conclusions .....</b>	<b>75</b>
<b>5.</b>	<b>References .....</b>	<b>77</b>

# 1. Introduction

## 1.1 Contextualization

Chemistry will always have a vital role in almost every aspect of modern society. Despite providing us with a vast array of useful products, the chemical industry has been subjected to close scrutiny and attention owing to concerns about its reliance on depleting fossil resources and its ecologically damaging chemical processes which release toxic and hazardous by-products and wastes that require stringent environmental control and special forms of effluent treatment. Furthermore, most of those products are not readily recyclable or degraded in nature after their useful lifetime.

The industry has come under increasing pressure to make chemical production more eco-friendly and efforts to shift the prime resource base of industry from fossil (non-renewable) to renewable feedstocks have recently gained momentum, primarily because of the rapid rise in the costs of mineral oil and an increasing concern about the depletion of these resources in the near future. Governments around the world are increasing the fines levied for pollution, the costs of waste disposal, and penal taxation for the storage of large quantities of dangerous chemicals and are introducing new chemical legislation, to improve the levels of protection of human health and the environment from chemical risks, as our environmental awareness keeps growing.<sup>1-4</sup>

Worldwide, it is increasingly believed that the management, conservation and utilization of natural resources need be improved and that making industry more sustainable can provide the means for reducing environmental impacts while yielding goods and services that can provide jobs, reduce poverty and improve the quality of life for a growing world population.

Sustainable development is clearly the most difficult challenge that humanity has ever faced and is the main aspiration/ambition for the 21st century. According to the World Commission on Environment and Development (Brundtland 1987) it is understood as “... *a process of change in which the exploitation of resources, the direction of investments, the orientation of technological development, and institutional change are all in harmony and enhance both current and future potential to meet human needs and aspirations...* (It is) the

*set of strategies and actions that have the objective of meeting the needs and aspirations of the present generation without compromising the ability to meet those of the future.”.*<sup>3,5-6</sup>

Its aim is to balance economic development, social equity and environmental quality. Sustainable development recognizes that the well being of ecosystems, the economy and communities are inseparably linked and that our quality of life depends on balancing each of these three pillars. Its goals can only be achieved if its three dimensions – social, economic and environmental – are satisfied simultaneously (Figure 1).

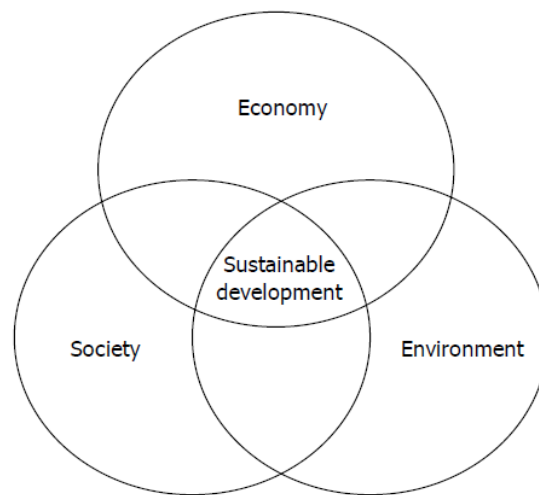


**Figure 1** The three components of sustainable development.

Developing a sustainable bio-based economy that uses eco-efficient/friendly (bio)processes and renewable bioresources is one of the key strategic actions for this century. Shifting to a more bio-based economy offers hope both for developed and developing countries. For developing countries, it presents the opportunity to use their technological capabilities for national security of energy and chemical supply. For developed countries, it provides the potential to leapfrog the age of fossil fuels and petrochemicals to the age of more environment-friendly biofuels and biochemicals that can be produced locally, improving the economy and quality of life.

Visionary thinking is therefore required among governments, industry as well as the environmental and research communities to shape an ideal approach to achieved sustainable development which, as mentioned earlier, presupposes that its three dimensions – social, environmental and economic – are simultaneously verified.<sup>5,7</sup>



## 1.2 Chemistry Contribution to Sustainable Development

The United Nations Conference on Environment and Development (UNCED), held in Rio de Janeiro in 1992, provided the fundamental principles – the Rio Declaration – and the comprehensive program of actions – the Agenda 21 - to achieve sustainable development in the 21st century. Adopted by more than 180 governments across the globe, and strongly reaffirmed at the World Summit of Sustainable Development, held in Johannesburg in 2002, Agenda 21 remains totally relevant, addressing the pressing problems of today and encouraging the environmentally sound and sustainable use of renewable natural resources, interestingly in chapter 4 “Changing consumption patterns”.<sup>8</sup> Chemistry contribution to the implementation of the Rio Declaration and Agenda 21, including its on-going advancements,<sup>9</sup> is green/sustainable chemistry.

The concept of “Green Chemistry” was introduced in the early 1990s by the American Environmental Protection Agency (US-EPA) by the organic chemists Paul Anastas and John Warner, in order “*to promote chemical technologies that reduce or eliminate the use or generation of hazardous substances in the design, manufacture and use of chemical products*”.<sup>10</sup> It is supported by a set of 12 principles formulated by considering aspects of the full cycle – from raw material to product use and fate - and which, if fulfilled, allow greener approaches. The use of renewable feedstocks, alternative non-toxic solvents, and selective catalysts instead of stoichiometric reactants, in order to minimize waste, as well as the design of safer and biodegradable chemicals, and the implementation of innovative, cleaner and less energy consuming technologies and processes, are just a few examples.<sup>4,10-</sup>

- P** – Prevent waste
- R** – Renewable materials
- O** – Omit derivatization Steps
- D** – Degradable chemical compounds
- U** – Use safe synthetic methods
- C** – Catalytic reagents
- T** – Temperature, pressure ambient
- I** – In process monitoring
- V** – Very few auxiliary substances
- E** – E-factor, maximize feed in products
- L** – Low toxicity of chemical products
- Y** – Yes, it is safe

**Figure 2** Condensed principles of green chemistry.<sup>12</sup>

According to the latest Global Footprint Network Report,<sup>13</sup> strategically released days before the Copenhagen Summit, so as to encourage the debate and increase the awareness about the urgency of an effective plan of actions for the conservation and management of depleting and renewable resources, in 2006, humanity used the equivalent of 1.4 Earths to support its consumption (Figure 3). This means that it took the Earth approximately a year and four months to regenerate the resources used by humanity in that year.

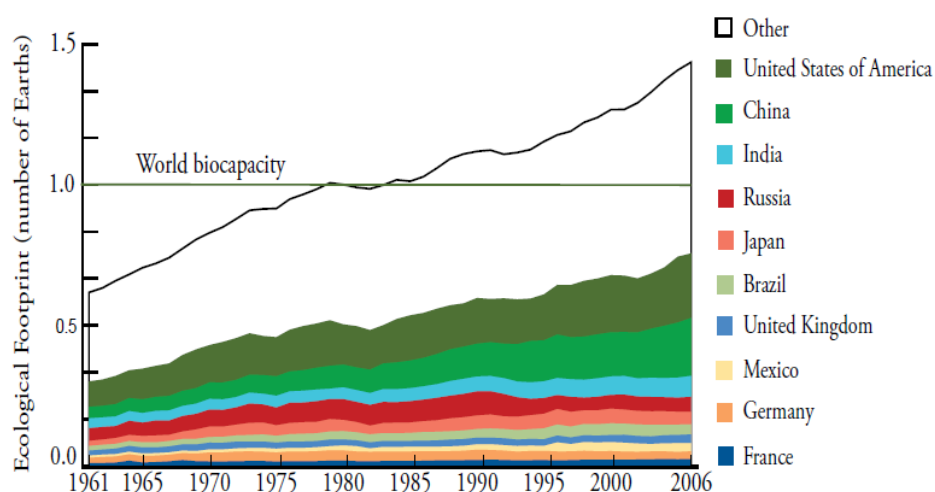


**Figure 3** Humanity's Ecological Footprint by country, 1961-2006 (reprinted from [13]).

If everyone in the world lived like an average resident of the United States or the United Arab Emirates, the biocapacity of more than 4.5 Earths would be required to support humanity's consumption rates. The average European resident has an Ecological Footprint of consumption of 4.5 global hectare (gha), half that of the average American, but still well above both than the world average of 2.6 gha and what is sustainably available per person. We are demanding nature's services – using resources and creating CO<sub>2</sub> emissions – at a rate 44% faster than what nature regenerate and reabsorb. This ecological overshoot (Figure 4) and its effects in terms of climate change, flooding, deforestation and desertification might be contributing to the slight decline in the earth's biocapacity - the amount of resources nature can produce- in recent years, or eventually end up in ecosystem collapse, in a world where population and human demand are continuously growing.<sup>13-15</sup>

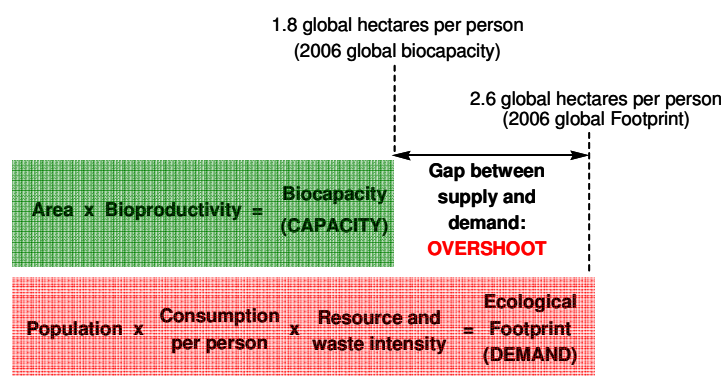


**Figure 4** Footprint and biocapacity factors that determine global overshoot.

The transposition of the “sustainable chemistry” concept to practice and the 21st century real world is not meant to be an easy task for chemists, who are regularly confronted with new and demanding challenges. Chemists, in straight collaboration with chemical engineers, are at the forefront of this global revolution, playing a vital role in the search for feasible pathways towards sustainable development. *“It has become imperative that chemists lead in developing the technological dimension of a sustainable civilization”*, stated Dr. Terry Collin, an awarded green chemistry expert and director of the Institute for Green Science at Carnegie Mellon University, to Science Magazine.<sup>2</sup>

Chemistry can make important contributions to the conservation of resources by development of:<sup>14</sup>

- More efficient and environmentally benign chemical products and processes;
- Chemical Products derived from renewable resources;
- Products that allow the consumer to use resources more efficiently;
- A product design that fits into a recycling concept.

Thus, chemists are expected to develop products that not only perform well but, compared to their conventional counterparts, are more durable, less toxic, easily recyclable and biodegradable at the end of their useful life. Such products shall be derived as much as possible from renewable resources and manufactured in environmentally acceptable ways involving less consumption of energy and raw-materials, and contribute minimally to net generation of greenhouse gases.<sup>3,16-17</sup>

The transition from a traditional fossil fuel based economy to a sustainable biobased economy which utilizes renewable raw materials is surely one of the major scientific and technological challenges of the 21st century.<sup>12</sup>

### **1.3 Renewable Feedstocks – Vegetable Oils**

In the last century the supply of raw materials for the chemical industry underwent radical changes (Figure 5). Whereas at the beginning of the 19th century the demand for basic chemicals was entirely satisfied by renewable raw materials, from about 1900 it came to rely increasingly on coal. The advent of crude oil revolution, in the 1940s, provided an inexpensive liquid fuel source that helped to industrialize the world and improved standards of living. In the next following 40 years it remained by far the most important source.<sup>18</sup> Nearing the end of the last century, however, fossil resources dwindling together with their unpredictable price fluctuations and the ever-increasing environmental concerns, raised serious questions about the medium-term pursuit of their exploitation and have encouraged chemical industry to reinvest on renewable resources – biomass - as alternative feedstocks.

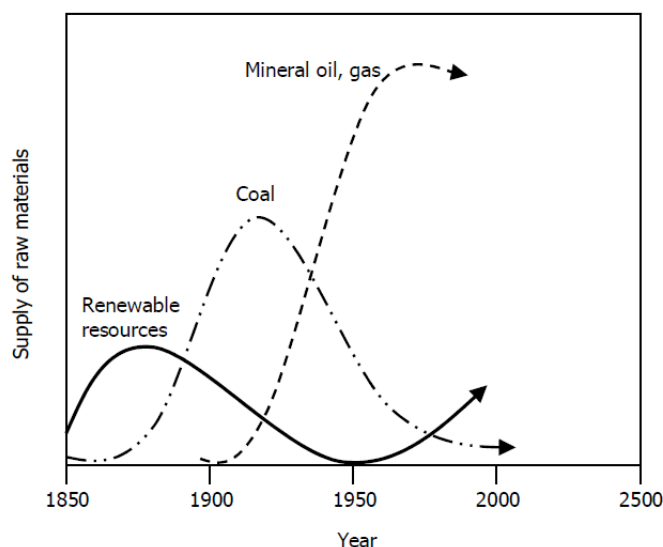


**Figure 5** Changing sources of feedstock for the chemical industry (reprinted from [19]).

Biomass ready availability, its renewable character as well as its potential to effectively tackle global warming, by minimizing greenhouse gases emissions, makes it the only sustainable alternative carbon source to fossil fuels.<sup>20-23</sup>

The flurry of initiatives that followed aiming to exploit biomass potential as an alternative energy source, was also extended to research activities in the area of replacing the major petro-derived commodity chemicals by biomass derived derivatives. New results addressing to both issues are reported daily.<sup>e.g.[24-27]</sup> The scientific series “Renewable Feedstocks” published by the FNR (Agency of Renewable Resources, Gulzow, Germany)<sup>28</sup> frequently reports on selected topics of the use of renewables, and recently, various reviews<sup>1,24-25,29-33</sup> summarizing the state of the art in research on biomass conversion into value-added chemical products such as fine and specialty chemicals, biofuels and polymers, to name only a few, were published as well.

Polysaccharides (cellulose, hemicelluloses and starch), sugars, proteins, wood and plant oils are just a few examples of renewable raw materials to which academic and industrial researchers have been devoting increasing attention.<sup>34-35</sup> Amongst them, vegetable oils are the most widely used for the chemical and polymer industries and still, they are considered to be amid the most promising raw materials for other purposes, owing to their excellent environmental credentials, which include their ready availability, low price, inherent biodegradability, low toxicity and their many versatile applications.<sup>36</sup>

In the chemical industry plant oils are used as an ingredient or component in many manufactured products, such as surfactants (soaps), lubricants, plasticizers, cosmetic products, monomers (e.g. dimer acids and polyols) and agrochemicals. In addition, they have been used for decades in paint formulations, as flooring materials and for coating and resin applications.<sup>37-38 (and refs therein)</sup>.

Vegetable oils compose about 80% of the global oil and fat production, with 20% (with a decreasing tendency!) being of animal origin.<sup>39</sup> The annual global production of the main vegetable oils was of 128 million tons (Mt) in 2007/08, increased to 132 Mt in 2008/09 and is expected to reach 137 Mt in 2009/2010.<sup>40</sup> It represents a growth at a steady pace of about 3.3 % per year. It is noteworthy that, despite making up the greatest proportion of the current consumption of renewables by the chemical industry, only around 15% of these raw materials are used as precursors to the synthesis of new chemical commodities. The remaining is used for animal (about 5%) and human (*ca.* 80 %) consumption. In recent years, though, with the increasing production of biodiesel, this ratio has been changing, and the share of oil and fat consumption between food, feed, and industrial applications is now closer to 74:6:20.<sup>41</sup> This remarkable increase, offers chemists a new window of opportunities because biodiesel, as fatty acid methyl ester, can also be used as chemical feedstock.<sup>e.g. 22,24,42</sup>

## 1.4 Vegetable Oils: Composition and Chemistry

Vegetable oils are part of a large family of chemical compounds known as lipids. Their major constituents are triglyceride molecules, which have the three-armed structure depicted on Figure 6. Triglycerides are fatty acid triesters of glycerol.

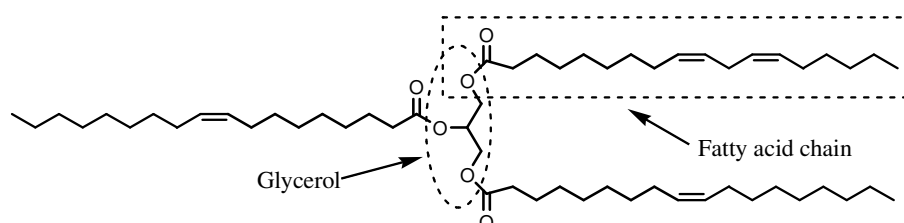


**Figure 6** Triglyceride molecule (TG), the major component of vegetable oils and fats (fatty acid chains vary according to the oil considered; here we depicted a soybean oil TG)

The fatty acids may be all different, two may be different, or may be all alike. Typically, fatty acids present in common oils can vary between 14 and 22 carbon atoms in chain length and contain 0-3 double bonds (DB) which, most of the times, are in a non-conjugated sequence (*i.e.* double bonds separated by a bis-allylic group) and exhibit a *cis* configuration. The number of known fatty acids is very large, and some have other functionalities other than double bonds, such as hydroxy and epoxy groups. The fatty acid composition of the most common oils is listed in Table 1, and their chemical representative structures are depicted on Table 2.

**Table 1** Main fatty acids composition of different commodity oils.<sup>34,43</sup>

Oils	Fatty Acid (%)					Double Bonds (DB) <sup>a</sup>
	Palmitic	Stearic	Oleic	Linoleic	Linolenic	
Soybean*	11.0	4.0	23.4	53.3	7.8	4.6
Palm	42.8	4.2	40.5	10.1	---	1.7
Rapeseed/Canola*	4/4.1	2/1.8	56/60.9	26/21.0	10/8.8	3.8/3.9
Sunflower*	5.2	2.7	37.2	53.8	1.0	4.7
Groundnut	11.4	2.4	48.3	31.9	---	3.4
Tung*	---	4.0	8.0	4.0	---	7.5
Cottonseed	21.6	2.6	18.6	54.4	0.7	3.9
Olive	13.7	2.5	71.1	10.0	0.6	2.8
Corn*	10.9	2.0	25.4	59.6	1.2	4.5
Linseed*	5.5	3.5	19.1	15.3	56.6	6.6
Sesame	9	6	41	43	1.0	3.9
Castor*	1.5	0.5	5.0	4.0	0.5	2.7
Coconut	9.8	3.0	6.9	2.2	---	---
Fish*	10-22		11-25	---	---	---
Palm kernel	8.8	2.4	13.6	1.1	---	---

\* used as precursors for polymers synthesis purposes; <sup>a</sup> Average number of DB per triglyceride

**Table 2** Most common fatty acids in natural oils and fats.<sup>34,43</sup>

Acid	Structure
Myristic	
Palmitic	
Palmitoleic	
Stearic	
Oleic	
Linoleic	
Linolenic	
$\alpha$ -Eleostearic	
Ricinoleic	
Vernolic	
Licanic	

Triglycerides possess multiple reactive sites where chemical reactions can take place: the C=C double bonds, the ester groups, the allylic positions, and the  $\alpha$ -carbonyl position (Figure 7). However, by the end of the 80's, more than 90% of triglyceride transformations arose predominantly from reactions at the carboxylic functionality, with less than 10% referring to chemical modifications of the alkyl chain. By then, the basic oleochemicals produced were: free fatty acids, methyl esters, fatty amides, fatty alcohols and fatty amines, with glycerol as by-product.

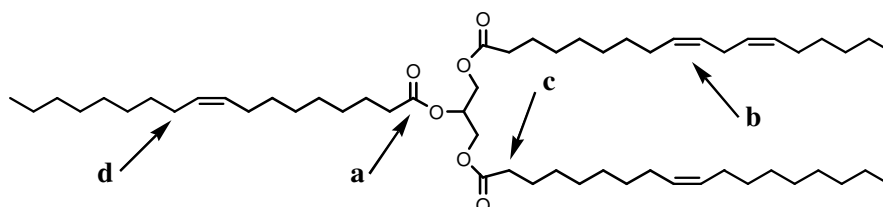


**Figure 7** Triglyceride molecules can undergo reaction at different reactive positions: (a) the ester groups, (b) the double bonds, (c) the  $\alpha$ -carbonyl positions and (d) the allylic positions.



After a period of relatively stagnation, research on this field has recently regained momentum. Increasing attention is now being focused on the functionalization of the unsaturated alkyl chains, due to its potential to considerably extend the range of valuable compounds obtainable from oils and fats (Figure 8). Fatty acids functionalization through enzymatic and microbial reaction pathways has even been tackled, on our continuous pursuit for innovative and greener methodologies.<sup>44-48</sup> The chemical possibilities of renewable oils and fats are endless and still very far from being thoroughly explored and therefore, research on this area is imperative, as part as of the general concern for sustainability.

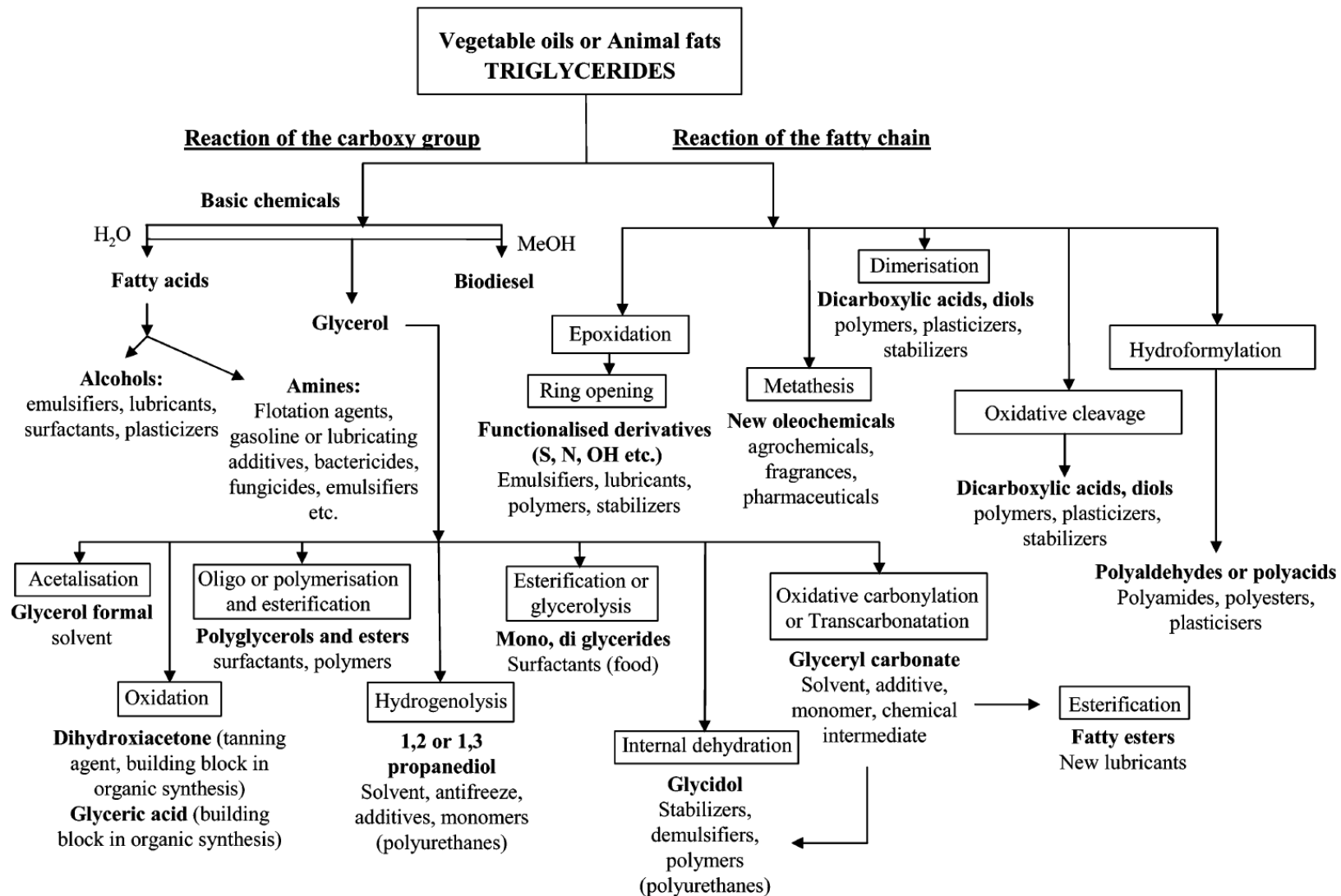


**Figure 8** Production of valuable products from fats and oils (reprinted from [25]).

## 1.5 Polymers from Vegetable Oils

Polymers are quantitatively the most important products of the chemical industry for our everyday life. The majority of the existing polymers are derived from non-renewable, fossil sources.

Currently, materials and energy consumption are no longer the only concern surrounding polymers production. Due to the worldwide spread overuse and the actual consumption patterns, in which materials are used only once and then discarded, polymers are contributing to the increasing amount of solid waste, as a high percentage of all plastics produced from fossil resources are non-biodegradable.

Moreover, efforts such as recycling and combustion in incinerating plants need to be carefully considered from the economic and ecological perspectives.

Owing to this serious environmental problem and the finite nature of the non-renewable resources, biomass has been seen as the only effective sustainable feedstock for both energy and materials production. Therefore, presently, there is a growing interest in producing materials from renewable resources, notably, vegetable-oil based polymers. In addition to being biodegradable, these biopolymers are, in many cases, cheaper than their petroleum-based counterparts. Since after their useful lifetime they are decomposed and reabsorbed by the biomass regrowth, in theory, they are “CO<sub>2</sub> neutral”. The life cycle of vegetable-oil based polymers is shown in Figure 9.

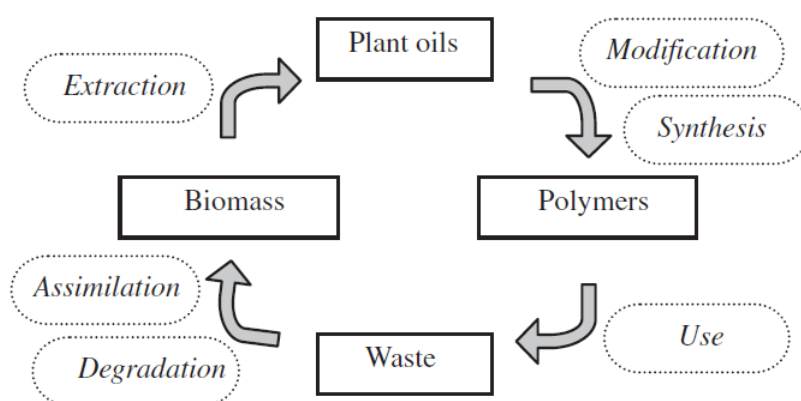


**Figure 9** Life cycle of polymers based on triglyceride oils (reprinted from [49]).

### 1.5.1 Chemical Modification and Polymerization

Triglyceride molecules contain C=C double bonds that can be directly polymerized through a free radical or a cationic mechanism. The free radical polymerization of triglyceride molecules has received little attention due to the presence of chain-transfer reactions to the many allylic positions in the molecule, whereas cationic polymerization has been extensively studied by Larock's group.<sup>50</sup>

Considerable efforts have now been devoted to triglyceride modifications to make them more prone to polymerization. These modifications consist of:

- Introducing polymerizable groups into the aliphatic chains with higher aptitude to polymerize (pathway A, Figure 10), and
- The reduction triglycerides to monoglycerides through a glycerolysis reaction<sup>51</sup> (pathway B)

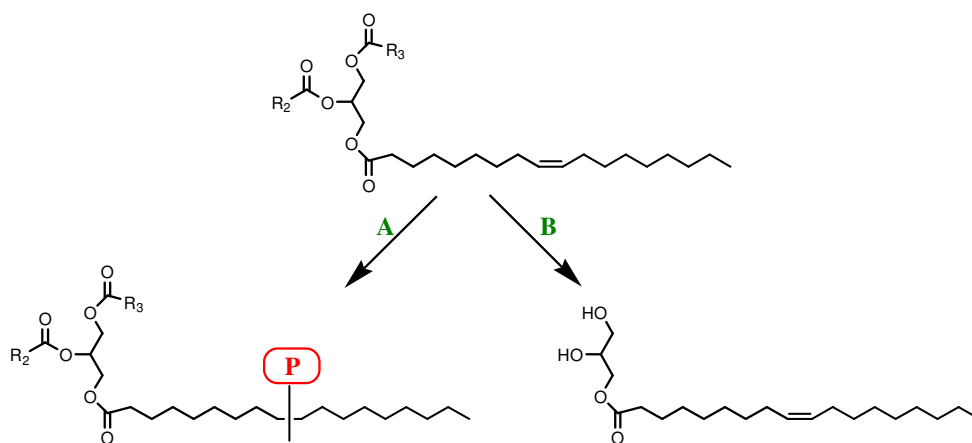


**Figure 10** General modification pathways: incorporation of polymerizable groups along TG's aliphatic chains (A) and reduction of the triglycerides to monoglycerides (B). P stands for polymerizable moiety.

The first approach, notably, has gained increasing prominence in recent years for its potential to considerably extend the range of compounds obtainable from oils, particularly in the polymer domain.<sup>22,24,43,49-50,52</sup>

However, most of the times, the introduction of polymerizable moieties in triglyceride's unsaturated aliphatic chains can't be carried out directly due to the low reactivity of the C=C double bonds and hence, a suitable platform must be chosen prior to the functionalization reaction. One of the most popular and effective routes to achieve it is

through epoxidation. Due to the high reactivity of the oxirane ring, TG epoxides are useful intermediates and provide abbreviated pathways to several functional derivatives that would not be readily accessible otherwise. Of all the routes to oxirane<sup>53-54</sup>, the least hazardous and most cost-effective procedure is the Prilezhaev reaction, *i. e.*, the epoxidation of alkenes with *in situ* generated peracids. Epoxidation of vegetable oils is usually carried out with performic or peracetic acid formed within the reaction medium from hydrogen peroxide and the corresponding acid, in the presence of acidic catalysts, either strong inorganic acids or acidic ion exchanger resins.<sup>53-56</sup>

## 1.6 Self-Healing Polymeric Materials

For centuries, mankind has been fascinated by living nature's faculty to spontaneously repair damage. One of the most striking examples is human body's skin – minor cuts and bruises are healed completely, whereas more severe injuries may lead to scars. Nevertheless, in either case, the operational capability of the system is largely restored. Artificial, man-made self-healing polymeric materials remained a pipe dream for centuries but the will to make this dream come true has been considerably fuelled over the last decade and it's not longer an illusion or utopia. Their synthesis has become a newly emerging paradigm and a fascinating area of research. Inspired by the natural process of blood clotting or repairing of fractured bones, scientists are trying to incorporate the same concept into engineering materials. The first steps have been taken but we still have a long path ahead. More than half of all publications on self-healing polymers are no more than five years old, and several reviews articles, including two books, report the latest advances and gather the most remarkable achievements.<sup>57-60</sup>

Self-healing materials have the ability of repairing or recovering themselves when suffering mechanically or thermally induced damage, which can occur autonomously<sup>61-62</sup> (*i.e.* without any intervention) or be activated by external stimuli<sup>63-65</sup> (*i.e.* needs human intervention/external triggering, such as heat), once or multiple times.

As virtually all materials are susceptible to degradation and deteriorate with time, repairing is indispensable to enhance their reliability and lifetime. Polymers are no exception - they have a finite lifetime, as their inherent properties degrade with age through accumulated

stresses and strains (wear-to-tear), and usually/most of them end up in landfills or incinerated after their functional use.

### **1.6.1 Design Strategies**

The cracking or breaking of a material starts at the microscopic level, and usually goes unnoticed until the material fails and requires mending. Mending at the macroscopic level can be done with adhesives, but doesn't restore the original properties of the polymer. Mending at the microscopic level, though, as enabled by a reversible polymerization process, makes it possible, and this process can be repeated many times. Such reversible polymerizations would involve the formation and cleavage of covalent bonds. The development of supramolecular chemistry has brought a new approach to tackle this issue – through polymerizations based on the formation and severing of non-covalent interactions.<sup>65</sup> Moreover, the recent advances in composite manufacture have allowed the development of “smart” materials, where one-time healing is achieving without the necessity of a reversible polymerization process, through strategies such as microcapsule (Figure 11) and hollow fiber embedment (Figure 12).

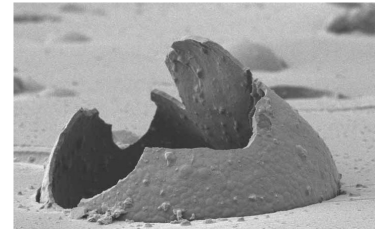
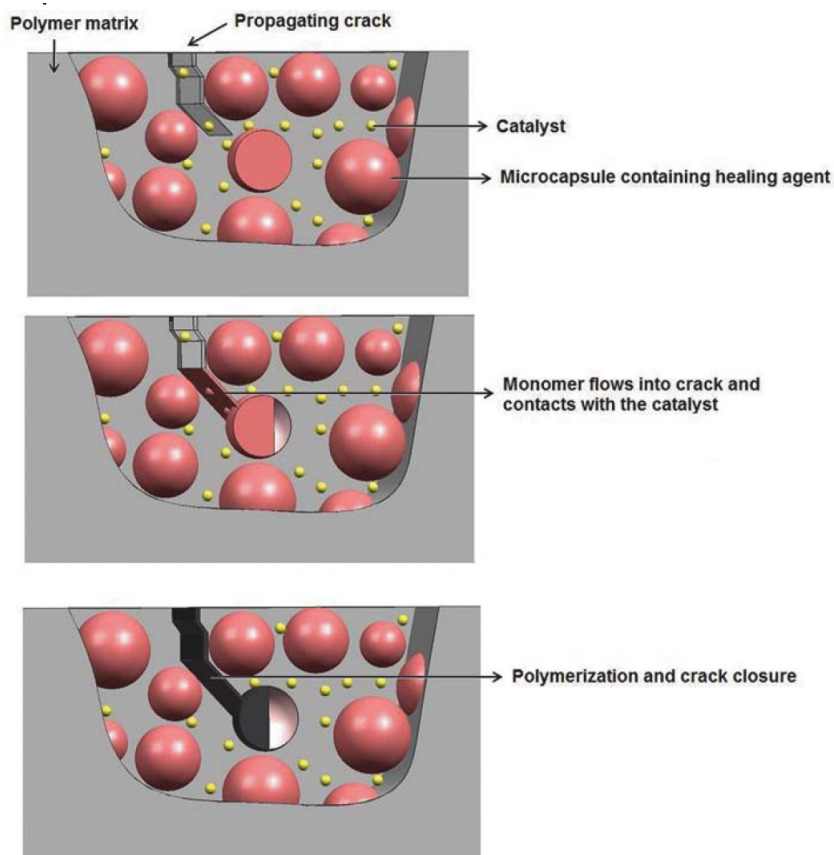


**Figure 11 (Left)** The self-healing concept using embedded microcapsules (reprinted from [58]). A microencapsulated liquid monomer healing agent is embedded in a structural polymer matrix containing a catalyst capable of polymerizing the healing agent. When the material is damaged cracks occur, rupturing the microcapsules and releasing the healing agent into the crack plane through capillary action. The healing agent contacts the catalyst, triggering polymerization that bonds the crack faces closed. **(Right)** SEM micrograph of a fracture surface showing a broken microcapsule embedded in a thermosetting polymer matrix. Microcapsule diameter is approximately 100 μm (reprinted from [66]).

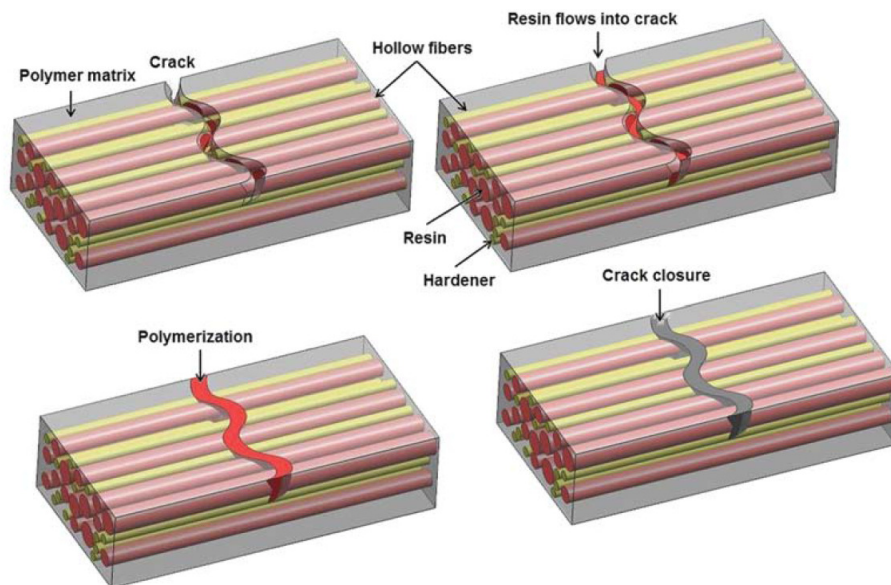


**Figure 12** Schematic representation of self-healing concept using hollow fibers or tubes (reprinted from [58]).

Different strategies to design self-healing materials have been developed and improved over the years according to the type of material considered. Materials such as plastics/polymers, paints/coatings, metals/alloys, and ceramics/concrete have distinct self-healing mechanisms. The different strategies of designing self-healing materials are as follows:<sup>58</sup>

- Release of healing agent
- Reversible cross-links
- Miscellaneous technologies
  - Electrohydrodynamics
  - Conductivity
  - Shape memory effect
  - Nanoparticle migration
  - Co-deposition

Due to space limitations and practical purposes we will just refer to the “Reversible Cross-links” strategy, focusing on the thermally reversible crosslinked polymeric systems based on the Diels-Alder (DA) and Retro-Diels-Alder (RDA) reactions. Those predesigned to undergo self-repairing and which have demonstrated to be mendable will be discussed with



detail. This strategy represents a highly promising route to introduce self-healing properties to polymeric systems.

### 1.6.2 Diels-Alder based Crosslinked Polymers

The Diels-Alder reaction is one of the most important and deeply studied reactions in organic chemistry. It consists in a [4+2] cycloaddition between a conjugated diene and a substituted alkene, commonly termed by dienophile, to form a cyclic product called adduct (Figure 13). The Diels-Alder reactions enable the formation of two carbon-carbon  $\sigma$  bonds, in a specific manner, and require very little energy to take place.

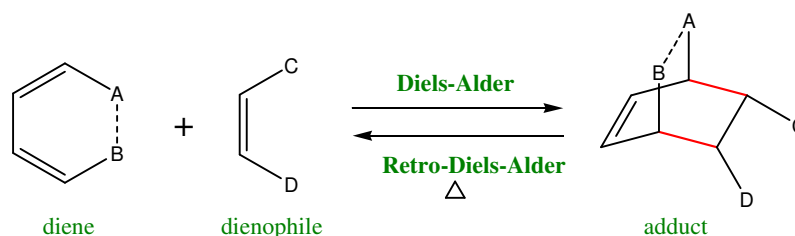


**Figure 13** Reaction Scheme of the Diels-Alder and Retro – DA reactions.

One of the most relevant aspects of the Diels-Alder reaction for re-mendable polymers is its thermal reversible character, through the so-called retro-Diels-Alder (RDA) reaction. A temperature rise will favour the RDA reaction and thus, shift the equilibrium towards the monomeric, oligomeric, or noncross-linked state of the polymeric systems. Major classes of thermally reversible polymers are made by exploiting the Diels-Alder (DA) reactions.

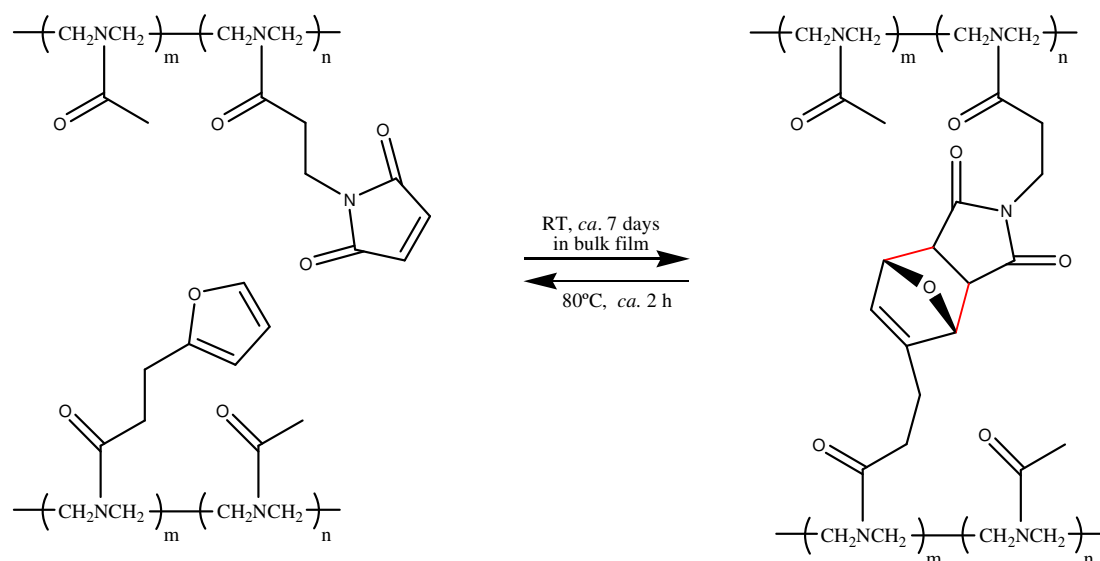
In the present work, the option for furfurylamine as the polymerizable agent/moiety meets one of our group's research lines –the synthesis of furan-based new polymers. Furan's pronounced dienic properties makes it specially suitable for the Diels-Alder (DA) thermoreversible coupling reactions with maleimides (dienophile). This remarkable feature applied to macromolecular synthesis will give rise to a new class of polymers with unique properties, such as self-mendability and network recyclability.

Two types of reversible polymer based on the DA-RDA reaction sequence have been prepared:

- (i) polymers where the pendant groups cross-link through successive DA coupling reactions, for example, crosslinked polymer networks from linear thermoplastics bearing pendant furan or maleimide groups;
- (ii) Polymers where the backbone itself is constructed through successive DA coupling reactions involving multifunctional complementary monomers, for example, a di- or trifunctional furan derivative and a bis-maleimide.

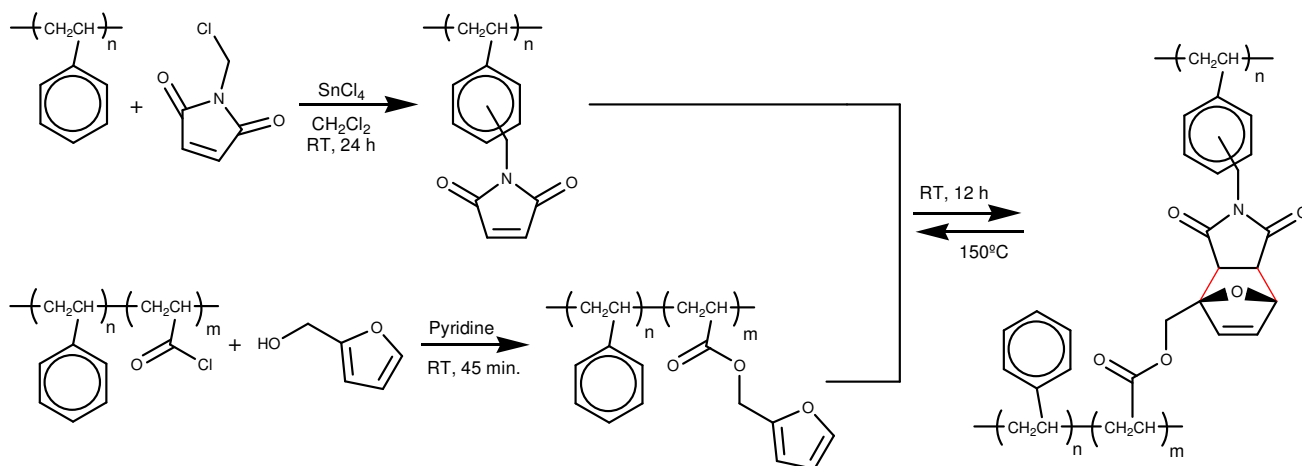
The first report about the incorporation of furan/maleimide moieties into polymers chains for the purpose of attaining thermal reversible self-healing was reported in 1969 by Craven.<sup>67</sup> Efforts devoted by the scientific community to this field resulted in several articles and patents, all concerning the production of a thermally reversible cross-linked polymeric network based on DA coupling reactions between furan and maleimide units, either as pendant groups (for reversible cross-linking), or as part of the polymer backbone (for reversible polymerization).

Stevens and Jenkins tackled this idea in their pioneering work,<sup>68</sup> in 1979, but only a decade later it was brought up again. Saegusa and coworkers reported the first example of a thermally reversible network through covalent bonds.<sup>69</sup> They described the cross-linking of modified *N*-acetyleneimine (PAEI) polymer chains with furan and maleimide pendant moieties by means of DA/RDA reaction sequence (Scheme 1). These authors claimed that mixing the two modified complementary polymers in bulk resulted in a highly cross-linked material which, heated at >80 °C for at least 2 hours in a polar solvent (methanol/water mixture, nitromethane), dissolved itself and regenerated the two starting precursors at quantitative yield.



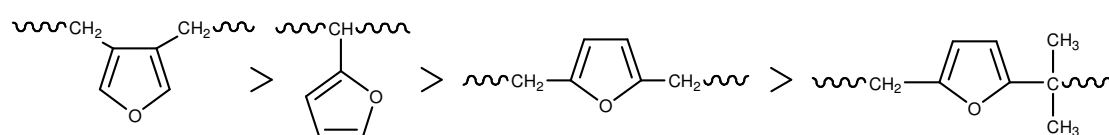
**Scheme 1** Reversible polymer cross-linking via Diels-Alder cycloaddition reaction between pendant furan and maleimide groups.

Later, Canary and Stevens described the reversible cross-linking of polystyrene bearing maleimide pendant groups with di-2-furfuryl adipate (Scheme 2).<sup>70</sup> However, the RDA reaction of the system was achieved only at 150°C, which posed serious limitations to the viability of the system due to the ensuing thermal instability of furfuryl moieties.



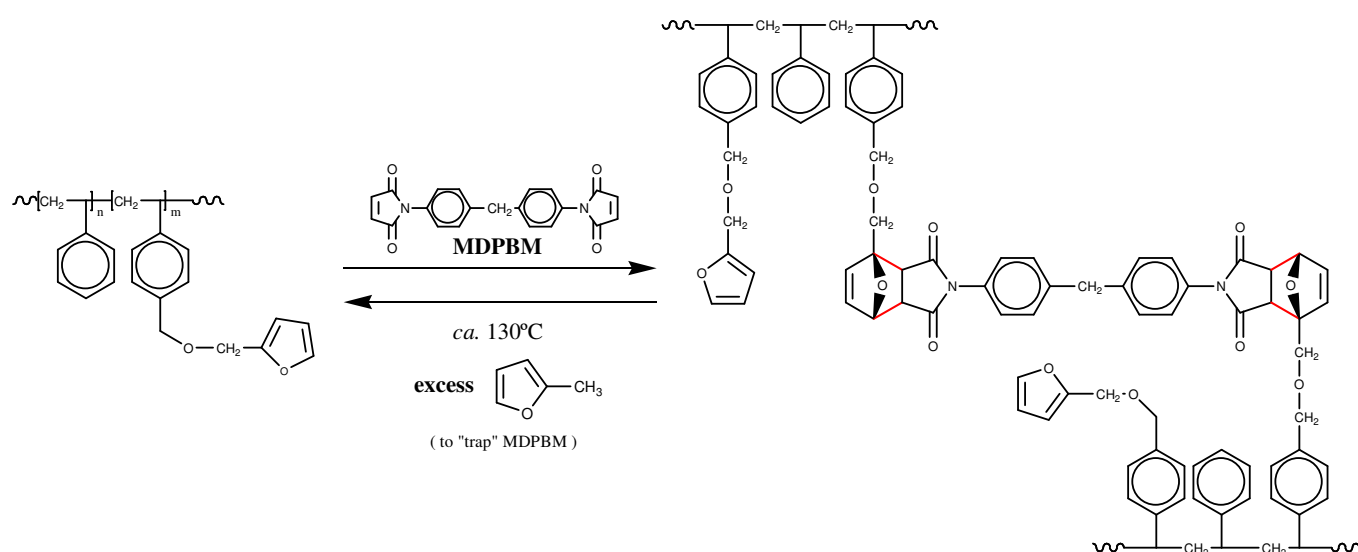
**Scheme 2** Reversible cross-linking of polystyrene *via* Diels-Alder cycloaddition reaction between pendant furan and maleimide moieties.

Gandini and coworkers have also given noteworthy contributions to this research field. They explored the Diels-Alder coupling reaction of two sets of furan-containing polymers: (i) polyurethanes bearing the heterocycle in different topological emplacements, *i.e.*, either as side group or within the main chain, or both positions and (ii) acrylic copolymers with variable furan content, with mono- and di-dienophiles (*N*-Methylmaleimide and *N,N'*-methylenediphenyl-bis-maleimide, MDPBM, respectively).<sup>71</sup> They found that furan's reactivity to DA reaction is very sensitive to the enchainment of the heterocycles within the macromolecular backbone, and follows the trend:



Overall, crosslinking these polymers and copolymers with a bisdienophile in solution was easily achieved but, surprisingly, the opposite operation, based on the thermal reversibility of DA cycloadducts, did not take place satisfactorily. The authors suggested that aromatization of the imino heterocycles (adduct rings) was taking place, giving rise to irreversible crosslinks.

Later, the same group presented a study concerning the DA-based modifications of styrene copolymers bearing pendant 2-furfuryloxy moieties with MDPBM, and the thermal reversibility of the systems by means of RDA (Scheme 3).<sup>72</sup>



**Scheme 3** Reversible polymer cross-linking via Diels-Alder cycloaddition reaction between furan and maleimide groups of styrene and MDPBM, respectively.

Spectroscopic evidence indicated that DA-modification, *i. e.*, cycloadduct formation, was achieved in high yields, and that the retro-Diels-Alder reaction could be carried out successfully at *ca.* 130°C and by using an excess of furan trap (2-methylfuran, that reacted with the released MDPBM bisdienophile).

For high cross-linking densities (50/% furan moieties), however, the RDA reactions did not regenerate the copolymers in their original form, suggesting some cycloadducts were losing their ability to revert to the original structures. Authors argued that this was probably due to side reactions which modified the adducts and inhibited their aptitude to undergo the RDA pathway. Nevertheless, a purely kinetic problem, *i.e.*, incomplete reaction, wasn't excluded. A similar study concerning copolymers with elastomeric properties has been performed as well.<sup>73</sup> An acrylic copolymer bearing furan pendants and an oligoether-bridged bis-maleimide were cross-linked to yield a high flexibility system.<sup>73</sup> The reverse synthetic approach was also successfully explored, where an elastomeric polydimethylsiloxane (PDMS) modified with pendant maleimide moieties was cross-linked with a flexible difuran derivative (Figure 14).

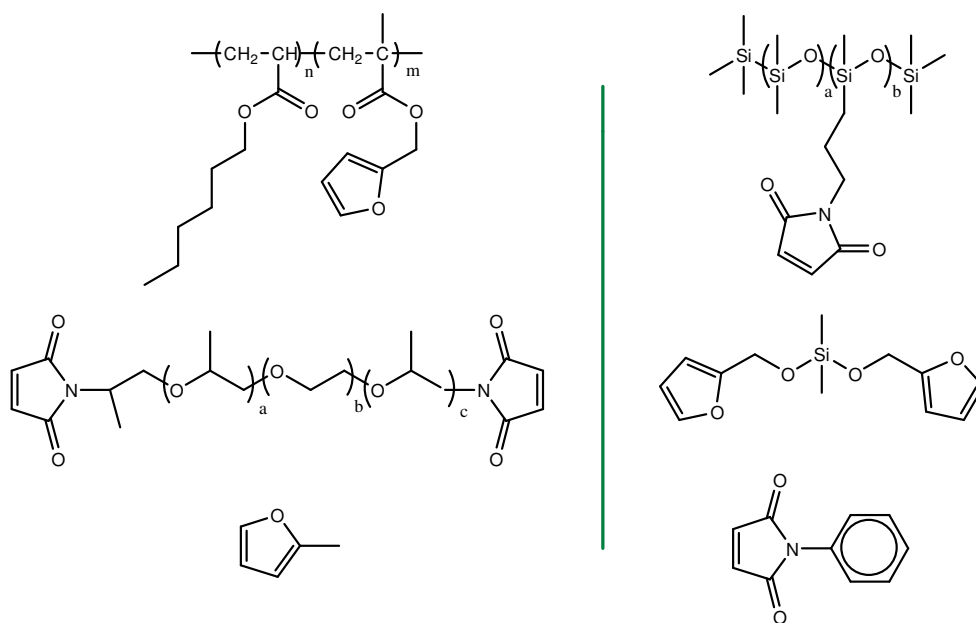


**Figure 14** Chemical structures of the copolymers, coupling agents and “traps” used. From top to bottom, left to right: Poly(hexyl acrylate-co-furfuryl methacrylate)s; PDMS modified with *N*-n-propylmaleimide pendant moieties; Poly(ethylene oxide)bis(2-propylmaleimide); Bis(2-methoxy-furan)dimethylsilane; 2-methylfuran; *N*-phenylmaleimide.

The de-cross-linking *via* RDA was accomplished by heating the networks at high temperature (*ca.* 90°C) in the presence of an excess of complementary monofunctional reagent, used as trap for the bifunctional molecule. The initial linear copolymers were restored quantitatively.

Huglin and coworkers also have contributed to this field. They conducted a systematic study on the mechanical and swelling properties of the network produced by the Diels-Alder reaction between poly(styrene-co-furfuryl methacrylate) and *N,N'*-bismaleimido-4,4'-diphenylmethane (MDPBM).<sup>74-76</sup> Kinetics studies for both DA cross-linking and RDA de-cross-linking reactions were performed as well, by following the decay/increase in UV absorbance of the maleimide group at 320 nm. DA process was shown to follow second order kinetics whereas the reverse process (RDA) obeyed to first order kinetics.

Early reports concerning the synthesis of low DP polymers through DA reaction between bis-furan and bis-maleimides monomers demonstrated the feasibility of such polymerizations<sup>77-82</sup> and supported much of the upcoming work. Gandini and Goussé also have dedicated themselves to the preparation and study of a number of low DP polymeric

systems based on difuran and bis-maleimide monomers.<sup>83</sup> They even took a step further, by preparing a molecular structure bearing both a furan and a maleimide moiety-2-furfurylmaleimide (FM).<sup>84</sup> The polymerization was conducted at 150 °C and gave partially soluble products, suggesting the high temperatures necessary to promote its self-condensation through the Diels-Alder reaction were also responsible for some aromatization of the adducts. The <sup>1</sup>H NMR analysis of the soluble part indicated that DA oligomers have been formed.

Wudl and coworkers have also implemented the DA/RDA strategy to design thermally remendable polymers.<sup>63-64</sup> They first reported a highly cross-linked and transparent polymer (3M +4F = polymer (3M4F)) which showed an average mechanical strength recovery (*i.e.*, healing efficiency) of about 50% at 150 °C, and 41% at 120 °C.<sup>63</sup>

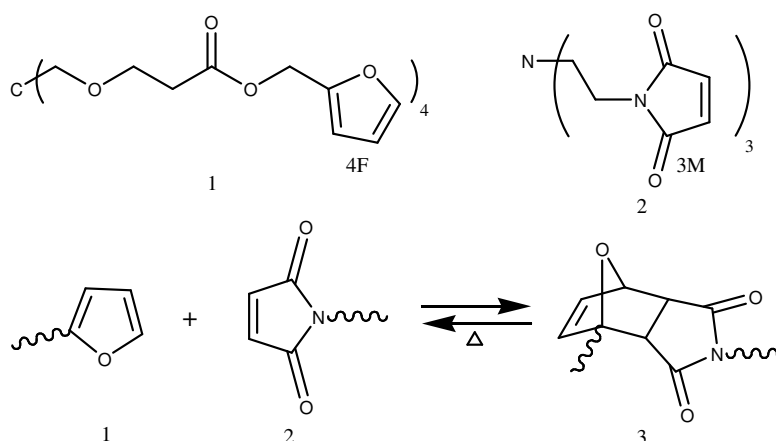


**Figure 15** Schematic showing formation of highly cross-linked polymer (3M4F) [polymer 3] using a multi-diene (four furan moieties, 4F) [monomer 1] and multi-dienophile (three maleimide moieties, 3M) [monomer 2] via DA reactions.

Multiple healing at or near the same interface was also observed although the critical load at fracture of the third cracking was about 80% of the second. This 20% drop from the second to the third healing cycle suggested that the original mechanical properties were not fully restored, *i.e.*, that the healed region had different mechanical properties than the starting original material.

Later on, they reported an improved solvent-free polymerizable system (Figure 16).<sup>64</sup> Polymer healing efficiency was assessed using a heating-quenching cycle of 115°C for 30

min., followed by cooling at 40°C for 6 hours. An average mending efficiency of about 80% was achieved for the first crack healing procedure, whereas for the second one the average value was 78%. The reported healing efficiencies however, were intended for relative comparison within their series of studies, rather than for absolute comparisons with other self-healing technologies. The influence of parameters such as crack length and crack bluntness on the critical load was not considered and therefore, more quantitative experiments were deemed necessary.

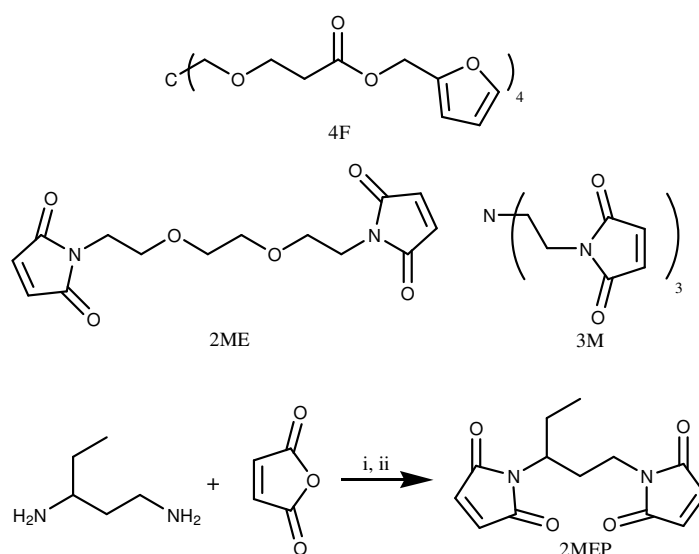


**Figure 16** A remendable polymer network (2MEP4F) with thermally reversible bonds was formed by mixture of a tetra-furan derivative (4F) and a bis-maleimide (2MEP) *via* DA reactions. (i) DMF; (ii) DMF, Acetic Anhydride, Triethylamine, Nickel Acetate Tetrahydrate

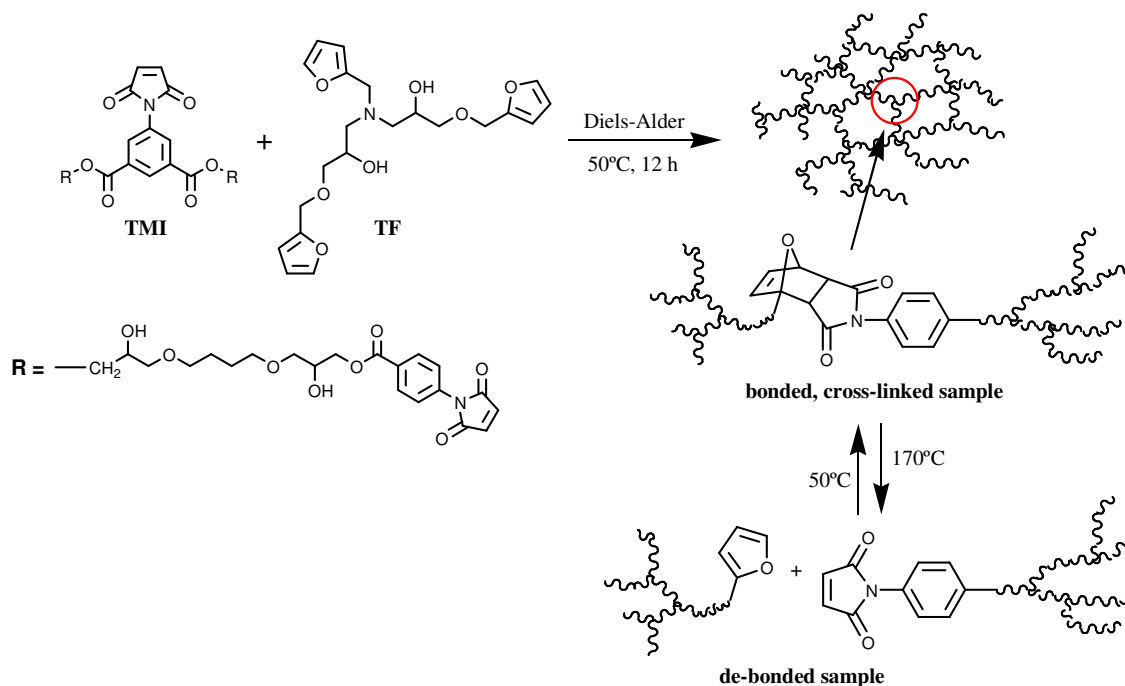
Since then, several other research groups have further contributed to this exciting field of research.<sup>85-91</sup>

Liu *et al.* have adapted Wudl's approach in their work.<sup>87</sup> They have synthesized multifunctional furan and maleimide compounds by simple routes, using epoxy compounds as precursors (Scheme 4). These precursors were strategically used, so as to incorporate the advantageous characteristics of epoxy resins, such as solvent and chemical resistance, thermal and electric properties as well as good adhesion, in the final cured polymer.

Besides that, the prepared furan and maleimide monomers had low melting points and were soluble in most common organic solvents: acetone, methanol, ethanol, ethylacetate



and tetrahydrofuran. Their solvent versatility makes them suitable for the current epoxy resins processing techniques. The use of solvents with low boiling temperatures, such as acetone, is beneficial, as it prevents the occurrence of cross-linking reactions during the solvent removal period.



**Scheme 4** Thermally reversible crosslinking reaction of TMI and TF through DA/RDA cycle.

Equivalent amounts of the trimaleimide (TMI) and Trifuran (TF) compounds were dissolved in acetone to produce a homogeneous solution. Then, the solvent was removed and the residue was left to react in an oven for 12 h at 50°C. A solid film was produced as the cross-linking between maleimide and furan moieties, from TMI and TF respectively, took place via DA reactions (DA). The debonding (retro-DA) process occurred upon heating the film sample at 170°C for 30 min.

The self-repairing property of TMI-TF cross-linked material was assessed using Scanning Electron Microscopic (SEM) technique. A fissure was made on the smooth and planar surface of the sample by knife-cutting, and the cut sample was then thermally treated at 120°C for 20 min. and at 50°C for 12 h. The high temperature stage was required to promote de-bonding and allow chain reformation, whereas the second to re-form/bond the cross-linked structure. After this treatment, the fissure of the sample was repaired, as it can be seen in Figure 17. Extending the treatment time to 24 h a fully recovered sample was

observed. However, the impact of the healing process on the mechanical properties of the previously damaged region was out of the scope of this study and therefore, not evaluated.

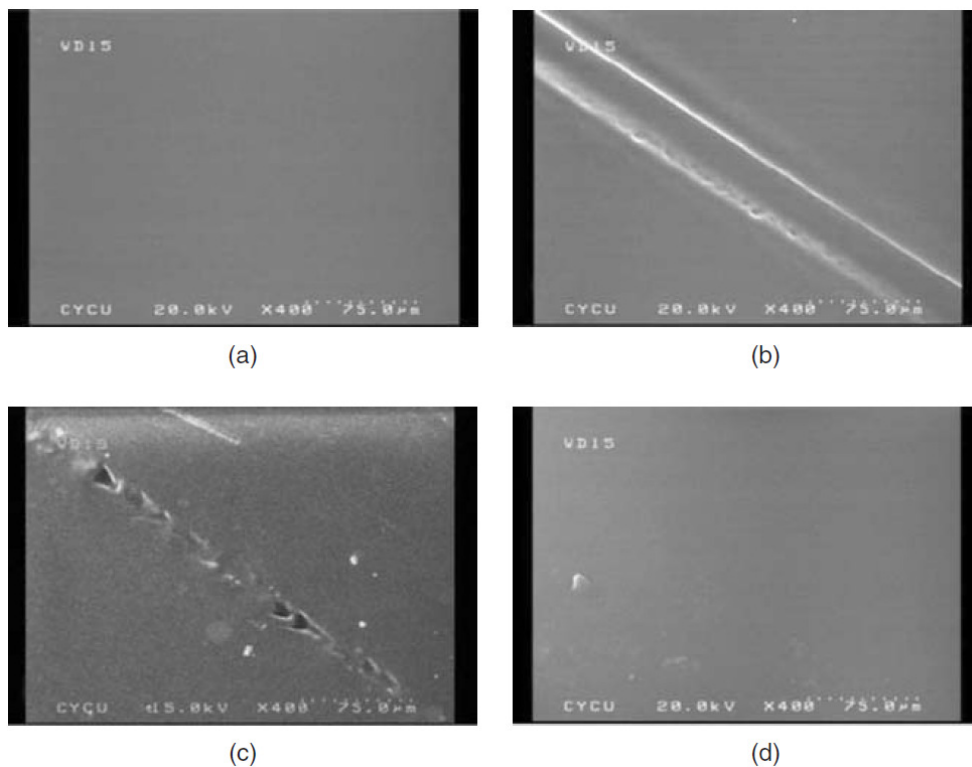


**Figure 17** Test of remendability. SEM micrographs of (a) starting TMI-TF cross-linked material, (b) knife-cutting sample, (c) thermally self-healed sample (50°C; 12h), and (d) thermally self-healed sample (50°C; 24h). Reprinted from [87].

Later Liu *et al.* reported the first investigation on thermally-reversible cross-linked polyamides and thermo-responsive polyamide gels.<sup>88</sup> They graft maleimide moieties onto the polyamide backbone (PA-MI) and cross-linked it in *N,N*-dimethylacetamide (DMAc), with a tri-functional furan compound (TF), at 30°C (Figure 18).

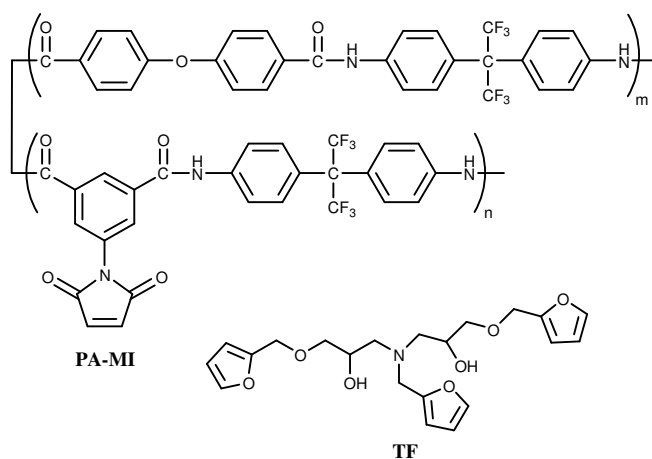


**Figure 18** Chemical structures of the trifuran derivative (TF) and the maleimide-containing polyamide (PA-MI) used in Liu's pioneering work on thermally remendable polyamide networks based on the DA/RDA reactions.

The resulting PA-MI/TF gels exhibited good thermo-reversibility, which was found to be adjustable by varying the maleimide content in the polyamide (Figure 19).

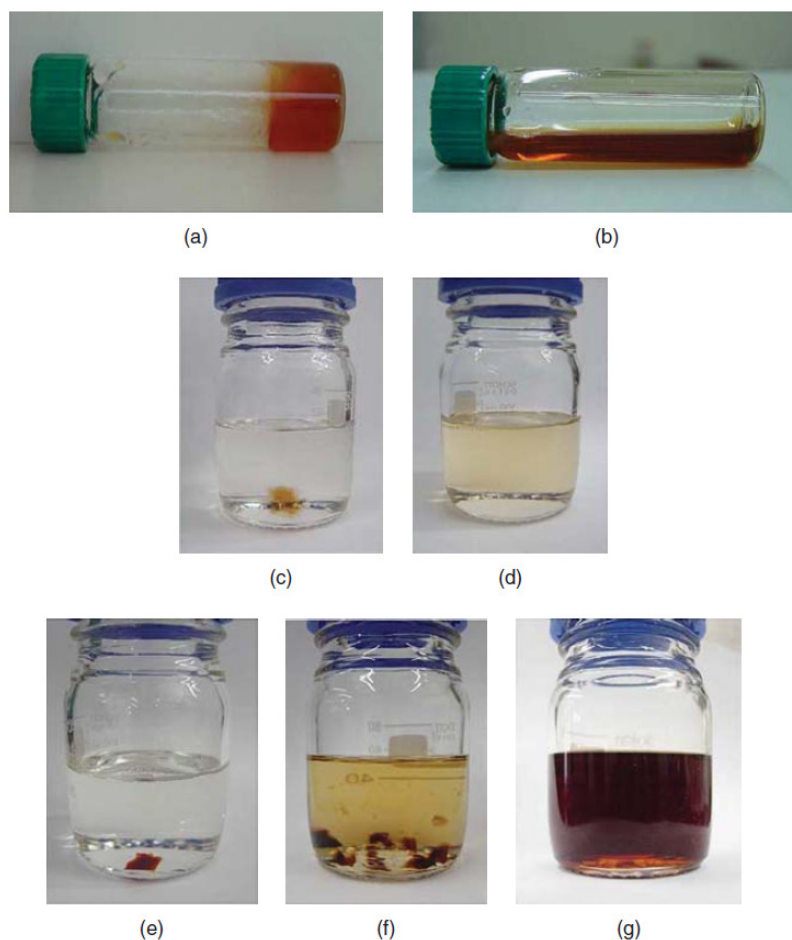


**Figure 19** Photographs of observation of thermally-reversible cross-linking behaviour of PA-MI/TF polymers. (PA-MI-1/TF polymers have the lowest cross-link density and PA-MI-10/TF polymers the highest). Polymer gel of PA-MI-1/TF in DMAc: (a) 30 °C, (b) 160 °C and cross-linked PA-MI-1/TF in DMAc: (c) 30 °C, 5 h, insoluble and (d) 120 °C, 2 h, soluble. Cross-linked PA-MI-10/TF polymer in DMAc: (e) 30 °C, 5 h, insoluble, (f) 120 °C, 5 h, partially soluble and (g) 160 °C, 5 h, soluble. Reprinted from [88].

Recently, they prepared modified polyamides bearing maleimide (PA-MI) and furan moieties (PA-F) in various amounts and examined the mechanical properties and the thermally reversible cross-linking behavior of the polymer networks obtained after mixing PA-MI and PA-F together in solution (DMAc), at 50°C (Figure 20).<sup>86</sup>

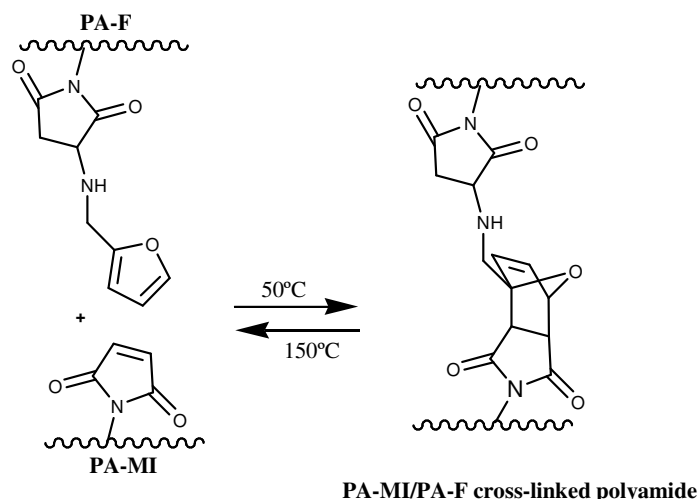


**Figure 20** Thermally reversible cross-linking reaction between polyamides modified with maleimide (PA-MI) and furan (PA-F) pendants. Polyamide structure is depicted in Figure 18. PA-F was prepared from PA-MI, by reaction with furfurylamine (FA) in the presence of acetic acid (DMAc, 110°C/96 h)

The ensuing PA-MI/PA-F films exhibited enhanced toughness and mechanical properties with respect to PA-MI and PA-F precursors, as well as self-repairing ability. However, only partial recover was observed for the cut films after the thermal healing treatment (Figure 21). This was attributed to the low mobility of high molecular polyamide chains in bulk.

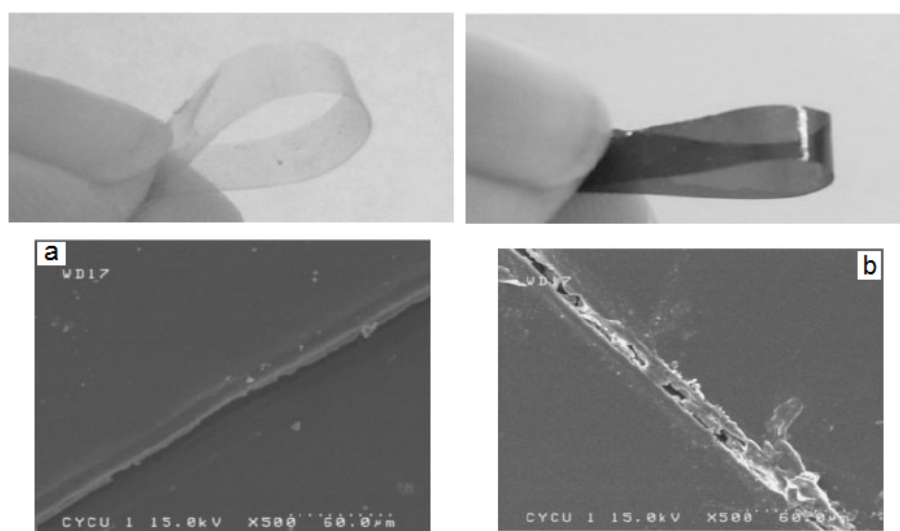


**Figure 21** Two top images: Appearance of PA-MI/PA-F cross-linked films showing high toughness. Two bottom images: Test of self-repairing ability of PA-MI-0.3/PA-F-0.3 cross-linked film. (a) Knife cut PA-MI-0.3/PA-F-0.3 cross-linked film surface; (b) thermally self-repaired PA-MI-0.3/PA-F-0.3 cross-linked film surface (120°C/3 h and 50°C/5 days). Reprinted from [86].

## 1.7 Scope

Interest in polymers from renewable resources is growing at a fast pace, as part of the general concern for sustainability. Vegetable oils are considered to be among the most promising renewable raw materials for development of innovative polymeric materials due to their ready availability, renewable character, low price, inherent biodegradability and chemical structure with multiple reactive positions. Within this realm, present research initiatives are focusing on the functionalization of the triglycerides unsaturated aliphatic chains with polymerizable moieties to create a large number of materials from which interesting thermophysical and mechanical properties are expected.

On this work we have challenged ourselves to synthesize a “self-healing” cross-linked polymeric material from soybean oil (SBO), through the DA/RDA thermo-reversible reaction sequence between furans and maleimides. The distinctive particularity of this work with respect to analogues stems from the building block itself, which has 100% renewable origin, rather than the strategy applied to attain the “self-healing” property. The monomeric units - SBO triglyceride molecules bearing furfuryl pendants (*abbrev.:* Furfuryl-SBO), were synthesized from soybean vegetable oil and furfurylamine, a derivative of furfural (the latter resulting from the acid hydrolysis of sugars).

Reaction conditions for the monomer preparation were optimized using epoxidized methyl oleate (EMO) as model compound. Structural characterization of both products – Furfuryl-SBO and Furfuryl-EMO - was carried out and will be discussed.

Furfuryl-SBO monomer was then crosslinked with 1,6-bismaleimido-hexane and *N*-tris(ethyl)maleimide at different Furan/Maleimide molar ratios. The polymerization progress and the thermal reversible behaviour of the ensuing DA-based polymer networks were monitored by  $^1\text{H}$  NMR. Results will be presented and discussed.

## 2. Experimental Procedures

### 2.1. Materials

Methyl oleate (Aldrich 99%), hydrogen peroxide (Fluka reactant, 30% solution), glacial acetic acid (99.7%, Panreac reactant), sulphuric acid (> 95%, Aldrich), toluene (99.7%, Riedel-de Haën reactant) and dichloromethane purchased from Fischer Scientific were used in the epoxidation procedure.

Catalysts,  $\text{SnCl}_4$  (1 M in  $\text{CH}_2\text{Cl}_2$ ),  $\text{ZnCl}_2$ ,  $\text{Zn}(\text{ClO}_4) \cdot 6\text{H}_2\text{O}$  and  $[\text{C}_1\text{Im}][\text{BF}_4]$  ( $\geq 98\%$ ) were supplied by Aldrich, V. P., Acros and Merck, respectively. Furfurylamine (> 99 %) was obtained from Acros, whereas ESBO from Shandong Longkou Longda Chemical Industry CO. Deuterated chloroform ( $\text{CDCl}_3$ , 99.8 atom%D) and 1,1,2,2-tetrachloroethane ( $\text{TCE-}d_2$ ) were purchased from Acros and Aldrich, respectively. Sample purification was carried out using: ethyl acetate, acetonitrile (extra dry, water content < 10 ppm), petroleum ether and  $\text{NaHCO}_3$  (99 + %), from Acros,  $\text{Na}_2\text{SO}_4$  from Pronalab,  $\text{NaCl}$  (99%) from Carlo Erba CO and silica supplied by Aldrich.

*N-methylmaleimide* (97%, Aldrich reactant) and *1,6-bismaleimido*hexane (Tyger Sci. Inc. reactant) were employed as received. *N-tris(ethyl)maleimide* had been previously synthesized in our laboratory to prepare thermoreversible polymer materials based on the DA/RDA reaction sequence strategy.<sup>92-93</sup>

$[\text{C}_1\text{Im}][\text{BF}_4]$  catalyst was dried under high vacuum for overnight prior to its use. Dichloromethane was dried with  $\text{CaH}_2$  under reflux and then distilled from the desiccant. It was stored inside an exsiccator with activated 3 Å molecular sieves.

Reagents for silylation: *N,O-bis(trimethylsilyl)trifluoroacetamide* (99% purity), trimethylchlorosilane (99% purity), pyridine (99% purity) and tetracosane (99% purity) were supplied by Sigma Chemicals.

## 2.2. Instrumentation

The microwave-assisted reactions were carried out in a microwave oven Monowave 300 from Anton Paar.

The FT-IR spectra were taken with a Mattson 7000 spectrophotometer working in the ATR mode. Each spectrum was an average of 256 scans taken with  $4\text{ cm}^{-1}$  resolution in the  $500\text{--}4000\text{ cm}^{-1}$  range.

Gas chromatography–mass spectrometry (GC–MS) analyses were carried out with a Trace GC Ultra 2000 instrument equipped with a mass selective detector DSQ II and a DB-1 J&W capillary column ( $30\text{ m} \times 0.32\text{ mm i.d.}$ ,  $0.25\text{ }\mu\text{m}$  film thickness). Helium at a flow rate of  $1.8\text{ ml/min.}$  was used as carrier gas. The conditions adopted for these analyses were: Ramp 1 - initial temperature,  $80\text{ }^{\circ}\text{C}$  for  $5\text{ min.}$ ; heating rate,  $4\text{ }^{\circ}\text{C/min.}$  till  $260\text{ }^{\circ}\text{C}$ ; Ramp 2 – initial temperature,  $260\text{ }^{\circ}\text{C}$ ; heating rate,  $2\text{ }^{\circ}\text{C/min.}$ ; final temperature,  $285\text{ }^{\circ}\text{C}$ , held for  $8\text{ min.}$ ; injector temperature,  $250\text{ }^{\circ}\text{C}$ ; transfer-line temperature,  $285\text{ }^{\circ}\text{C}$ ; and split ratio of 1:33.

$^1\text{H}$ - and  $^{13}\text{C}$  NMR spectra were acquired on a Bruker Avance spectrometer operating at  $300$  and  $75\text{ MHz}$ , respectively, using  $\text{CDCl}_3$  or  $\text{TCE-}d_2$  as solvent. Chemical shifts ( $\delta$ ) were reported in parts per million, relative to the tetramethylsilane ( $\text{Me}_4\text{Si}$ ) internal standard (TMS,  $\delta = 0.00\text{ ppm}$ ).

Nitrogen elemental analyses were performed in a Carlo Erba 1108 Elemental Analyser.

ESI-MS analysis was carried out in a Linear ion trap LIT LXQ (ThermoFinnigan). The HPLC fractions were dissolved in methanol and directly injected into the ESI source by means of a syringe pump, at flow rate of  $8\text{ }\mu\text{L.min}^{-1}$ . Optimal ESI conditions were: nitrogen sheath gas  $30\text{ psi}$ , spray voltage  $4.7\text{ kV}$ , capillary temperature  $275^{\circ}\text{C}$ , capillary voltage  $-7.0\text{ V}$  and tube lens voltage  $-71.8\text{ V}$ . MSn experiments were performed on mass-selected precursor ions using standard isolation and excitation configuration. The collision energy used was between  $20\text{--}40\text{ V}$ .



## 2.3. Syntheses

### 2.3.1. Epoxidation of Methyl Oleate (MO)

Into a 25-ml two-necked round-bottom flask equipped with a reflux condenser, a dosing funnel and a magnetic stirrer was placed 1 ml (2.92 mmol) of 99% methyl oleate, 150  $\mu$ l (2.62 mmol) of 99.7% glacial acetic acid, 15  $\mu$ l ( $2.67 \times 10^{-1}$  mmol) of 95% concentrated sulphuric acid and 2 ml of toluene. The reaction mixture was then degassed with dry nitrogen and placed in an oil bath at 60-65 °C under magnetic stirring. After allowing the reaction mixture to heat up to the desired temperature, 5 ml (48.5 mmol) of 30% H<sub>2</sub>O<sub>2</sub> were added dropwise from the dosing funnel during half an hour. This precaution was taken to prevent overheating of the system due to the exothermic nature of epoxidation reactions. The mixture was stirred at 60-65 °C for 24 h.

When the reaction was complete, the mixture was poured into a separatory funnel and extracted with dichloromethane. The collected organic fraction was washed successively with dilute sodium carbonate solution until the pH was neutral, and then with saturated sodium chloride solution and finally water. The solvent was removed in a rotary evaporator after drying the organic fraction over anhydrous sodium sulphate.

### 2.3.2. Synthesis of Furfuryl-MO

Table 3 gathers all the tests carried out aiming to target the highest selectivity and conversion towards the furfuryl-MO derivative. The efficiency of several catalysts in different reaction conditions (reactants molar ratio and temperature) was evaluated.

Each test, except for the microwave-assisted reactions, was carried in a Sovirel tube. All the reactants were introduced together into the vial which was then purged with dry nitrogen and placed in an oil bath at the specified temperature for a certain period of time. Sample purification was carried out as mentioned on Table 3.

**Table 3** Tests carried out to optimize the furfuryl-MO chemical synthesis.

Test	m (EMO) g	V (amine) μl	Catalyst	Molar ratio EMO:Amina:Cat.	Solvent ml	[Ref.]	T (°C)	t (h)	Remarks / Purification procedure
1	0.195	167	<b>Zn(ClO<sub>4</sub>).6H<sub>2</sub>O</b> 12 mg	<b>1:3:0.05</b>	<b>CH<sub>3</sub>CN</b> 0.5	94-95	80	~24	- Filtration with celite - CH <sub>3</sub> CN Evaporation ** - Dissolved in CH <sub>2</sub> Cl <sub>2</sub> - Extraction/Wash with H <sub>2</sub> O
2	0.195	167	<b>ZnCl<sub>2</sub></b> 21 mg	<b>1:3:0.25</b>	<b>CH<sub>3</sub>CN</b> 1	95-96	82	~24	- Filtration with silica - CH <sub>3</sub> CN evaporation - Dissolved in CH <sub>2</sub> Cl <sub>2</sub> - Extraction/Wash with H <sub>2</sub> O
3	0.050	15	<b>SnCl<sub>4</sub></b> 59 μl	<b>1:1:0.37</b>	<b>CH<sub>3</sub>CN</b> 0.5	97	80	~24	- As for test 2
4	0.050	29	<b>SnCl<sub>4</sub></b> 59 μl	<b>1:2:0.37</b>	<b>CH<sub>3</sub>CN</b> 0.5		80	~24	- As for test 2 + Org. fraction dried over Na <sub>2</sub> SO <sub>4</sub>
5	0.050	43	<b>SnCl<sub>4</sub></b> 59 μl	<b>1:3:0.37</b>	<b>CH<sub>3</sub>CN</b> 0.5		80	~24	- As for test 2 + Org. Fraction dried over Na <sub>2</sub> SO <sub>4</sub>
6	0.050	57	<b>SnCl<sub>4</sub></b> 59 μl	<b>1:4:0.37</b>	<b>No solvent</b>		40	~24	- Dissolved in CH <sub>2</sub> Cl <sub>2</sub> - Extraction/Wash with H <sub>2</sub> O - Org. fraction dried over Na <sub>2</sub> SO <sub>4</sub>
7	0.050	29	<b>SnCl<sub>4</sub></b> 59 μl	<b>1:2:0.37</b>	<b>Dry CH<sub>2</sub>Cl<sub>2</sub>*</b> 0.5		40	~24	- Molecular sieves 3 Å were added to the Sovirel tube prior to reaction - As for test 6
8	0.050	29	<b>ZnCl<sub>2</sub></b> 11 mg	<b>1:2:0.50</b>	<b>Dry CH<sub>2</sub>Cl<sub>2</sub></b> 0.5		40	~24	- Molecular sieves 3 Å were added to the Sovirel tube prior to reaction - As for test 6
9	0.050	29	<b>SnCl<sub>4</sub></b> 16 μl	<b>1:2:0.10</b>	<b>Dry CH<sub>2</sub>Cl<sub>2</sub></b> 0.5		40	~24	- Molecular sieves 3 Å were added to the Sovirel tube prior to reaction - As for test 6

Test	m (EMO) g	V (amine) μl	Catalyst	Molar ratio EMO:Amine:Cat.	Solvent ml	[Ref.]	T (°C)	t (h)	Remarks / Purification procedure
10	0.050	86	<b>SnCl<sub>4</sub></b> 59 μl	<b>1:6:0.37</b>	<b>No solvent</b>		80	~24	- Dissolved in CH <sub>2</sub> Cl <sub>2</sub> - Extraction/Wash: H <sub>2</sub> O - Org. fraction dried over Na <sub>2</sub> SO <sub>4</sub>
11	0.150	---	<b>SnCl<sub>4</sub></b> 178 μl	<b>1:0.37</b>	<b>No solvent</b>		80	~24	- As for test 10
12	0.050	57	<b>SnCl<sub>4</sub></b> 59 μl	<b>1:4:0.37</b>	<b>Dry CH<sub>3</sub>CN</b> 0.5		80	~24	- CH <sub>3</sub> CN evaporation** - Dissolved in CH <sub>2</sub> Cl <sub>2</sub> - Extraction/Wash with H <sub>2</sub> O - Org. fraction dried over Na <sub>2</sub> SO <sub>4</sub>
13	0.100	57	<b>[C<sub>1</sub>Im][BF<sub>4</sub>]</b>	<b>1:2:1.5<sup>#</sup></b>	<b>No solvent</b>		105	2	- CH <sub>3</sub> CN evaporation
14		143	81 mg	<b>1:5:2.3<sup>#</sup></b>				3	- Dissolved in AcOEt
15		143	128 mg	<b>1:5:2.3<sup>#</sup></b>				4	- Extraction/Wash with H <sub>2</sub> O (pH 5), aq. solution of NaCl (sat.) and H <sub>2</sub> O - Org. fraction dried over Na <sub>2</sub> SO <sub>4</sub>
16	0.100	143	<b>[C<sub>1</sub>Im][BF<sub>4</sub>]</b> 128 mg	<b>1:5:2.3<sup>#</sup></b>	<b>Dry CH<sub>3</sub>CN</b> ~ 2		120	20 min.	- <b>Microwave-assisted reactions</b> - As for above
17	0.0765								
18	0.0765								
19	0.0765								

Important data:  $d$  (furfurylamine) = 1.090 g/cm<sup>3</sup>;  $d$  ( SnCl<sub>4</sub> 1 M in CH<sub>2</sub>Cl<sub>2</sub>) = 1.419 g/cm<sup>3</sup>

\* - Predried with CaH<sub>2</sub> under reflux;

\*\* - Solubility tests have shown that CH<sub>3</sub>CN is soluble both in H<sub>2</sub>O and CH<sub>2</sub>Cl<sub>2</sub>. Its removal by evaporation prior to the extraction step avoids compound losses.

<sup>#</sup> - catalyst load corresponds to 50 % by weight of the reaction mixture (EMO + Furfurylamine)

As for the optimized synthesis, the procedure is as follow:

Into a 10 ml microwave reaction vial fitted with a magnetic stir bar were added 100 mg of EMO, 155 mg of furfurylamine (5 eq.), 127.5 mg of [C<sub>1</sub>Im][BF<sub>4</sub>] (50% by weight of reaction mixture) and ~ 2 ml of acetonitrile. The reaction mixture was then purged with dry nitrogen, placed inside the microwave oven and irradiated for 20 min. at 160 °C.

After the reaction was complete, the solvent was removed in a rotary evaporator and the residue dissolved in ethyl acetate, transferred to a separatory funnel and washed with acidic water (pH 5), followed by a saturated solution of sodium chloride and distilled water, to remove the ionic liquid catalyst and the free unreacted furfurylamine. The organic fraction was then dried over sodium sulphate before removing the solvent in a rotary evaporator.

Furfuryl-MO was isolated from the residue by silica-gel column chromatography with a 7:3 (v/v) mixture of petroleum ether/ethyl acetate.

### **2.3.3. Synthesis of Furfuryl-SBO**

Five tests were carried out with the purpose of synthesizing a furfuryl-SBO derivative with a high substitution degree. The experimental conditions for each test are summarized on Table 4. For the microwave-assisted aminolysis trials, reaction conditions were adjusted on the basis of the previously optimized furfuryl-MO synthetic procedure. Each test, except for the microwave-assisted reactions, was carried in a Sovirel tube. All the reactants were introduced together into the vial which was then purged with dry nitrogen and placed in an oil bath at the specified temperature for a certain period of time. Sample purification was carried out as mentioned on Table 4.

**Table 4** Tests carried out for furfuryl-SBO chemical synthesis.

Test	m(ESBO) g	V(amine) μl	Catalyst mg	Molar ratio ESBO:Amine:Cat.	Solvent ml	T (°C)	t (h)	Remarks/Purification procedure
1	0.100	76	<b>ZnCl<sub>2</sub></b> 16	<b>1:8:1.1</b>	<b>No solvent</b>	80	~24	- Dissolved in CH <sub>2</sub> Cl <sub>2</sub> - Extraction/Wash with H <sub>2</sub> O - Org. fraction dried over Na <sub>2</sub> SO <sub>4</sub>
2*	0.100	76	<b>SnCl<sub>4</sub></b> 176 μl	<b>1:8:1.7</b>	<b>Toluene</b> 0.5	80	~24	- Toluene evaporation - Dissolved in CH <sub>2</sub> Cl <sub>2</sub> - Extraction/Wash with H <sub>2</sub> O - Org. fraction dried over Na <sub>2</sub> SO <sub>4</sub>
3**	0.100	226	<b>[C<sub>1</sub>Im][BF<sub>4</sub>]</b> 104 or 35	<b>1:24:5.8 (a)</b>	<b>Dry</b>	150	1	- <b>Microwave-assisted reactions</b> - CH <sub>3</sub> CN evaporation
4**				<b>1:24:1.9 (b)</b>	<b>CH<sub>3</sub>CN</b>	150		- Dissolved in AcOEt - Extraction/Wash with H <sub>2</sub> O (pH 5), aq. solution of NaCl (sat.) and again with H <sub>2</sub> O
5**				<b>1:24:5.8</b>	~2 ml	105		- Org. fraction dried over Na <sub>2</sub> SO <sub>4</sub>

- Important data:  $d$  (furfurylamine) = 1.090 g/cm<sup>3</sup>;  $d$  (SnCl<sub>4</sub> 1 M in CH<sub>2</sub>Cl<sub>2</sub>) = 1.419 g/cm<sup>3</sup>;  $M_w$  (ESBO) = 945 g/mol

- \*  $n(\text{C}=\text{C})/\text{mol ESBO} = 4.5$ ; \*\*  $n(\text{C}=\text{C})/\text{mol ESBO} = 4.0$

- (a) and (b) - catalyst load corresponds to 50 and 10 % by weight of the reaction mixture (EMO + Furfurylamine), respectively

The best results were achieved with the following experimental procedure:

Into a 10 ml microwave reaction vial fitted with a magnetic stir bar were added 100 mg of ESBO, 247 mg of furfurylamine (24 eq.), 104 mg of [C<sub>1</sub>Im][BF<sub>4</sub>] (30% by weight of reaction mixture) and ~ 2 ml of acetonitrile. The reaction mixture was then purged with dry nitrogen, placed inside the microwave oven and irradiated for 20 min. at 150 °C.

After the reaction was complete, the solvent was removed in a rotary evaporator and the residue dissolved in ethyl acetate, transferred to a separatory funnel and washed with slightly acidic water (pH 5), followed by a saturated solution of sodium chloride and distilled water, to remove the ionic liquid catalyst and the free unreacted furfurylamine. The organic fraction was then dried over sodium sulphate before removing the solvent in a rotary evaporator.

### 2.3.4. DA-based Polymer Synthesis

Tests were carried out using 1,6-bismaleimido-hexane and *N*-tris(ethyl)maleimide as crosslinking agents, at different Furan:Maleimide (units) molar ratio (Table 5). The test with *N*-methylmaleimide was used as model system. The trifunctional furfuryl-soybean oil derivative (3FA-SBO) and the maleimide compound were added to a sample holder, dissolved in a few drops of TCE-*d*<sub>2</sub> and transferred to a NMR tube. The volume of deuterated solvent was then adjusted to 1/3 of tube capacity and placed in an oil bath at 65 °C. Polymerization progress was monitored by <sup>1</sup>H NMR

The thermoreversible nature of DA-based materials was investigated by placing the tubes in an oil bath at 110 °C. De-polymerization progress was monitored by <sup>1</sup>H NMR as well.

**Table 5** Furan:Maleimide moieties molar ratio employed on the several DA-based polymerization tests with maleimides.

Maleimide	m (3FA-SBO) mg	m (Maleimide) mg	Furan: Maleimide Initial*	Furan: Maleimide Final*
<i>N</i> -methylmaleimide <b>MM</b>	17.0	4.5	<b>1:1</b>	---
1,6-bismaleimido-hexane <b>BM</b>	40.1	3.30	<b>1:0.25</b>	<b>1:0.5</b> (by adding more 3.8 mg of BM)
	75.0	20.0	<b>1:0.8</b>	---
<i>N</i> -tris(ethyl)maleimide <b>TM</b>	55.5	12.0	<b>1:0.70</b>	<b>1:1.3</b> (by adding more 9.9 mg of TM)

- \* Molar ratio between complementary single units

- Assuming that 3FA-SBO was the only derivative formed; M (3FA-SBO) = 1256 g/mol;

- M (MM) = 111.1 g/mol; M (BM) = 276.29 g/mol; M (TM) = 386.36 g/mol;

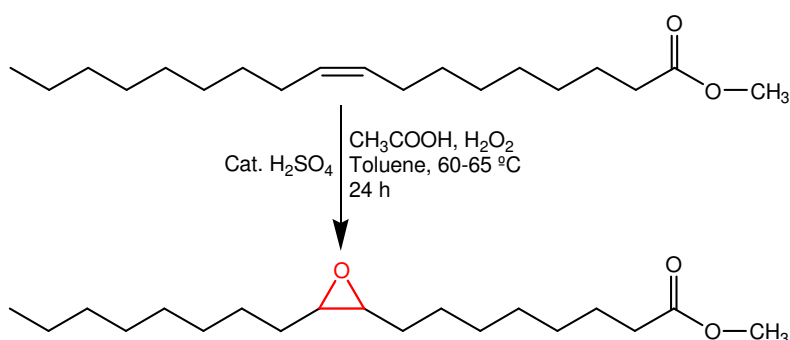
### 3. Results and Discussion

#### 3.1. Epoxidized Methyl Oleate (EMO)

##### 3.1.1. Synthesis of EMO

In the reaction sequence, we first started with methyl oleate (MO) and epoxidized it to methyl 9,10-epoxyoctadecanoate (EMO). The oxirane precursor was the functionalization platform chosen for this study, as its higher reactivity provides abbreviated pathways to several functional derivatives which wouldn't be readily achieved otherwise.

Epoxidation was carried out *via* hydrogen peroxide and acetic acid catalyst, *i.e.* by *in situ* generated peracetic acid standard pathway (see experimental section), which, of all the routes to oxiranes, it's the least hazardous, and the most cost-effective environment-friendly procedure (Scheme 5).



**Scheme 5** Methyl-oleate epoxidation reaction scheme.

##### 3.1.2. Structural Characterization of EMO

Epoxidation of methyl oleate (MO) to EMO was confirmed by Proton Nuclear Magnetic Resonance ( $^1\text{H}$  NMR) and GC-MS (Gas Chromatography associated with Mass Spectrometry) analyses. The disappearance of the signal assigned to the olefinic protons ( $\delta \sim 5,3$  ppm),<sup>eg. 98-99</sup> together with the emergence of new resonances at  $\delta \sim 2,9$  ppm, typical of those of epoxide protons,<sup>eg. 96,100-101</sup> and the upfield shift of  $\text{H}_8$  and  $\text{H}_{11}$  protons peak, are consistent with the conversion of MO to EMO (Figure 22). In addition, the

typical features assigned to the rest of the molecular structure were kept unchanged - terminal  $\text{-CH}_3$ ,  $\alpha\text{-CH}_2$ , and  $\text{O-CH}_3$  at  $\delta$  0.88, 2.31 and 3.67 ppm, respectively.<sup>eg. 102</sup> No resonances attributable to side reaction product groups such as  $\text{-OCOCH}_3$  (acetyl),  $\text{-OOH}$  (hydroperoxide),  $\text{-OH}$  (hydroxyl),  $\text{-CO}$  (carbonyl) or even  $\text{-OOCOCH}_3$  (peroxoacetyl) were detected,<sup>56</sup> meaning that both (regio)selectivity and conversion to the epoxidized product are high.

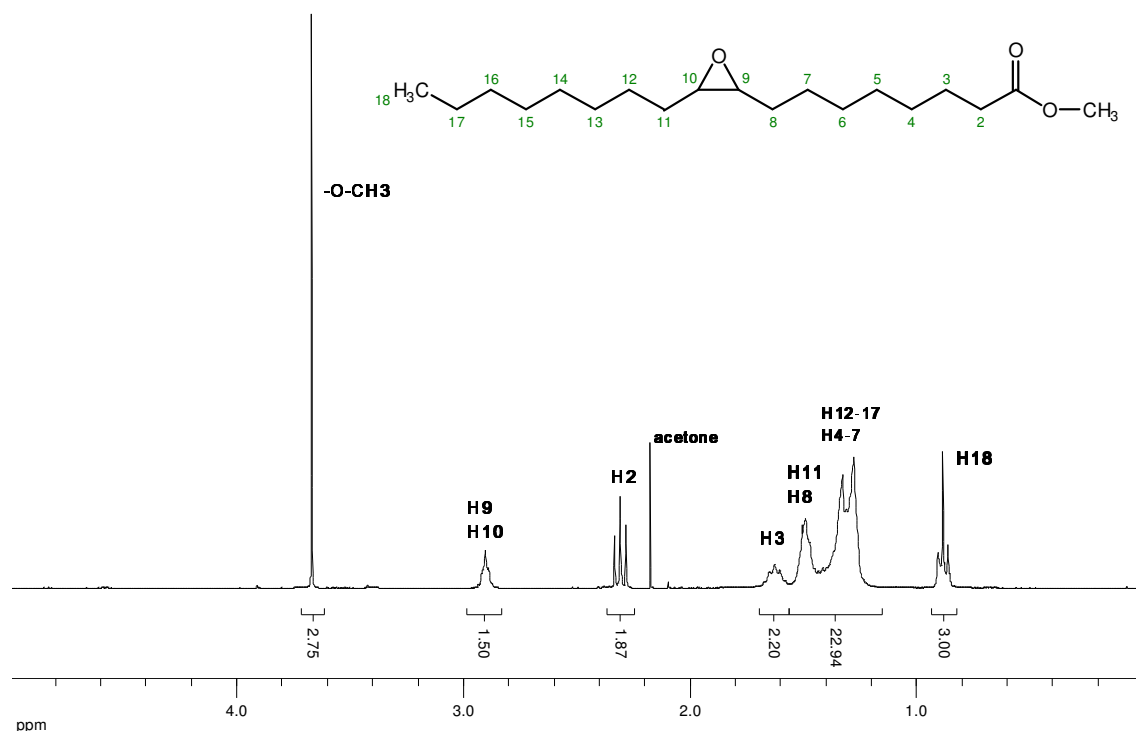


**Figure 22**  $^1\text{H}$  NMR spectrum of epoxidized methyl oleate (EMO) in  $\text{CDCl}_3$  and corresponding peak assignments.

MO epoxidation was further confirmed by GC-MS. The chromatogram exhibited two peaks: the most intense at 38,32 min., referring to the major component, and a second, at 42,57 min (Figure 23). The former peak was attributed to EMO and the latter corresponded to the TMS derivative of the corresponding fatty ester diol. The most useful diagnostic ion in the mass spectrum of EMO it's attributed to the intense peak at  $m/z = 155$  and results from  $\text{C}_8\text{-C}_9$  bond heterolytic cleavage (Figure 24), whereas for the TMS-derivatized fatty diol, the spectral peaks at  $m/z = 215$  and  $259$ , both assigned to fragments bearing silylated  $\text{-OH}$  groups, constitute a clear-cut evidence of its formation. Diol origin remains unknown, but it seems more likely to have been formed during the derivatization process rather than



in the epoxidation reaction ( $^1\text{H}$  NMR spectrum is assigned to a single structure). Admitting the last hypothesis, EMO was obtained with  $\sim 95\%$  yield, as estimated by GC. In both compound mass spectra the long series of related ions at  $m/z = 41, 55, 69, 83, 97, 111$ , etc., characteristic of the fragmentation of the aliphatic chain of the fatty ester of general formula  $[\text{C}_n\text{H}_{2n-1}]^+$ , was detected (Figure 24). We were expecting, however, the series  $[\text{C}_n\text{H}_{2n+1}]$  to prevail. The molecular ion at  $m/z = 74$  is attributed to McLafferty rearrangement (R 1,5-H).

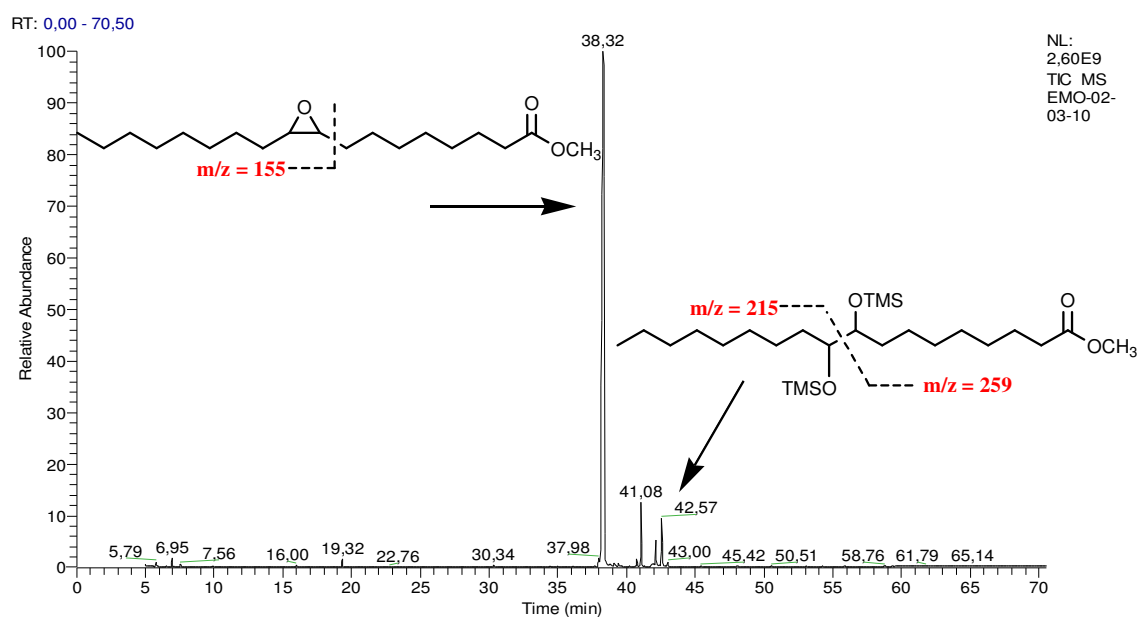


**Figure 23** GC chromatogram of the MO epoxidation products. From left to right: EMO, internal standard (tetracosane, Rt 41,08 min.) and the diol derivative.

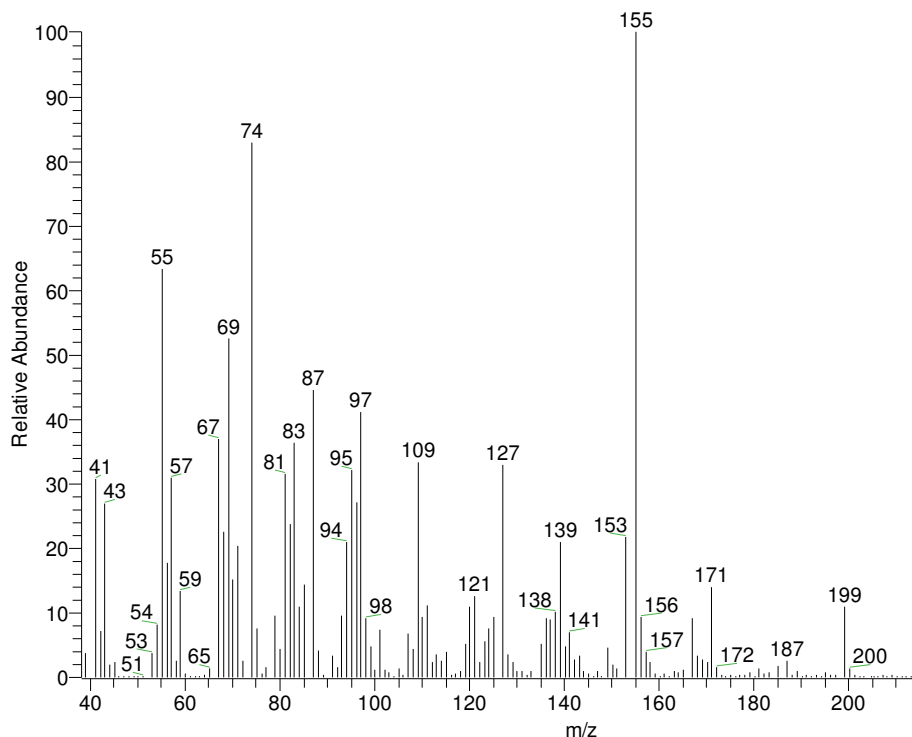


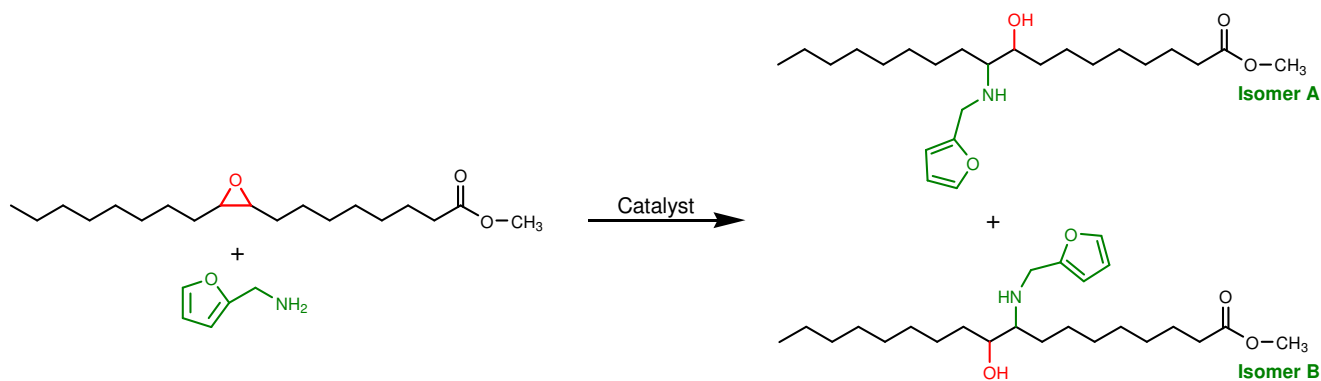
**Figure 24** Mass spectrum of EMO.

## 3.2 Furfuryl-Functionalized Methyl Oleate (Furfuryl-MO)

### 3.2.1 Synthesis of the Furfuryl-MO Derivative

The outcome of the first tests on the synthesis of furfuryl-derivatives, from reaction of EMO with furfurylamine, was considered unexpected albeit much more useful for the purpose in mind, and therefore, worthy of further investigation.

Two amine derivatives were expected to be produced (Scheme 6), but GC-MS analysis of the reaction mixture (after TMS derivatization) revealed it was far more complex, with many products being formed (Figure 25).



**Scheme 6** Epoxide ring-opening reaction by furfurylamine. Two regioisomeric (β-aminohydroxyl) products were expected.

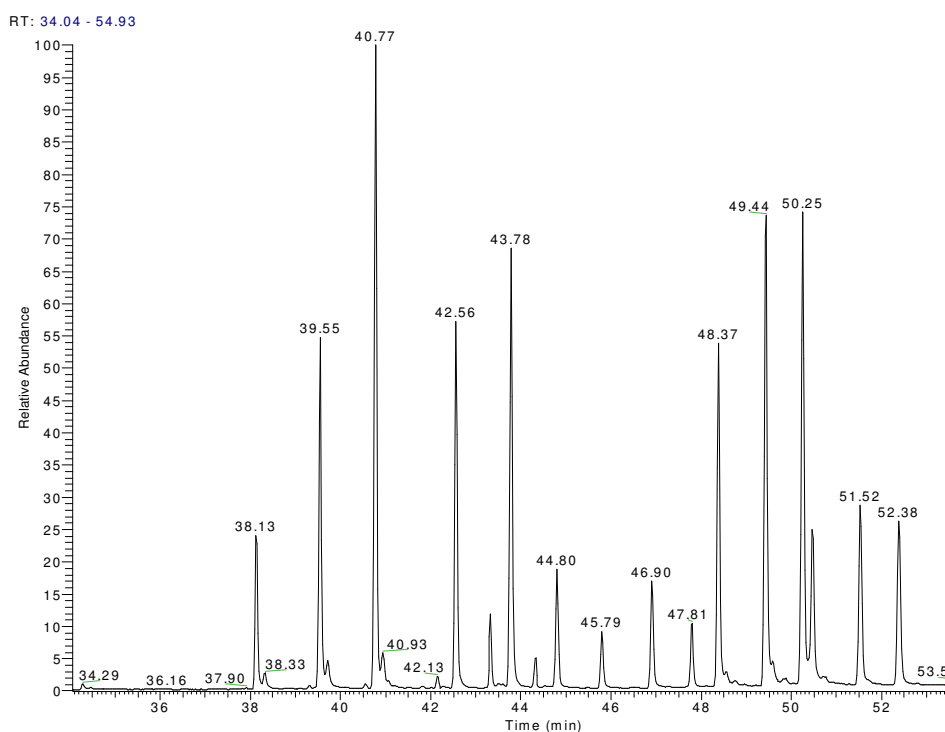


**Figure 25** GC chromatogram of the products of the reaction between methyl 9,10-epoxyoctadecanoate and furfurylamine.

The main peaks were tentatively identified based on their characteristic fragmentation which, typically, occurs by cleavage of the C<sub>9</sub>-C<sub>10</sub> bond. The mass of the two main fragments produced would then allow identifying the chemical structure of the pendant moieties attached to C<sub>9</sub> and C<sub>10</sub> and, ultimately, the compound's structure. The structures we were able to identify are depicted on Figure 26. Intriguingly, none of the two predicted monofurfuryl derivatives (Figure 26) was apparently present.

Amongst the detected compounds, the one eluted at Rt 48.37 min. showed a fragmentation pattern which seemed compatible with the bisfurfuryl product structure. This derivative was totally unexpected. Further analyses weren't carried out at the time due to difficulty in isolating the compound from the complex reaction mixture. However, even though it wasn't confirmed by any other analysis technique, the assignment seemed a straightforward, clear cut evidence.

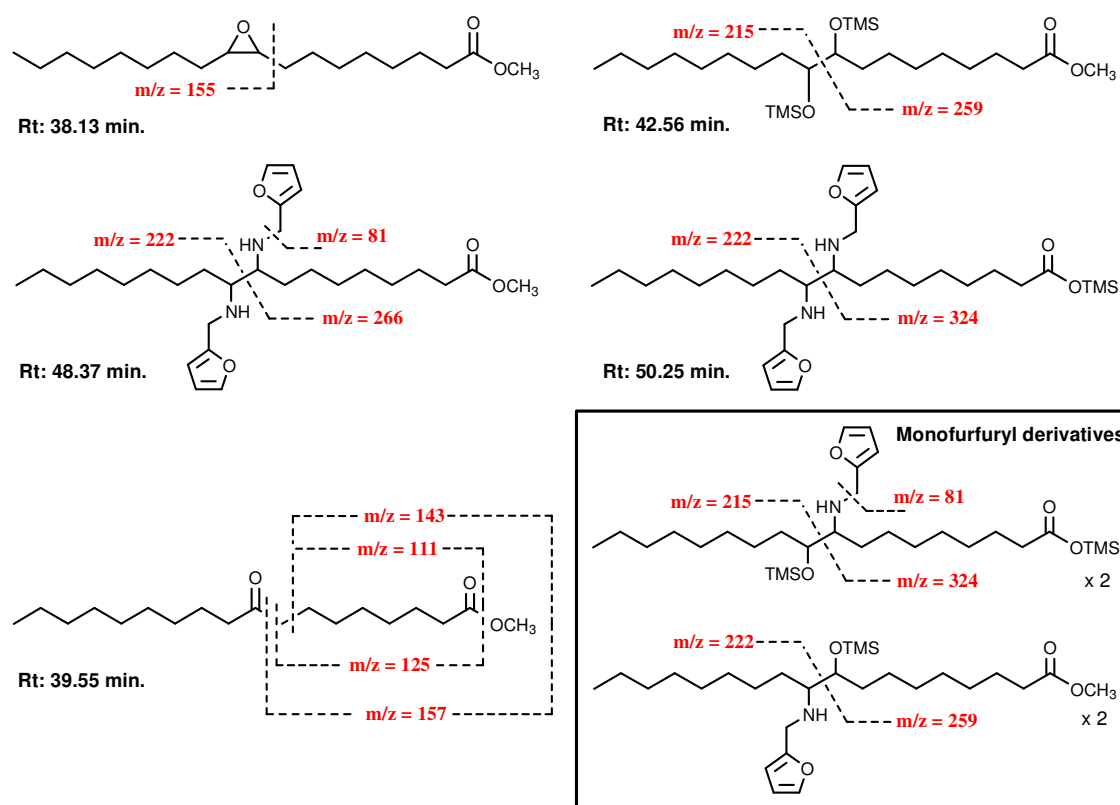


**Figure 26** End-product compounds after aminolysis and silylation reactions, identified by GC-MS. Despite being expected, no traces of the monofurfuryl isomers were detected. From top to bottom, left to right: EMO; vicinal diol; vicinal di-amine (or bisfurfuryl) derivatives (middle row) and the ketone.

Every ion fragment on the corresponding MS spectrum could be easily understood considering the vicinal bisfurfuryl derivative, as shown in Figure 27.

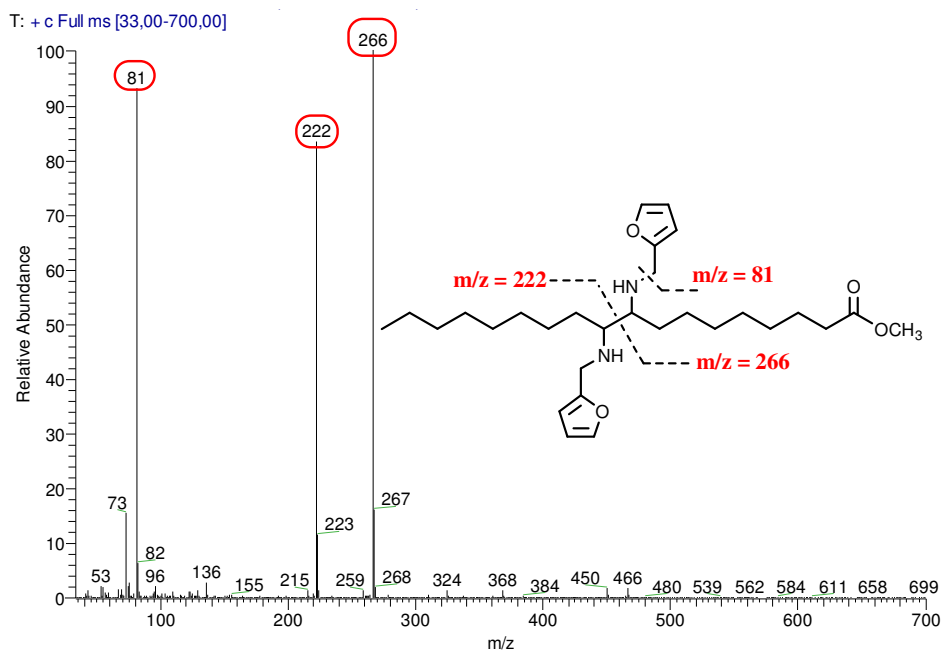


**Figure 27** Mass spectrum of the vicinal di-amine derivative. Its main  $m/z$  fragment ions are assigned.

Although unexpected, the bisfurfuryl derivative was far more interesting than the monofurfuryl counterpart, because, in this case, polymerizable structures could be obtained directly from MO. This unexpected feature would dismiss the need to prepare bisfurfuryl derivatives from diepoxidized linoleic acid.

Based on these preliminary results we focused on the optimization of the reaction towards the presumed bisfurfuryl derivative, in order to maximize EMO conversion and selectivity to the desired product which, could then be “easily” fractionated from the reaction mixture by preparative chromatographic techniques. The acquired knowledge on this stage would then be applied to synthesize (multi)furfuryl-functionalized monomers directly from a renewable resource, *i.e.*, vegetable oils, rather than from one of its chemical derivatives (MO).

Several reaction conditions and catalysts were tested so as to improve the yield of the desired product. Table 3 gathers the reaction conditions used for each trial.

The catalysts (Lewis acids) tested were chosen so that amine-initiated cross-linking reactions were prevented. Strong acid catalysts such as  $\text{BF}_3$  are inefficient to carry out the aminolysis reaction as they tend to complex with the epoxy oxygen too strongly and

activate the epoxy group more than desired. This enhanced electrophilicity of the two carbons of the epoxy rings leads to higher reactivity and crosslinking reaction which is obviously undesirable.

Of all the catalysts tested, the ionic liquid 1-Methylimidazolium tetrafluoroborate, [C<sub>1</sub>Im][BF<sub>4</sub>], proved to be the most effective.

Microwave-assisted aminolysis at 160 °C/20 min., for a 1:5 EMO/furfurylamine molar ratio and a catalyst load of 50% (by weight of reaction mixture), gives the desired product in high yields (up to 93%) and improved reaction selectivity towards the desired derivative to 93% (Figure 28). These values could even be higher if one finds out that the diol (Rt 42.4 min.) is formed during the silylation process rather than as by-product of the aminolysis reaction.

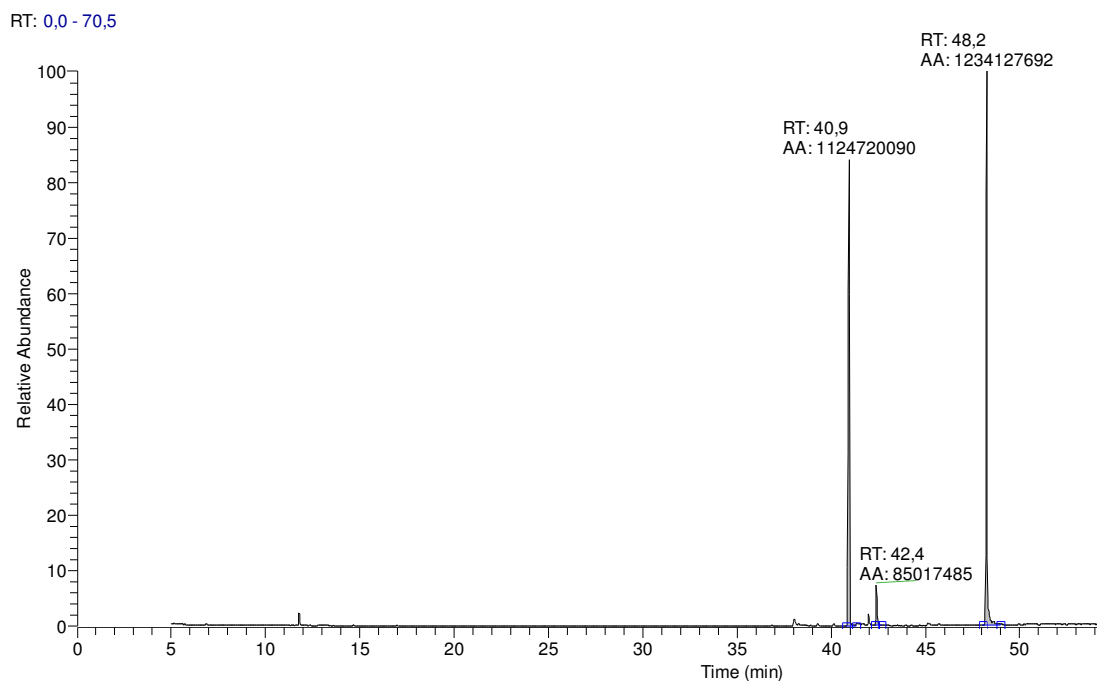


**Figure 28** GC chromatogram of the reaction mixture. From left to right: internal standard (tetracosane), diol and the bisfurfuryl derivative.

Under these conditions it became possible to purify the desired component by preparative chromatography and carry out a detailed spectroscopic characterization of the reaction product.

### 3.2.2 Structural Characterization of Furfuryl-MO Derivative

After a laborious column chromatography purification, to isolate the presumed (vicinal) diamine derivative from the remaining components of the reaction mixture, *i.e.*, vicinal diols, unreacted EMO and some other minor compounds, such as the corresponding ketone and amide molecules, we proceeded to its structural characterization by  $^1\text{H}$ ,  $^{13}\text{C}$  NMR and ESI-MS.

Surprisingly, the structure we had previously anticipated, using GC-MS, was not in agreement with that proposed by  $^1\text{H}$  and  $^{13}\text{C}$  NMR.

The  $^1\text{H}$  NMR analysis clearly confirmed the functionalization of epoxidized methyl oleate with a furfuryl moiety (Figure 29) by the disappearance of the signal assigned to oxirane/epoxide protons resonances (at  $\delta \sim 2.9$  ppm) and the emergence of new resonances characteristic of the furan ring protons of furfurylamine groups (at  $\delta > 6.0$  ppm).

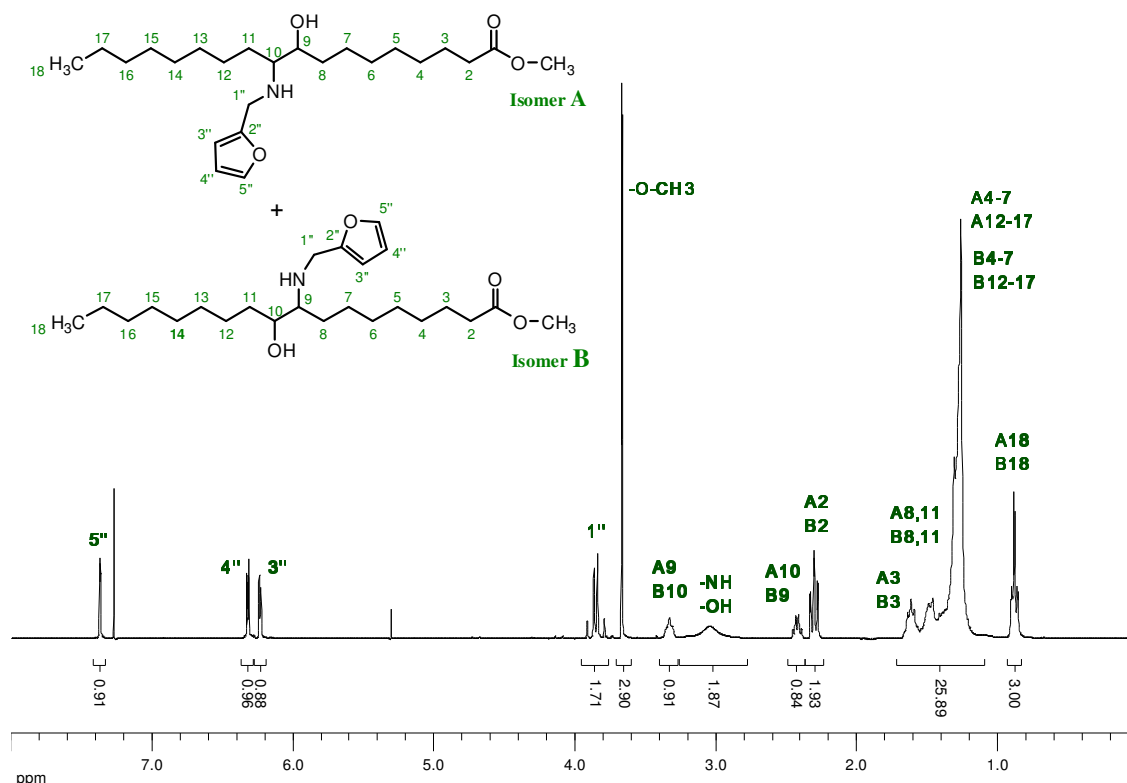


**Figure 29**  $^1\text{H}$  NMR spectrum of the furfurylamine-functionalized ( $\beta$ -aminohydroxy) methyl oleate derivative and corresponding peak assignment. The two possible structural isomers formed are depicted, although it's not possible to differentiate one from another using  $^1\text{H}$ .

The integration values of the proton signals are an unequivocal proof that our first assumptions were incorrect: the mono-amine ( $\beta$ -aminohydroxy) derivative is the single aminated product formed. This conclusion was further corroborated by ESI-MS, as discussed below.

In the  $^1\text{H}$  NMR spectrum, the assignment to furfurylamine moiety is straightforward from coupling patterns and intensities:  $\text{H}_3$  (d),  $\text{H}_4$  (dd) and  $\text{H}_5$  (d) in decreasing shielding ( $\delta$  6.1, 6.3 and 7.5 ppm, respectively). However, the signal assigned to the  $-\text{CH}_2$  group ( $\text{H}_1$  protons), which appeared as a singlet at  $\delta$  3.82 ppm for free unreacted furfurylamine (Figure 30), appears now as a double doublet (at  $\delta \sim 3.8$  ppm), suggesting there's no free rotation along the  $\text{N}-\text{CH}_2$  bond and that both protons have different chemical environments.

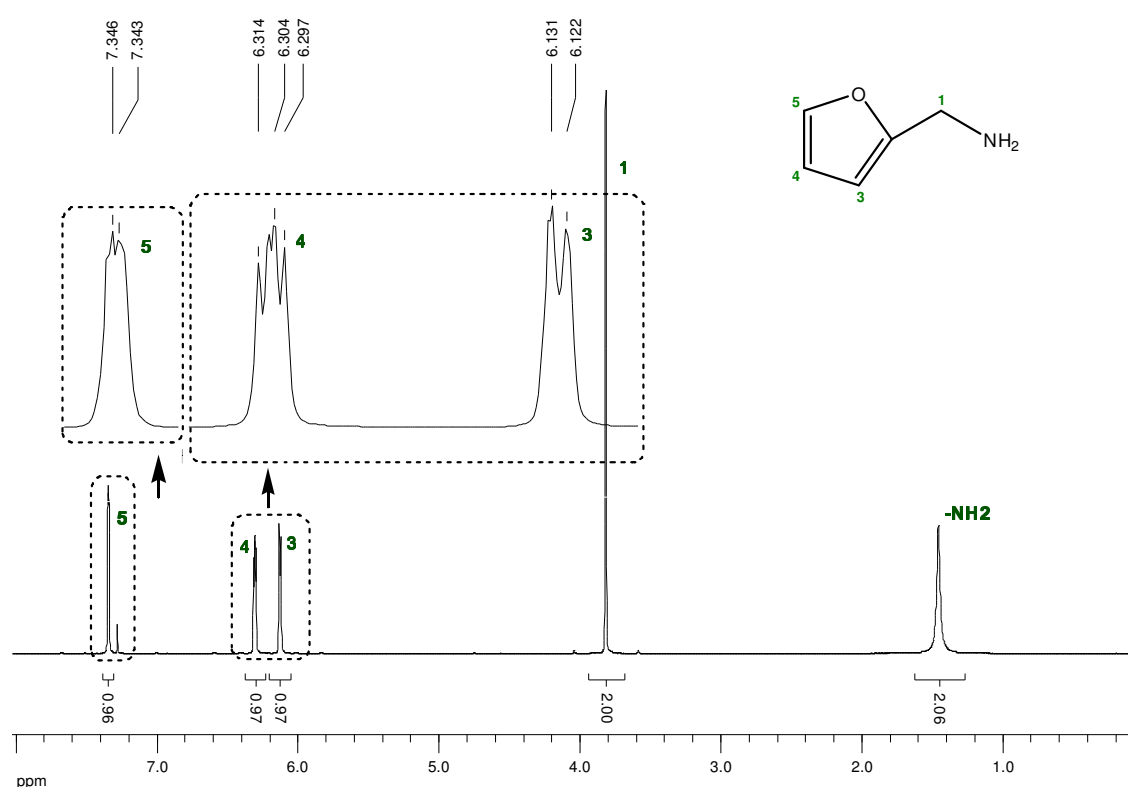


**Figure 30**  $^1\text{H}$  NMR spectrum of furfurylamine in  $\text{CDCl}_3$  and signals assignments. Expansions of furan ring peaks are shown.

Formation of a five membered ring involving an intramolecular hydrogen bond between nitrogen and the  $\beta$ -OH group, as depicted in Figure 31, would prevent free  $\text{N}-\text{CH}_2$  bond rotation and freeze their spatial arrangement. This seemed a reasonable explanation to



justify the signal multiplicity but still, no evidence of hydrogen bonding was perceived on the  $^1\text{H}$  NMR spectrum. If such was the case, a new resonance at  $\delta \gg 10$  ppm should have emerged. Alternatively, the multiplicity of  $\text{H}_{1'}$  protons is more likely to result from a steric hindrance effect, which sets distinctive chemical environments for both protons.

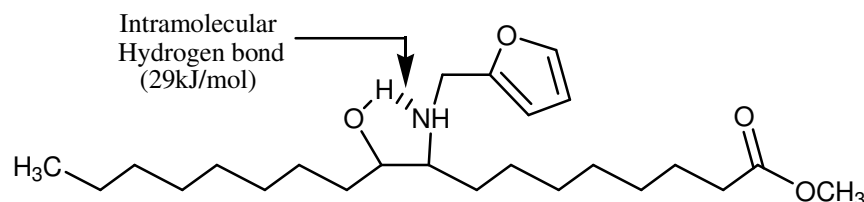


**Figure 31** Intramolecular hydrogen bonding in furfurylamine-functionalized methyl oleate. The participation of the nitrogen atom in the five-membered ring prevents free rotation along  $\text{N-CH}_2$  bond and sets distinct chemical environments for each methylene proton ( $\text{NCH}_2$ -2-Furan).

Apart from the set of signals assigned to the furfuryl moiety,  $^1\text{H}$  NMR spectrum of the aminated product revealed also the emergence of three new resonances ( $\delta \sim 2.42$ , 3.04 and 3.33 ppm), as a result of the epoxide ring opening reaction. Protons  $\text{A}_9/\text{B}_{10}$  and  $\text{A}_{10}/\text{B}_9$  are assigned to resonances at  $\delta$  3.33 and 2.42 ppm, respectively, because the methine attached to oxygen is more downfield than that attached to nitrogen, whereas the broad NMR signal at  $\delta$  3.04 ppm and an integration value 2, to the labile protons  $-\text{NH}$  and  $-\text{OH}$ . These assignments were confirmed by COSY and  $^{13}\text{C}$ - $^1\text{H}$  HSQC and (Figure 32 and Figure 33). Organic chemists often combine these both analysis techniques to elucidate structural data on molecules that are not satisfactorily represented in a one-dimensional NMR spectrum. Using cross-peaks, one could discover much about the structure of the “unknown” molecule.

As for the protons of the structure backbone, we took advantage of having the assignments of epoxidized methyl oleate (Figure 22).

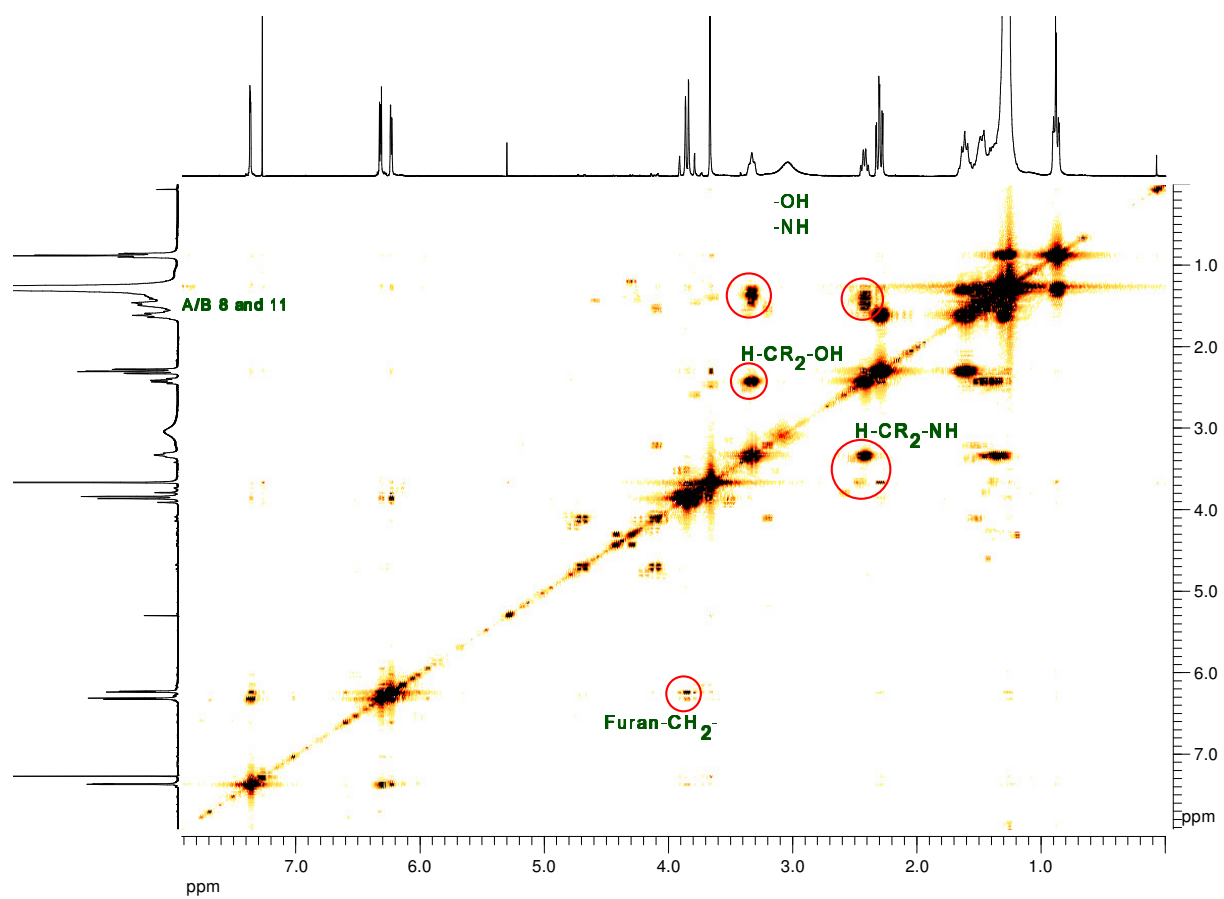


**Figure 32** COSY plot for furfurylamine-functionalized methyl oleate derivative.

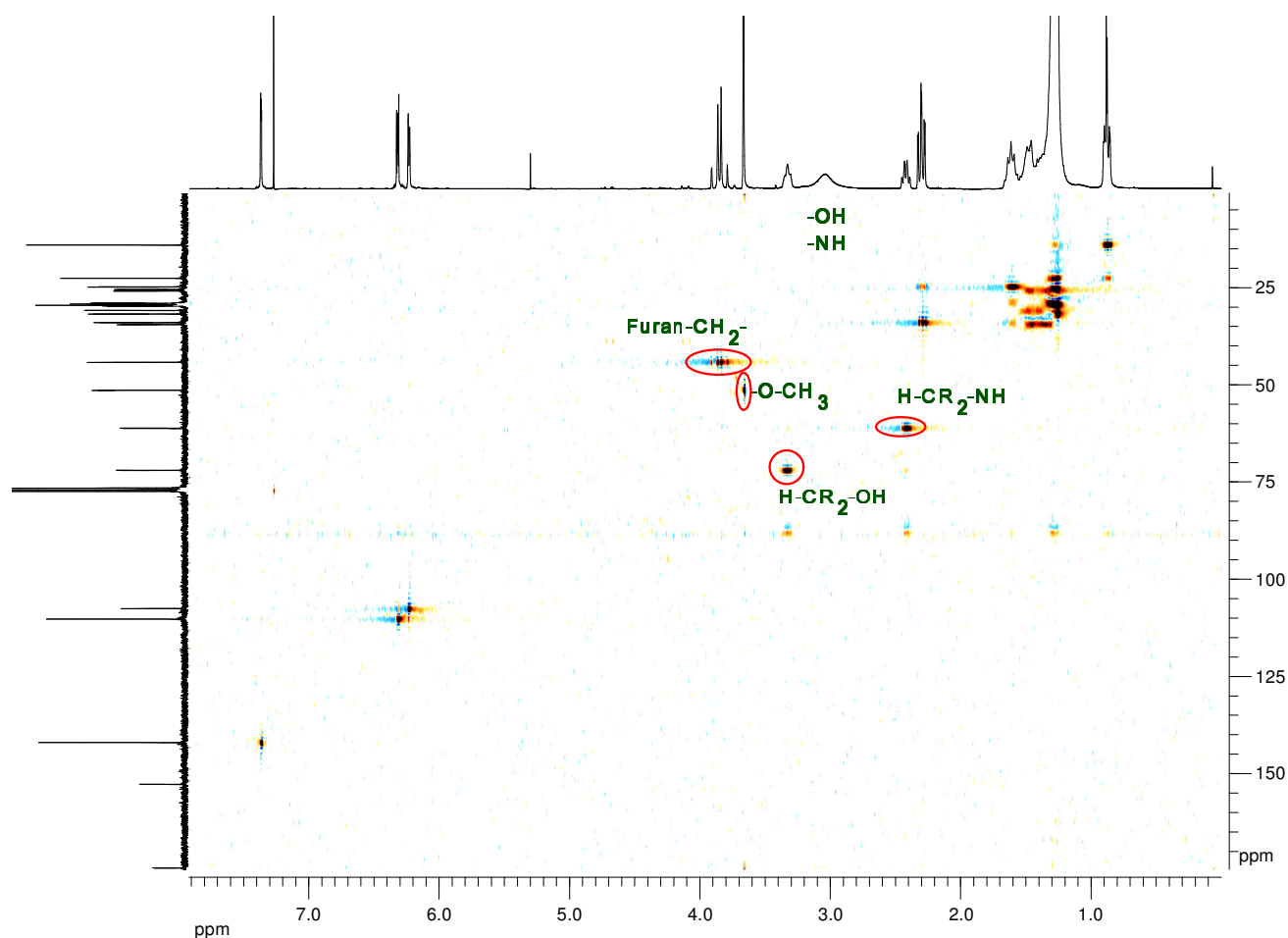
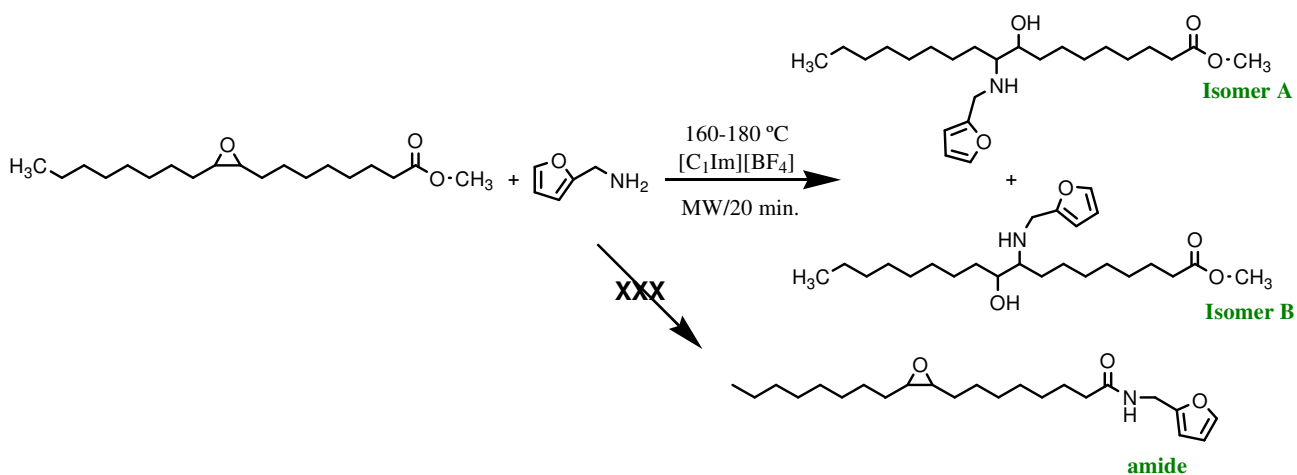


**Figure 33**  $^{13}\text{C} - ^1\text{H}$  HSQC plot for furfurylamine-functionalized methyl oleate derivative.

Still, it is important to emphasize that the peak assigned to the methoxy group protons of the fatty acid chain remains preserved, which suggests that no fatty amide is formed during the aminolysis reaction (Scheme 7).



**Scheme 7** Reaction of EMO with Furfurylamine catalyzed by 1-Methylimidazolium tetrafluoroborate.

The  $^{13}\text{C}$  NMR analysis of the product was consistent with the structure proposed by  $^1\text{H}$  NMR (Figure 34). Signals at  $\delta > 100$  ppm, assigned to the furan ring group carbon atoms ( $\text{C}_{2''}$ ,  $\text{C}_{3''}$ ,  $\text{C}_{4''}$  and  $\text{C}_{5''}$  at  $\delta$  153, 108, 110 and 142 ppm, respectively), together with those at 61 and 72 ppm, attributed to  $\text{A}_{10}/\text{B}_9$  and  $\text{A}_9/\text{B}_{10}$  carbons, in the same order, confirmed the occurrence of the aminolysis reaction and the synthesis of the mono-aminated ( $\beta$ -aminohydroxy) derivative as the single reaction product.

A clear-cut evidence of the formation of the vicinal di-amine product would be the presence of pairs of peaks closely located assigned to both furfurylamine moieties and, less perceptible, the absence of the signal corresponding to the methine proton attached to the oxygen ( $\text{A}_9/\text{B}_{10}$  peak). None of the evidence was detected, thus confirming the absence of the bisfurfuryl derivative.

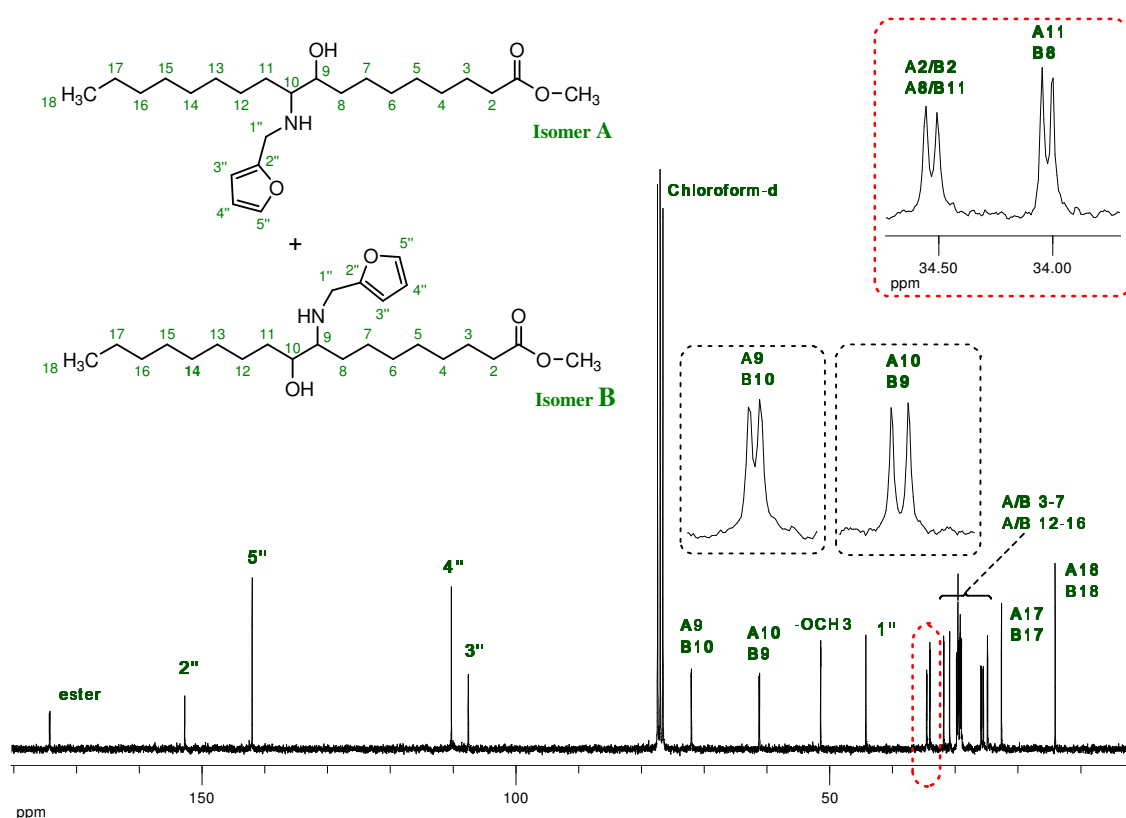


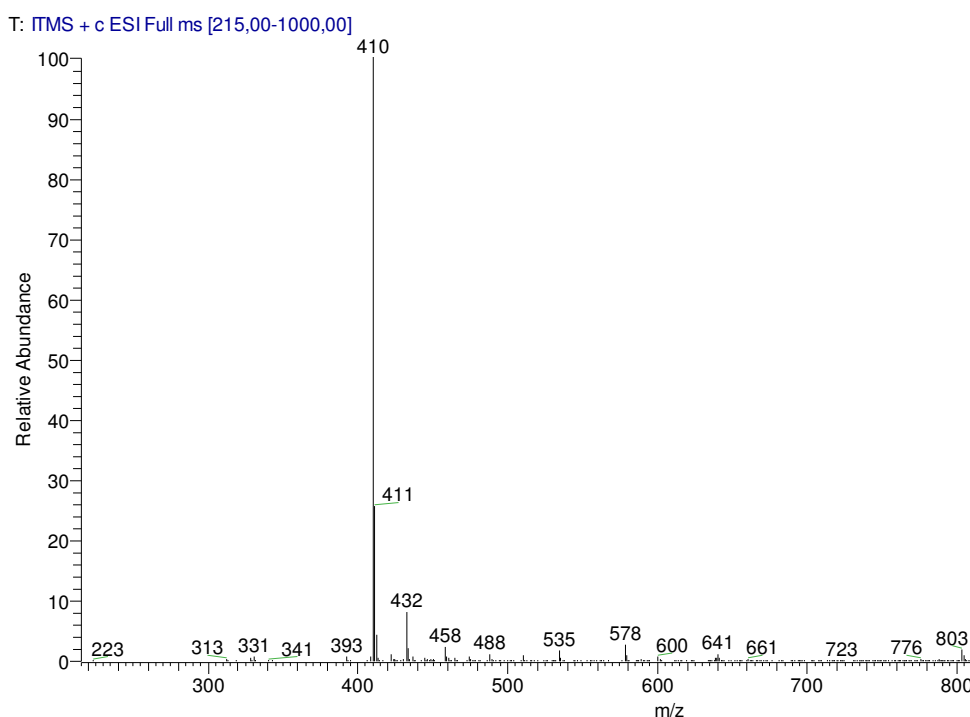
**Figure 34**  $^{13}\text{C}$  NMR spectrum of the aminated derivative and corresponding peaks assignments.

Interestingly, both isomers can be distinguishable in the  $^{13}\text{C}$  NMR spectrum recorded at 75.5 MHz. Expansions of the  $^{13}\text{C}$  NMR spectrum signals show that products A and B give distinctly peaks for all carbons, except for C-17 and C-18, and carbons from methoxy and

furfurylamine. Nevertheless, as depicted in Figure 34, peaks appear together in pairs, almost overlapping each other, which make their assignment hazardous.

$^{13}\text{C}$  spectrum also substantiates the previous conclusion that no fatty amide is formed, because only the carbonylic ester resonance ( $\delta$  174 ppm) is observed and the methoxy group remains intact ( $\delta$  51.4 ppm). If the fatty amide had also been formed, we would have observed another carbonylic resonance, slightly shifted upfield in comparison to the ester's, and assigned to the carbonylic carbon of the amide group.

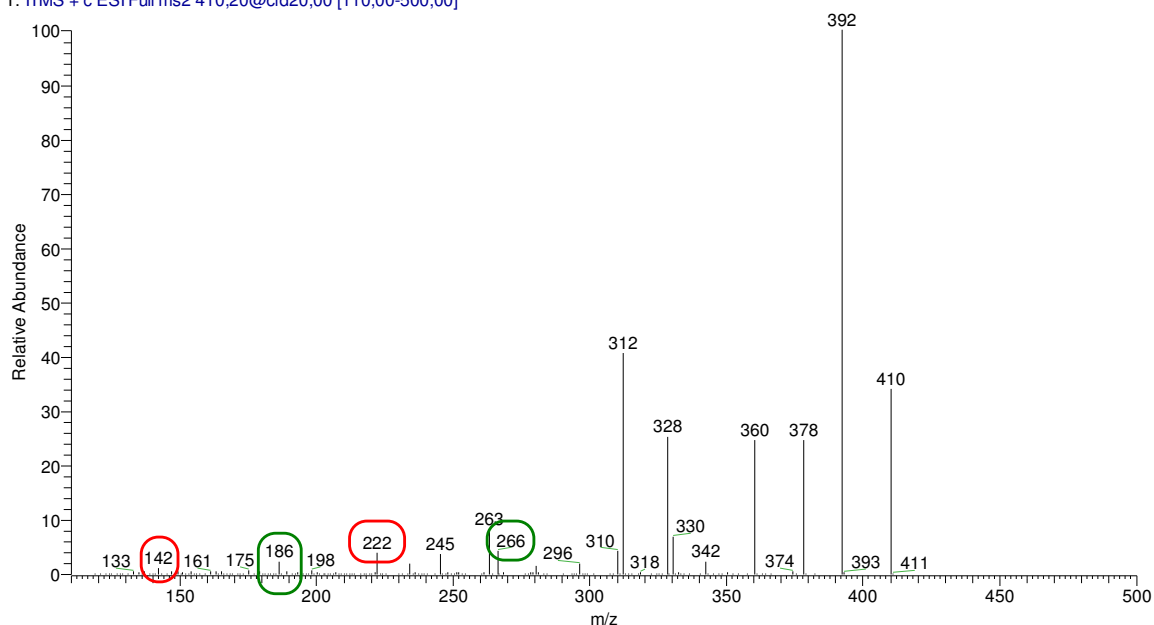
Additional evidence that the assigned product is correct was given by ESI-MS analysis. Besides detecting the molecular ion  $[\text{M} + \text{H}]^+$  (Figure 35), it allowed further structural characterization by MS/MS spectrometry (Figure 36). The mass to charge ratio ( $m/z$ ) for the product's molecular ion  $[\text{M} + \text{H}]^+$  was found to be 410.5, which is consistent with the molecular weight of the mono-aminated derivative – 409.6 g/mol.



**Figure 35** ESI spectrum of the aminolysis product. The mass to charge ratio ( $m/z$ ) for the product's molecular ion  $[\text{M} + \text{H}]^+$  was found to be 410.5, which is consistent with the molecular weight of the mono-aminated derivative – 409.6 g/mol.

The MS/MS spectrum of the (mono-)aminated compound and the fragment assignment are shown in Figure 36 and Table 6, respectively.

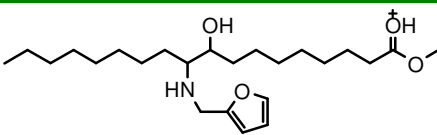
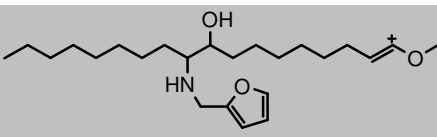
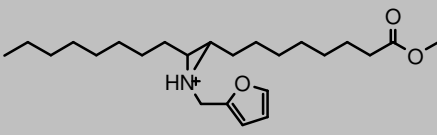
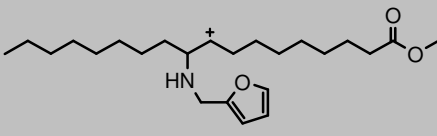
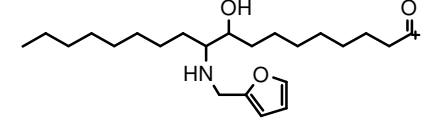
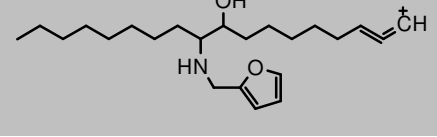
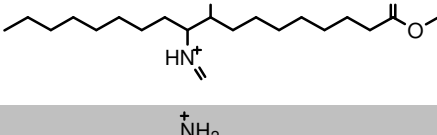
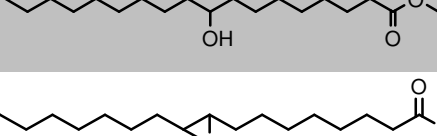
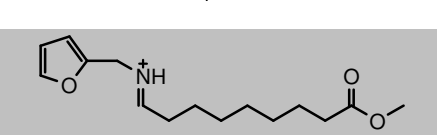

T: ITMS + c ESI Full ms2 410,20@cid20,00 [110,00-500,00]

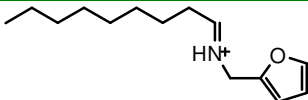
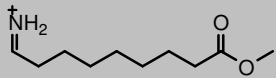
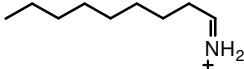


**Figure 36** ESI-MS spectrum of furfurylamine-functionalized methyl oleate.

The presence of isomers A and B was also confirmed using this technique. All peaks are common to both structures, excepting those highlighted (Figure 36). The latter peaks can be grouped in pairs:  $m/z = (266; 186)$ , and,  $m/z = (222; 142)$ , and are characteristic of isomer B and A, respectively. Peaks at higher  $m/z$  ratio are attributed to fragments resulting from C<sub>9</sub>-C<sub>10</sub> bond heterolytic scission, whereas the remaining (two) to those representing the loss of the Furan-CH<sub>2</sub>-(loss of 80 not 81) moiety from the latter structures.

**Table 6** m/z peak assignment to probable fragment structures.

m/z Peak	Fragment Structure*	From Isomer:
410		A + B
392		A + B
	and/or	
		A + B
	and/or	
		A + B
378		A + B
360		A + B
342		A + B
328		A + B
312		A + B
266		B

m/z Peak	Fragment Structure*	From Isomer:
222		A
186		B
142		A

\*Probable/Possible fragments structures.

Given the above data, it seems that GC-MS results are inconsistent. A closer look, however, reveals they are in good agreement. The GC column wasn't able to separate both isomers, which end up being fragmented together. The low intensity peaks at  $m/z = 259$  and 215 are assigned to the positively charged fragments bearing the  $-OH$  group, which result from  $C_9$ - $C_{10}$  homolytic scission of isomers A and B, respectively (Figure 37). Mechanistically, fragmentation by EI is triggered by the abstraction of an electron from the molecule, in this case, from the nitrogen or oxygen atoms. The disparity in peak intensity indicates that the positive charge is better stabilized on the fragment with N than on the fragment with O.

The GC-MS results were found to be misleading, as they lead us to the assumption/conclusion that the di-amine derivative was the product formed.



MW3' - Thesis Data #1750 RT: 48.25 AV: 1 NL: 1,31E8  
T: + c Full ms [33,00-700,00]

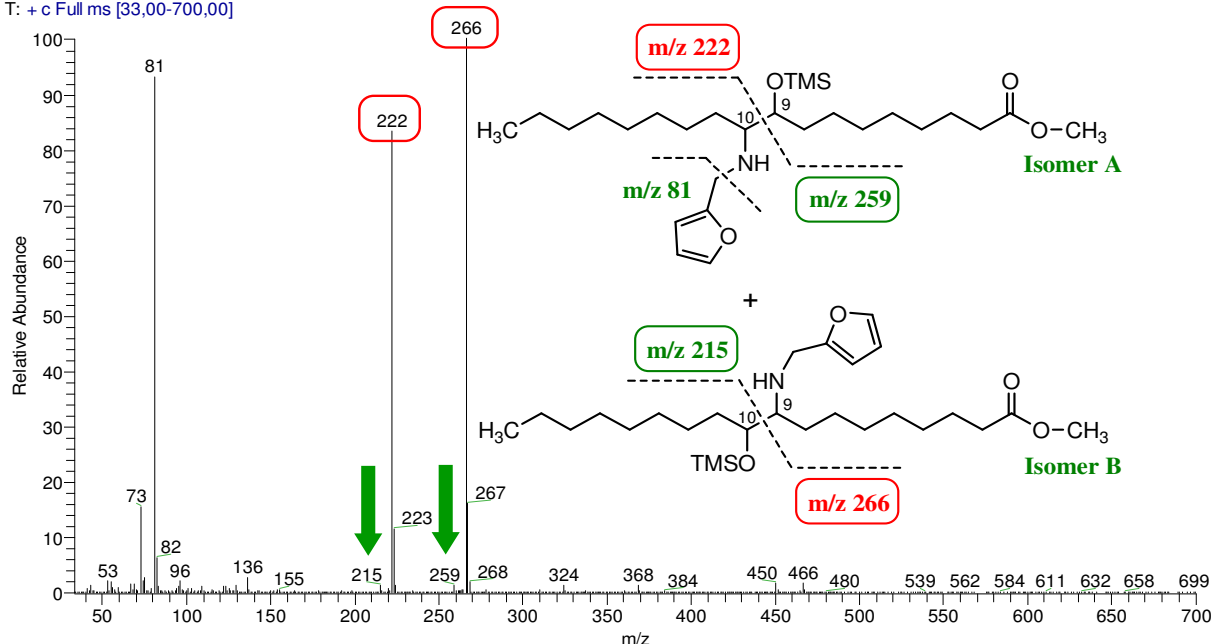


**Figure 37** Mass spectrum of the monofurfuryl-functionalized ( $\beta$ -aminohydroxy) methyl oleate (by EI).

Though our initial assumption was not confirmed– the presumed bisfurfuryl derivative was in fact a mixture of the two monofurfuryl isomers, this work helped to find the most suitable reaction conditions to the synthesis of the furfuryl-SBO.

### 3.3 Furfuryl-Functionalized Soybean Oil (Furfuryl-SBO)

#### 3.3.1 Synthesis of the Furfuryl-SBO derivative

As the synthesized monofurfuryl derivative wasn't suitable for polymerization purposes (functionality lower than 2!), we moved on directly to the functionalization of soybean oil (SBO), using as platform its oxirane derivative: epoxidized soybean oil (ESBO).

Tests were carried out employing three catalysts –  $\text{ZnCl}_2$ ,  $\text{SnCl}_4$  and  $[\text{C}_1\text{Im}][\text{BF}_4]$ , at different temperatures. Table 4 displays the reaction conditions for every test performed.

The best results were attained with the latter catalyst, as we had previously anticipated. The synthetic strategy adopted was the same as for the monofurfuryl-methyl oleate derivative, with a few modifications, targeting the highest substitution degree possible.

Optimally, for a 1:24 ESBO/furfurylamine molar ratio and a catalyst load of ~30% (by weight of reaction mixture), about 2.7 epoxy groups of ESBO (~68%) are converted to aminohydroxyl groups (microwave-assisted reaction at 150 °C/1 h), as determined by  $^1\text{H}$  NMR and elemental nitrogen analysis (the author refers you to the next pages).

### 3.3.2 Furfuryl-SBO Synthesis Reproducibility & Feasibility

To evaluate reaction reproducibility the synthesis of the Furfuryl-SBO was repeated several times and the products were analysed by  $^1\text{H}$  NMR. Our conclusions were supported by the integration values of the signals assigned to the furan ring protons (see next section for compound's  $^1\text{H}$  NMR characterization). The data is compiled on Table 7. Furthermore, degradation/decomposition of the triglyceride into its fatty acids constituents was suspected to take place and therefore, was investigated through  $^1\text{H}$  NMR, as well.

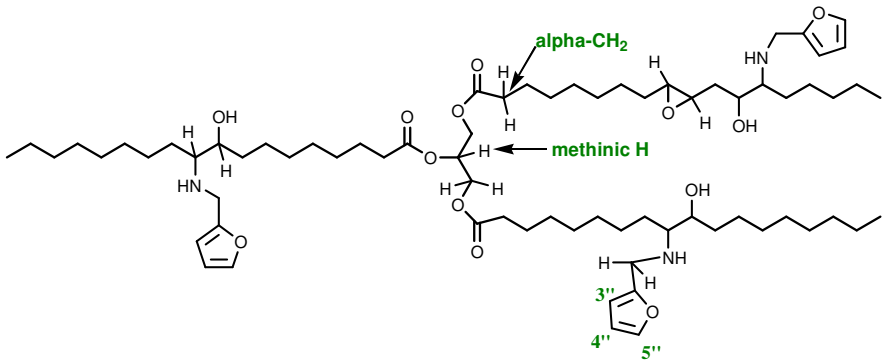
Upon decomposition, triglyceride molecules are break down into the corresponding fatty acids and glycerol, a trifunctional alcohol that is readily removed from the reaction mixture by liquid-liquid extraction with water.

The  $^1\text{H}$  NMR spectrum of a common triglyceride molecule reveals a clear resonance at 5.1-5.33 ppm, assigned to the methine proton of the glycerol backbone (Figure 38). It integrates to 1 (in relation to the terminal  $-\text{CH}_3$  resonance, at  $\delta$  0.90 ppm, which integrates to 9), and it's expected to keep integrating to 1 if the triglyceride's structure remains unaffected by the aminolysis reaction.

Smaller integration values are evidence of triglyceride decomposition into mono-, di-glycerides and, consequently, the presence of free fatty acids and/or derivatives in the reaction mixture. Furthermore, the triplet attributed to the  $\alpha$ -carbonylic protons- those bonded to the C atom adjacent to the carbonyl group – may also be used to evaluate the extent of sample deterioration/decomposition. In the unmodified soybean oil spectrum, this signal appears at  $\delta$  2.32 ppm (Figure 38), and it integrates to six protons - two  $\text{H}_\alpha$  per aliphatic chain ( $\times 3$ ). As for the methinic proton, its integration value shall remain unchanged after the amine-functionalization reaction.

Providing that correct spectral peak integration is available, we shall reach similar conclusions, regardless the chosen peak. The table below (Table 7) summarizes all the relevant data that supports the discussion.

**Table 7** Evaluation of aminolysis reaction reproducibility and feasibility (extent of triglyceride structure deterioration)

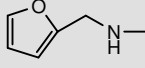
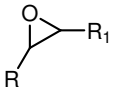
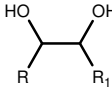
Furfuryl-SBO						
						
Reaction Reproducibility				Decomposition/Degradation		
N.º	$I_{H_5''}$	$I_{H_{3''+4''}}$	AD (%) $H_{5''}$ vs. $H_{3''+4''}$ *	$I_{H \text{ methinic}}$	$I_{\alpha-CH_2}$	
1	3.43	6.83	86 vs. 85	1.00	6.03	
2	2.71	5.60	68 vs. 70	0.69	6.00	
3	2.60	5.39	65 vs. 67	0.73	5.47	
4	2.65	5.22	66 vs. 65	0.87	6.08	
5	3.24	6.24	81 vs. 78	1.00	6.99	
6	2.64	5.27	66 vs. 66	0.84	6.84	
7	2.76	5.69	69 vs. 71	0.90	6.59	

\*AD: Aminolysis Degree; Calculations based on the assumption of four oxirane rings per triglyceride molecule ( $^1\text{H}$  NMR estimated)

With respect to the reproducibility of the furfuryl-functionalized soybean oil triglyceride, the scatter is rather typical of a first series of experiments on a novel system. Aminolysis degrees as high as  $\approx 85\%$  were obtained/attained (1.st experiment) but, for most of the essays, it ranged from 65 to 70%, meaning that the tri- and di-amine derivatives were the major products formed. A 100% aminolysis degree was expected if the tetra-amine

derivative was the only product. Slight variations of the solvent volume and/or catalyst mass seem the most likely explanation for the higher aminolysis degree for trials 1 and 5. The presence of free unreacted furfurylamine was prevented by washing the product with slightly acidic water (pH 5), and therefore, this hypothesis seems unlikely. Contradictorily, and excepting for the first essay, nitrogen elemental analysis of our product mixture revealed a nitrogen content above that predicted by  $^1\text{H}$  NMR technique and, in some cases, even touching the maximum value theoretically achievable– 4.2% (Table 8). Two hypotheses to justify these unexpected results were hence considered: the removal of the free unreacted furfurylamine wasn't successfully carried out and/or an extra nitrogen source, which could only be acetonitrile ( $\text{CH}_3\text{CN}$ ), was present. Soon, however, we abandoned them both. The former because a control test proved that the procedure used to eliminate the excess of furfurylamine was effective, and the latter, as no singlet at 2.10 ppm was detected in the  $^1\text{H}$  NMR spectra. A closer look at the  $^1\text{H}$  NMR spectra, however, revealed the presence of a residual solvent signal at  $\delta \sim 2.48$  ppm (singlet), assigned to methanol, but this would support the decrease in the N% content (as a consequence of C% and O% contents increase), with respected to the predicted value, rather than its increase. The origin of this apparent anomaly remains unclear, but we should bear in mind that the N% content measured will always be very small and, as a consequence, the uncertainty associated with the actual value, large.

**Table 8** Elemental nitrogen analyses results.

Elemental Nitrogen Analysis				
N.º		Predicted Range (%) <sup>a)</sup>		Exp. Value (%)
				
Essays	1	3.43	3.4 - 3.8	3.9
	5	3.24		3.9 <sup>b)</sup>
	3	2.60		4.2
	4	2.65	2.9 – 3.4	3.9 <sup>b)</sup>
	2	2.71		----
	6	2.64		3.9 <sup>b)</sup>
	7	2.76		3.9 <sup>b)</sup>

<sup>a)</sup> Assuming M (ESBO) = 945 g/mol; calculations took into account whether the reactive moieties remained unchanged, as epoxide moieties, or underwent H<sub>2</sub>O hydrolysis, giving vicinol diols – for both, the ranges were found to be similar.

<sup>b)</sup> These essays were analysed as a single sample; N% content of the mixture was expected to fall within the 2.9 – 3.4 % range.

Concerning decomposition or degradation, there's no evidence that they were occurring. Despite there are perceptible small variations in the relevant proton areas (H<sub>methinic</sub> and H<sub>α-CH<sub>2</sub></sub>), these can be neglected if we look at both peak integration values at the same time (Table 7). Furthermore, peaks assigned to triglyceride degradation compounds, such as amides and/or carboxylic acids, were not observed. In case of amide formation the α-CH<sub>2</sub> resonance would appear slightly displaced upfield, in comparison to the ester's.

This procedure has proven to be an effective and efficient methodology to “graft” furfurylamine moieties into triglycerides aliphatic chains. Optimally, each mole of ESBO when reacted with 24 molar equivalent of furfurylamine with ~30% by weight of reaction mixture of [C<sub>1</sub>Im][BF<sub>4</sub>] converts about 2.7 epoxy groups of ESBO to aminohydroxyl groups.

### 3.3.3 Structural Characterization of the Furfuryl-SBO Derivative

For comparison purposes, let us first characterize the epoxidized soybean oil by  $^1\text{H}$  NMR technique. The corresponding  $^1\text{H}$  NMR spectrum is shown in Figure 38. The proton resonances are annotated from 1 to 8 and their detailed assignment is given in Table 9.

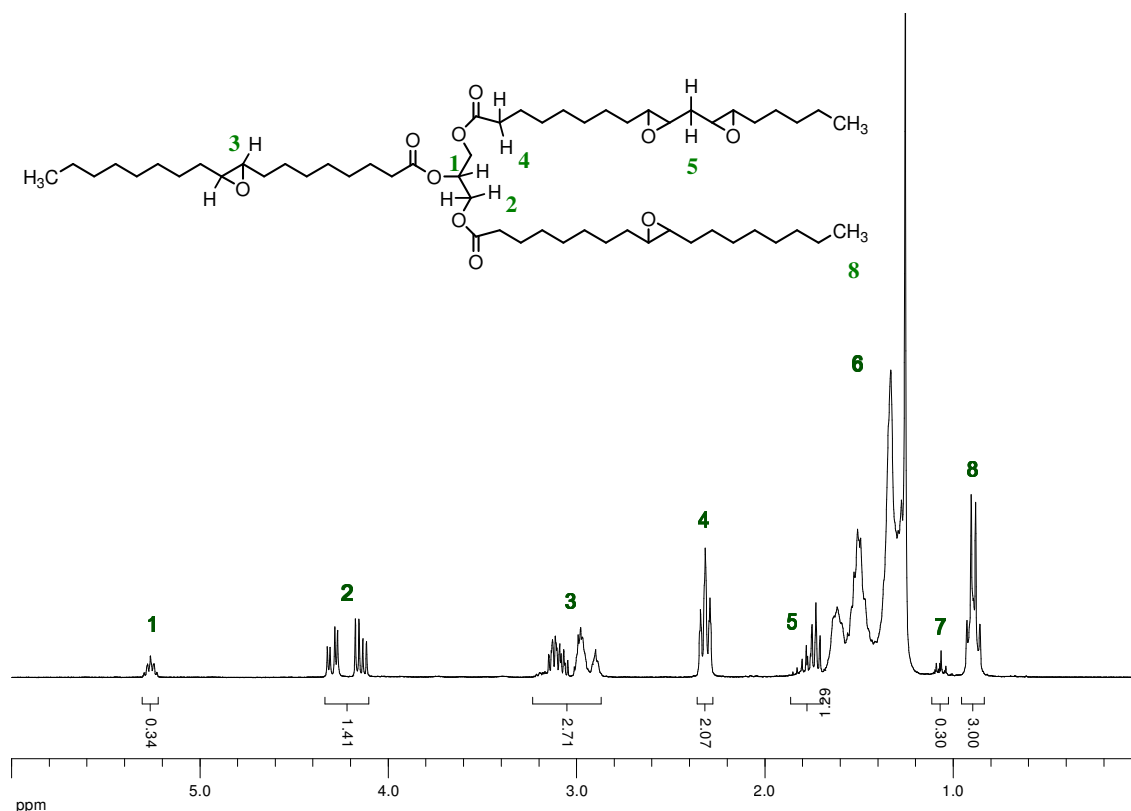


**Figure 38**  $^1\text{H}$  NMR spectrum of ESBO and corresponding proton signals assignment.<sup>eg. 55,96,98-99</sup>

**Table 9** ESBO proton signal assignments, <sup>eg. 55,96,98-99</sup>

Peak	$\delta$ (ppm)	Functional group
1	5.26	$>\text{CHOCOR}$ (methine proton)
2	4.32 - 4.11	$-\text{CH}_2\text{OCOR}$ ( methylene protons in glyceryl group)
3	3.15 - 2.89	$-\text{CH}(\text{O})\text{CH}-$ (Oxirane ring/epoxide protons)
4	2.32	$-\text{OCO}-\text{CH}_2-$ ( $\alpha$ – methylene protons)
5	1.80 - 1.71	$-\text{CH}(\text{O})\text{CH}-\text{CH}_2-\text{CH}(\text{O})\text{CH}-$ (methylene protons between adjacent epoxy rings/ di-epoxy methylene protons)
6	1.63-1.25*	$-\text{OCOCH}_2-\text{CH}_2-$ ( $\beta$ – methylene protons)
		$-\text{CH}_2-\text{CH}(\text{O})\text{CH}-$ (“allyl” methylene protons)
		All the others
7	1.06	$-\text{CH}_3$ ( terminal protons in linolenic fatty acid)
8	0.93 - 0.86	$-\text{CH}_3$ ( terminal protons in saturated, oleic and linoleic fatty acids)

\*Chemical shift decreases from top to bottom.

After the aminolysis reaction was complete, the end-product- the furfuryl-modified SBO- was characterized by  $^1\text{H}$  NMR as well. For a better understanding the two spectra have been superimposed (Figure 39). The  $^1\text{H}$  NMR spectrum of furfuryl-SBO, when compared with the corresponding epoxidized precursor, showed the emergence of new resonances typical of furan protons ( $\delta \sim 6.2$  and  $7.3$  ppm) along with the disappearance of the epoxide protons signal ( $\delta 2.7$ - $3.2$  ppm). Further evidence of the successfully incorporation of furfuryl moieties onto SBO was provided by the proton signals arising from the nucleophilic ring opening reaction, namely, the A and C signals ( $\delta 1.7$ - $2.2$  ppm), assigned to  $-\text{NH}$  and  $\text{H}-\text{C}-\text{NH}$ , respectively. Resonances corresponding to  $-\text{OH}$  and  $\text{H}-\text{C}-\text{OH}$  protons (B and D signals, respectively) may also be detected, though they’re much less perceptible.

The broad shape of the signals corresponding to furan ring protons results from the different positions of the furfuryl moieties along the aliphatic chains. Recall from the results with methyl oleate that two structural isomers are produced (A and B), depending on which carbon atom of the epoxy group the nitrogen attaches itself to. Moreover, in addition to oleic acid, SBO is also composed by linoleic and linolenic fatty acids (with two and three double bonds, respectively), which considerably widens up the number of possibilities, since the pendant furfuryl moiety can be found attached to a C-9, C-10, C-12,

C-13, C-15 or C-16 carbon atom. This sets slightly different chemical environments and translates into small chemical shift deviations, broadening the peaks.

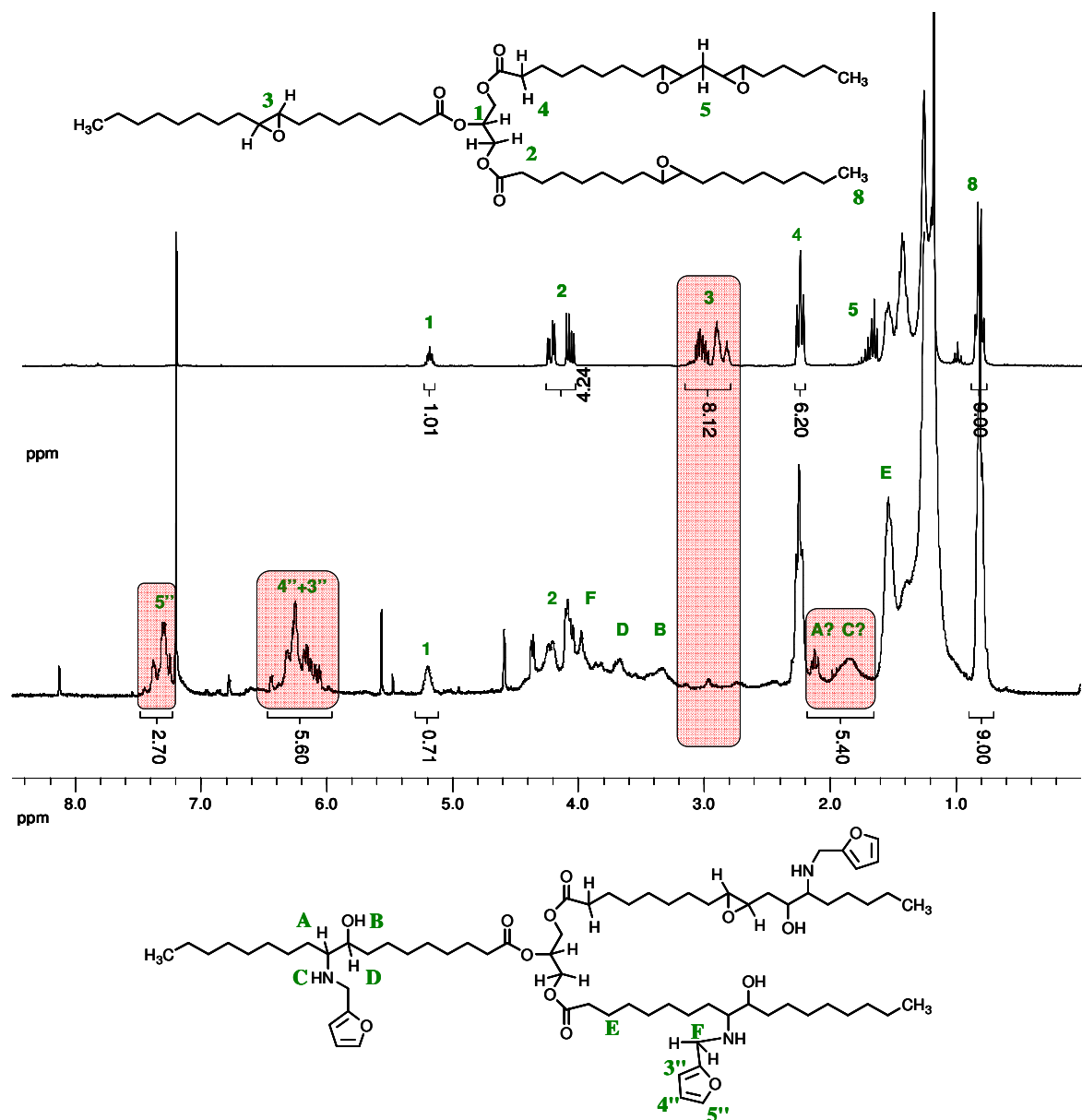


**Figure 39**  $^1\text{H}$  NMR spectrum of furfurylamine-functionalized SBO with ESBO's superimposed, for comparison purposes.

The functionalization of soybean oil triglyceride molecules with furfuryl moieties was also confirmed by FT-IR spectroscopy (Figure 40). The emergence of new bands characteristic of the furfuryl moieties, namely those assigned to furan C-H, C=C, C-N and N-H, together with that corresponding to the  $-\text{OH}$  groups, which arises from the oxirane ring opening



reaction, and the decrease of those attributable to the epoxide ring, constitutes further evidence of the successfully modification of ESBO with furfuryl pendant groups.

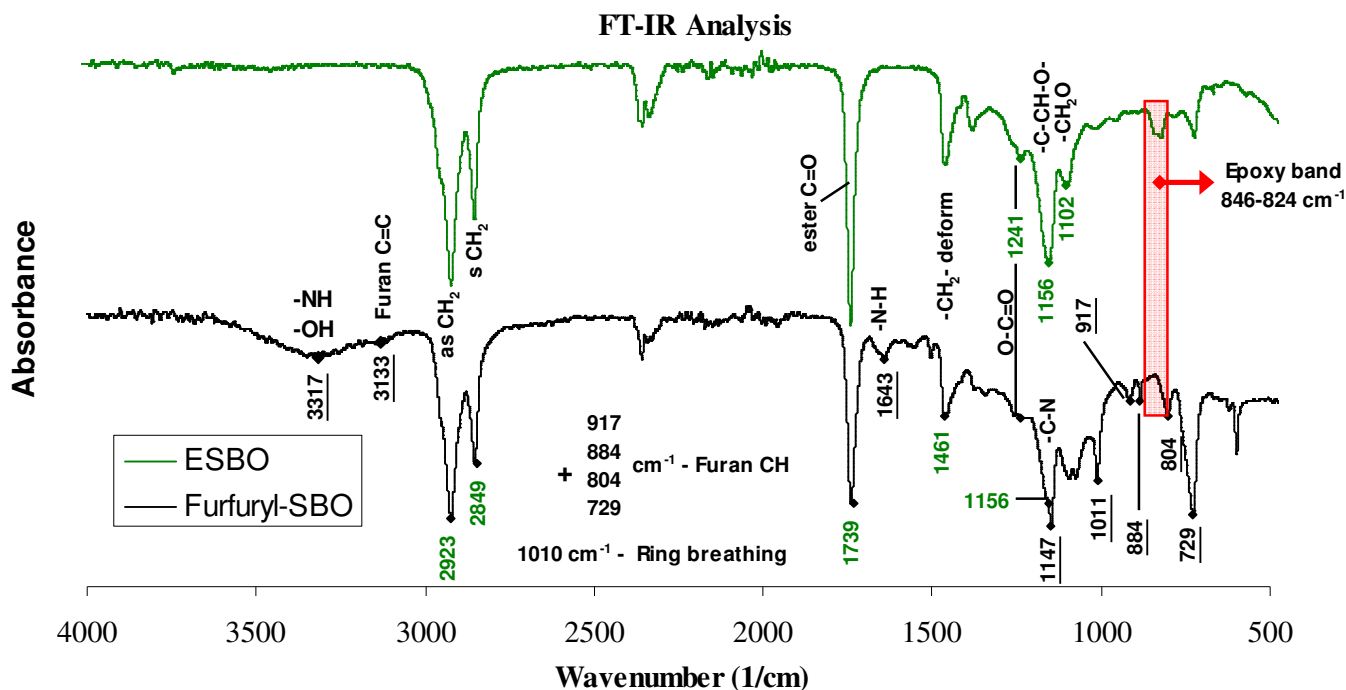


**Figure 40** FT-IR spectra of ESBO and furfuryl-ESBO with band assignment. Upper spectrum: ESBO. The underlined wavelengths correspond to bands assigned to the furfurylamine moiety.

Besides confirming the reaction, one other objective of FT-IR analysis was to measure the efficiency of the ring-opening reaction by estimating the fraction of unreacted epoxy groups remaining in the product oil.

From the spectrum of typical furfuryl-SBO products, one can see that the areas corresponding to epoxy bands were greatly reduced (Figure 40 and Figure 41). However, due to competing hydrolysis of the epoxy groups which, despite prevented, is likely to occur, as well as the emergence of furan C-H band at 804 cm<sup>-1</sup>, partially overlapping the 846-824 cm<sup>-1</sup> epoxy band, aminolysis reaction efficiency could not be estimated from the FTIR spectral integrations. This was accomplished instead by <sup>1</sup>H NMR, which indicated ~ 68% of the epoxy groups were converted to aminol, which is in reasonable agreement with the nitrogen elemental analysis results.

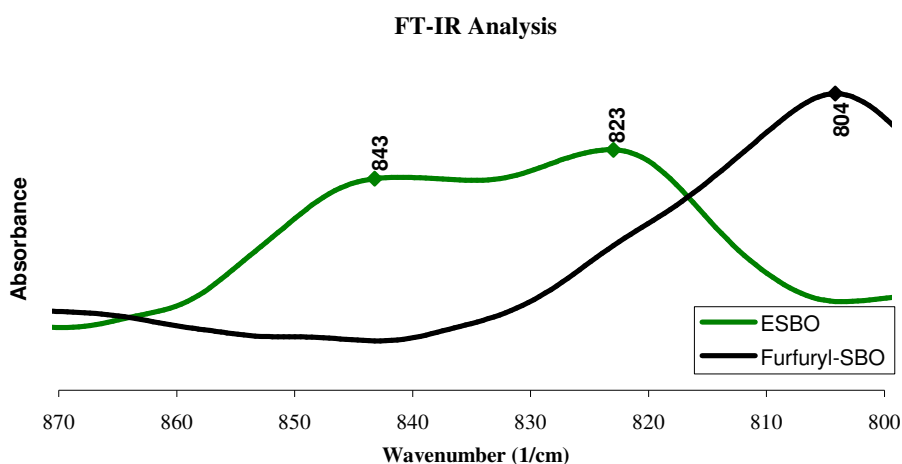


**Figure 41** Expansion of the FT-IR spectra epoxy region before and after oil functionalization. The epoxy absorbance band appears as two overlapping peaks centered at 843 and 824  $\text{cm}^{-1}$ . The band at 804  $\text{cm}^{-1}$  emerges for the furfuryl-SBO derivative and is assigned to furan C-H bond vibrations.

Furthermore, the furfuryl-SBO IR spectrum showed decreased ester carbonyl absorbance at 1740  $\text{cm}^{-1}$ , with respect to its precursor (ESBO), which we believed could indicate some hydrolytic side reaction of the amine on the ester function of the triglyceride. This hypothesis was soon discarded, as no evidence was found on the NMR data.

The most likely reason for the observed attenuation of the ester carbonyl absorbance of the aminohydroxy triglyceride is the change in molecular mass of these products compared with the oxirane precursor. Considering a tetra-oxirane triglyceride starting material (substantiated by  $^1\text{H}$  NMR spectroscopy), the product of a complete reaction, *i. e.*, SBO bearing four furfurylamine pendant groups, acquires an additional 388 mass units/mol. This increase is only in the carbon content of the derivatives with no corresponding increase in the ester carbonyl component.

### 3.4 Polymeric Materials Based on the Diels-Alder Reversible Reaction

Four trials were carried out at 65 °C, with TCE as solvent:

- One with *N*-methylmaleimide (MM), at 1:1 furan/maleimide molar ratio, used as model/control system.
- Two trials with 1,6-bismaleimido-hexane (BM):
  1. First using a 1:0.25 Furan:Maleimide groups molar ratio which later was modified to 1:0.50 by adding more BM to the solution;
  2. The other at 1:0.80 furan:maleimide groups molar ratio
- One with *N*-tris(ethyl)maleimide (TM), at 1:0.70 furan:maleimide groups molar ratio, then modified to 1:1.3 by adding more TM to the solution.

The chemical structure of the three maleimides is depicted on Figure 42.

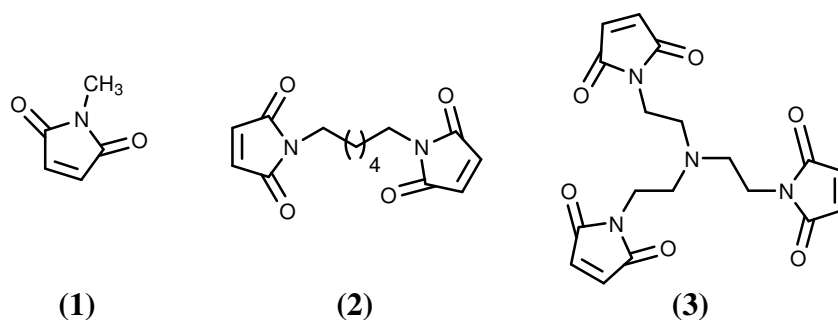


**Figure 42** Chemical structures of the maleimides used in this work: (1) *N*-methylmaleimide (MM), (2) 1,6-bismaleimido-hexane (BM), (3) *N*-tris(ethyl)maleimide (TM).

DA polycondensation progress (*i.e.*, adduct formation) was followed by  $^1\text{H}$  NMR through the progressive decrease in peak intensity of mono/bis/tris-maleimides CH=CH protons ( $\delta$  6.7 ppm). The case of *N*-methylmaleimide and 1,6-bismaleimido-hexane - 2.<sup>nd</sup> trial (Figure 43 and Figure 44, respectively) is discussed here as a typical situation.

DA polymerization could also be confirmed by the progressive decrease in the peak area of the monomer's  $\text{H}_{5''}$  proton and the corresponding increase on those arising from adduct formation [resonances assigned to protons b -  $\delta$  5.2 ppm, and c+d - 2.8 ppm].

Reactions proceeded slowly and the equilibrium was reached only after several days, when it was clearly shifted towards the adduct formation.

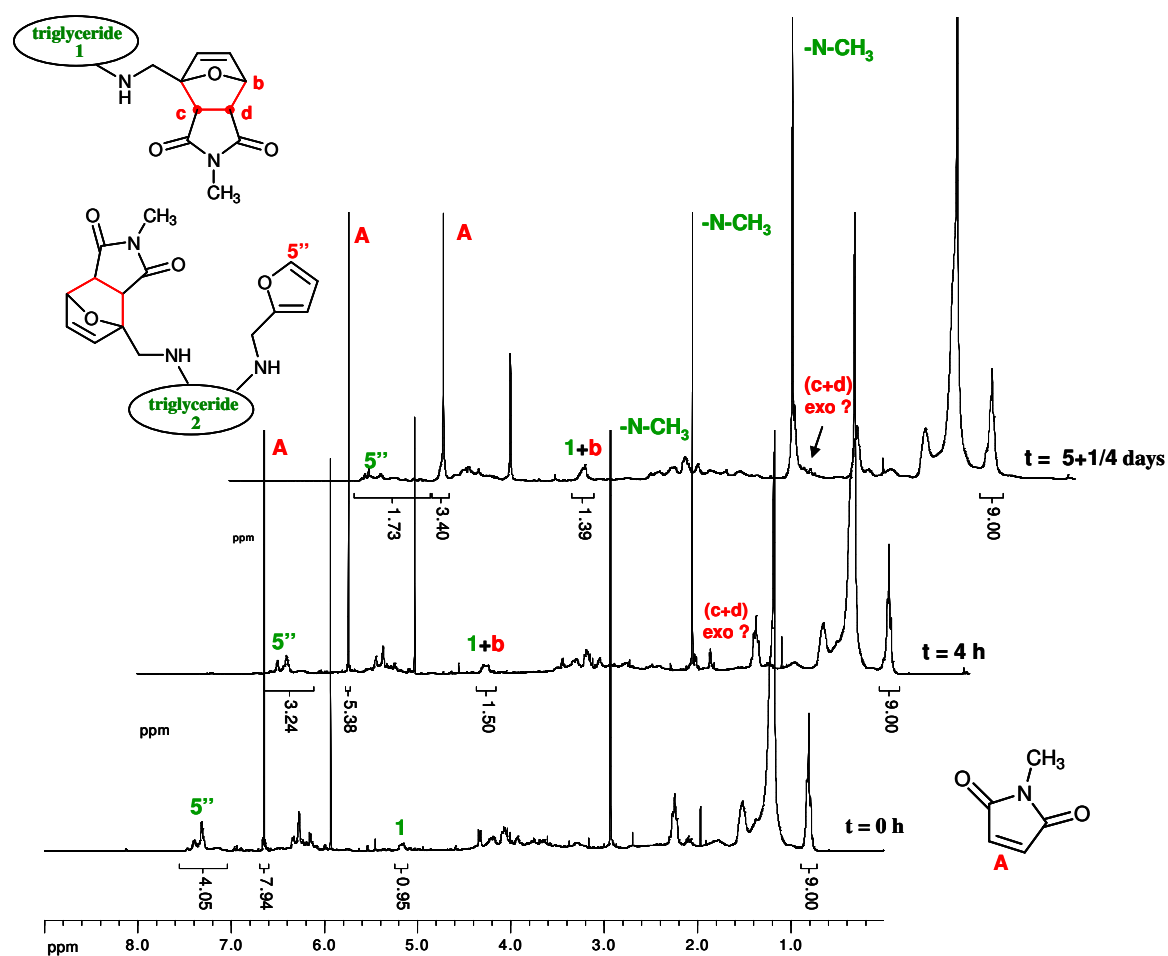


**Figure 43**  $^1\text{H}$  NMR spectra taken during the model DA reaction between Furfuryl-SBO derivative and *N*-methylmaleimide, at  $65^\circ\text{C}$  in TCEd2 (Furan:Maleimide molar ratio 1:1). Signal corresponding to c/d protons in endo adduct is not perceptible. Spectra were put into perspective. The progress of the reaction is better perceived by evaluating peak areas.

The model system proved that the system worked and that the DA polymerization progress could be followed by  $^1\text{H}$  NMR successfully.

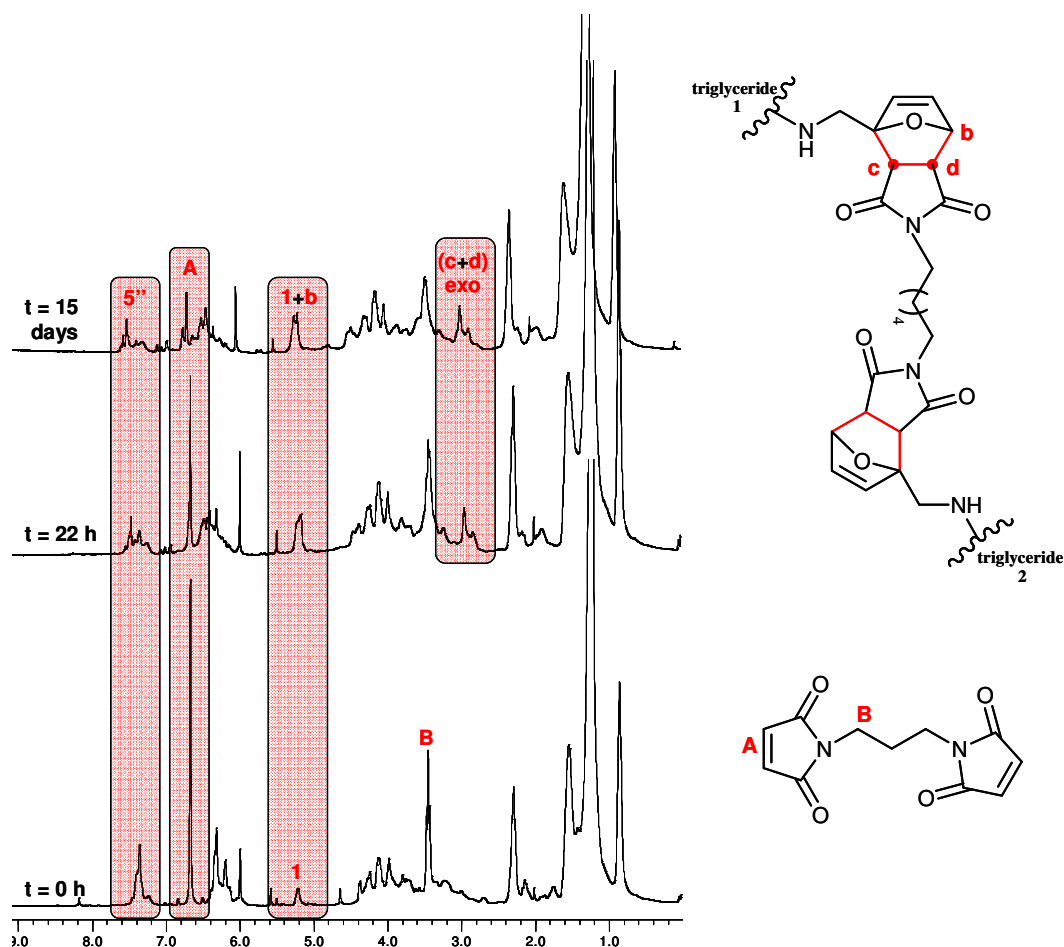


**Figure 44**  $^1\text{H}$  NMR spectra taken during the DA polymerization reaction at  $65^\circ\text{C}$  in  $\text{TCEd}_2$ , with 1,6-bismaleimidohehexane as dienophile (Furan:Maleimide molar ratio 1:0.8). After  $\sim 6$  days at  $65^\circ\text{C}$ , reaction was left to occur at room temperature (top spectrum). Signal corresponding to c/d protons in endo adduct is not perceptible.

Concurrently, and only for the essays carried out with the bi- and tri-functional cross-linking agents, the viscosity of the medium increased as the reaction proceeded.

In these circumstances, we were expecting the material to undergo one of the two phenomena, at a critical point:

- Gel formation, if at least one molecule of the cross-linking polymer had grown to the dimensions of the order of the sample, or
- Precipitate, if the polymer phase had separated from the medium due to poor thermodynamic compatibility.

However, none of the phenomena had been observed. We formulated two hypotheses to try to explain this unexpected behaviour. Most likely, the reason is a combination of them both.

### **Hypothesis 1:**

The stoichiometric condition related to the gel point and molecules bearing at least two furfuryl functions is not associated to furan:maleimide molar ratios higher than unity, *i.e.*, an excess of the crosslinking agent might be required to promote gelation or, the systems contained non-negligible proportions of monofunctional modified triglyceride (*i.e.*, only one furan moiety) that disrupt the formation of the polymeric network.

### **Hypothesis 2:**

Picturing the worst scenario, our calculations suggest that a value as high as 50 % of single reacted pendant BM molecules in the cross-linked polymer may be present which, obviously, poses serious limitations to the gelation or precipitation of the material (Box 1). If such is the case, adduct/crosslinking density might be just too low to observe any of the macroscopic changes referred above. Moreover, polymerization with BM proceeded slowly, taking 15 days to halve the initial amount of furan groups.

We believe this is attributable to kinetic constraints and not to any intrinsic property of the system. Even with a tri-functional maleimide, we still didn't observe any changes apart from the increased viscosity.

**Box 1** Logical reasoning behind the calculation of singly reacted pendant BM molecules content.

t	Unreacted Furan Units H <sub>5''</sub>	BM Maleimide Hs A	Unreacted Maleimide Units (A/2)	Maleimide Units Consumed
0 h	2.70	3.43	1.715	0
15 days	1.40	0.91	0.46	$\frac{3.43 - 0.91}{2} = 1.26$

For each singly reacted pendant BM molecule, one maleimide group remains to react (1:1 stoichiometry). Assuming all the unreacted maleimide groups are in this form, and not as unreacted BM molecules, 0.46 units of singly reacted pendant BM molecules are present. This represents roughly 50% of all BM molecules, whether partially or entirely reacted. The percentage was calculated as demonstrated below:

N.° of fully reacted BM molecules:  $\frac{1.26 - 0.46}{2} = 0.40$

Content in singly reacted pendant BM molecules:

$$\frac{0.46}{0.46 + 0.40} \times 100 = 53\%$$

We must highlight this was a preliminary study, conducted to evaluate the feasibility of the system rather than focused on the polymeric materials obtainable. At this stage a full understanding and control of the system are fundamental prior to the development of new vegetable-oil based polymers based on this approach.

The thermo-reversible character of the crosslinked polymers was then investigated. The retro-DA reaction was carried out at 110 °C for 24 h (Figure 45) and followed by <sup>1</sup>H NMR through the increase in peak intensity of bis/tris-maleimides CH=CH and monomer's H<sub>5''</sub> protons, as well as the decrease on those arising from adduct formation. As we had anticipated, the reaction is thermo-reversible. Interestingly, the RDA reaction was relatively fast, with the starting materials being almost fully regenerated within 4 hours. This behaviour was expected because, on the one hand, the RDA reaction was carried out at a

higher temperature (110 C), which increased the polymer chain mobility, and, on the other hand, it is a monomolecular reaction where a single molecular structure is “broken” down into the starting materials and, as such, it is not diffusion-dependent. Opposingly, DA reaction relies on the successful encounters between two complementary reactive moieties and therefore, materials diffusion in the solvent medium plays an important role.

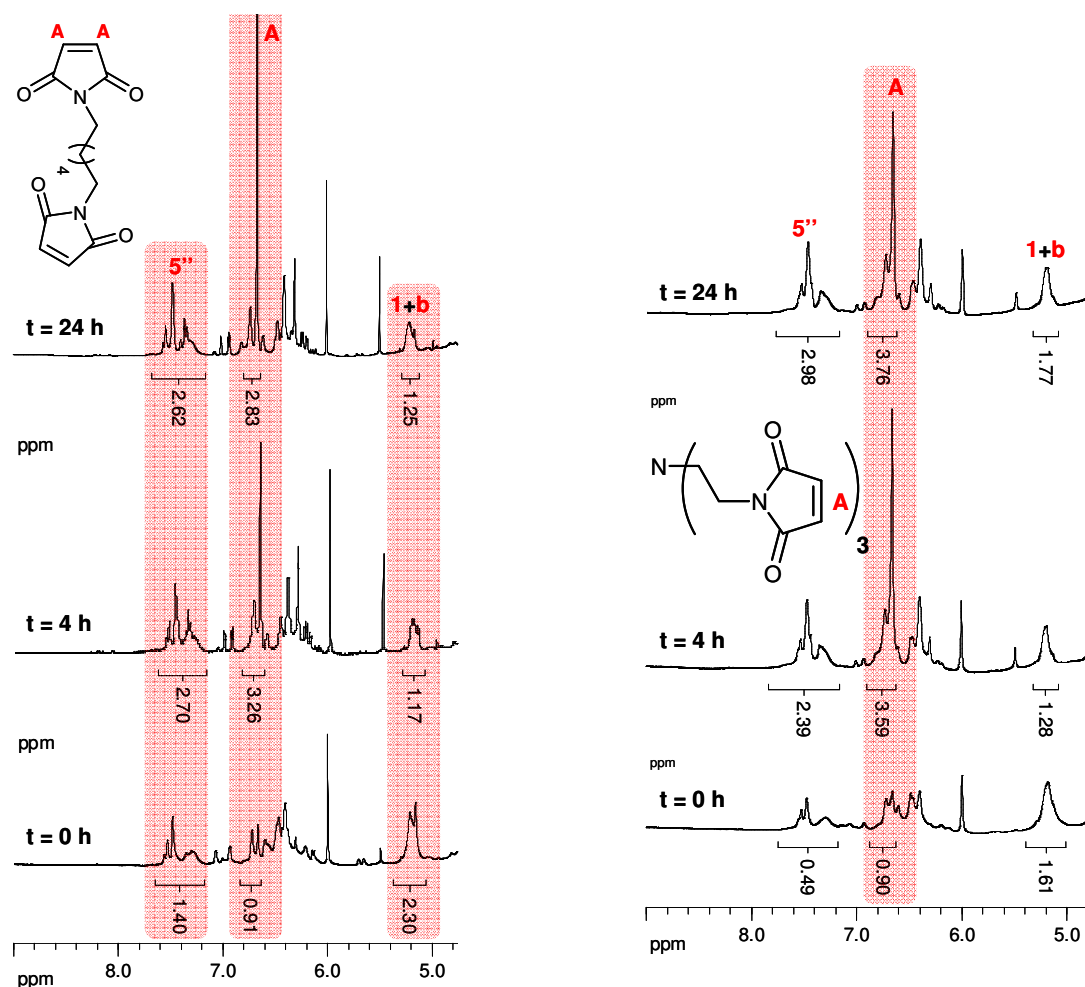


**Figure 45**  $^1\text{H}$  NMR spectra taken during the RDA reaction at 110°C in TCED<sub>2</sub>, with 1,6-bismaleimidohexane (Furan:Maleimide molar ratio 1:0.8, **left side**). and *N*-tris(ethyl)maleimide (Furan:Maleimide molar ratio 1:1.13, **right side**) as dienophiles. **5''**- C-5 furan ring proton; **1** – triglyceride's methinic proton.



## 4. Conclusions

To the best of our knowledge, this is the first time that the synthesis of a thermo-responsive vegetable oil-based cross-linked polymeric network is reported, using the DA/RDA reaction sequence approach. The simplicity and feasibility of the system, together with the renewable character, ready availability and low cost of the precursor materials involved, opens vegetable oils to a new context of applications within the synthesis of macromolecular structures with unique properties, such as self-mendability and network recyclability.

Soybean oil triglyceride molecules bearing furfuryl pendant groups, Furfuryl-SBO, were prepared from reacting epoxidized soybean oil (ESBO) with furfurylamine, *via* an aminolysis microwave-assisted reaction. Optimally, for a 1:24 ESBO/Furfurylamine molar ratio and a catalyst load of ~30% (by weight of the reaction mixture), it was found that about 2.7 epoxy groups of ESBO (~68%) were converted to aminohydroxyl groups. Reaction conditions were adjusted on the basis of the previously optimized Furfuryl-methyl oleate synthetic procedure. The polymeric materials were prepared by crosslinking Furfuryl-SBO with multifunctional maleimides - 1,6-bismaleimido-hexane and *N*-tris(ethyl)maleimide, at 65 C. The polymerizations proceeded slowly and the maleimide was never fully consumed, most likely due to kinetic reasons. Chain entanglement, steric hindrance and repulsion, along with the difficulty for complementary reactive moieties to find each other (as medium viscosity increased!) justify the low reaction rate.

Interestingly, the reverse operation (RDA reaction) was relatively fast, with the starting materials being almost fully regenerated within 4 hours. As with any preliminary work, applications to these materials can't be pointed out yet. Further studies must be carried out to get a full understanding and control of the system.



## 5. References

- 1 Clark, J. H., Deswarte, F. E. I. & Farmer, T. J. The integration of green chemistry into future biorefineries. *Biofuels Bioproducts & Biorefining-Biofpr* **3**, 72-90 (2009).
- 2 Collins, T. Toward Sustainable Chemistry. *Science* **291**, 48-49 (2001).
- 3 Gavrilescu, M. & Chisti, Y. Biotechnology - a sustainable alternative for chemical industry. *Biotechnology Advances* **23**, 471-499 (2005).
- 4 Hatti-Kaul, R., Tornvall, U., Gustafsson, L. & Borjesson, P. Industrial biotechnology for the production of bio-based chemicals - a cradle-to-grave perspective. *Trends in Biotechnology* **25**, 119-124 (2007).
- 5 OECD. The Application of Biotechnology to Industrial Sustainability. (OECD, Publications Paris, 2001).
- 6 Brundtland, G. *Our Common Future*. (Oxford University Press, Oxford (UK) 1987).
- 7 Bull, A. T. Biotechnology for industrial sustainability. *Korean Journal of Chemical Engineering* **18**, 137-148 (2001).
- 8 ONU. Report of the United Nations Conference on Environment and Development. (ONU, Rio de Janeiro, 1992).
- 9 European Technology Platform for Sustainable Chemistry SusChem. Putting Sustainable Chemistry into Action. (SusChem 2006).
- 10 Anastas, P. T. & Warner, J. C. *Green Chemistry - Theory and Practice*. (Oxford University Press, New York (USA) 1998).
- 11 Tufvesson, P. *Lipase Catalysed Synthesis of Speciality Chemicals* Ph.D. thesis, Lund University, (2008).
- 12 Sheldon, R. A., Arends, I. & Hanefeld, U. *Green Chemistry and Catalysis*. (Wiley-VCH, Weinheim( Germany) 2007).
- 13 Ewing, B. *et al.* Ecological Footprint Atlas 2009. (Global Footprint Network, Oakland, 2009).
- 14 Metzger, J. O. & Eissen, M. Concepts on the contribution of chemistry to a sustainable development. Renewable raw materials. *Comptes Rendus Chimie* **7**, 569-581 (2004).
- 15 Halls, C., Humphrey, S., Loh, J. & Goldfinger, S. Living Planet Report 2008. 45 (WWF (World Wildlife Fund), ZSL (Zoological Society of London), GFN (Global Footprint Network), Gland, Switzerland, 2008).
- 16 Gavrilescu, M. & Nicu, M. *Source reduction and waste minimization*. 2<sup>th</sup> edn, (Ecozone Press, Iasi 2005).
- 17 Gavrilescu, M. Cleaner Production as a Tool for Sustainable Development. *Environmental Engineering and Management* **3**, 45-70 (2004).

- 18 Boschen, S., Lenoir, D. & Scheringer, M. Sustainable chemistry: starting points and prospects. *Naturwissenschaften* **90**, 93-102 (2003).
- 19 Puig, G. L. i. *Biobased Thermosets from Vegetable Oils - Synthesis, Characterization, and Properties* Ph.D. thesis, Rovira i Virgili University, (2006).
- 20 IEA. World Energy Outlook 2006. (OECD/IEA, Paris (France), 2006).
- 21 IPCC. The Physical Science Basis. (IPCC, Cambridge (UK) and New York (USA), 2007).
- 22 Metzger, J. O. Fats and oils as renewable feedstock for chemistry. *European Journal of Lipid Science and Technology* **111**, 865-876 (2009).
- 23 Roper, H. Renewable raw materials in Europe - Industrial utilisation of starch and sugar. *Starch-Starke* **54**, 89-99 (2002).
- 24 Biermann, U. *et al.* New syntheses with oils and fats as renewable raw materials for the chemical industry. *Angewandte Chemie-International Edition* **39**, 2206-2224 (2000).
- 25 Corma, A., Iborra, S. & Velty, A. Chemical routes for the transformation of biomass into chemicals. *Chemical Reviews* **107**, 2411-2502 (2007).
- 26 Kamm, B., Gruber, P. R. & Kamm, M. *Biorefineries - Industrial Processes and Products*. (Wiley-VCH, Weinheim (Germany) 2006).
- 27 Olah, G. A., Goeppert, A. & Prakash, G. K. S. *Beyond Oil and Gas*. (Wiley-VCH, Weinheim (Germany) 2006).
- 28 <http://www.fnr-server.de/cms35/index.php?id=139>, FNR (Agency of Renewable Resources), Gulzow (Germany). (Viewed May 2010)
- 29 Bozell, J. J. & Petersen, G. R. Technology development for the production of biobased products from biorefinery carbohydrates-the US Department of Energy's "Top 10" revisited. *Green Chemistry* **12**, 539-554 (2010).
- 30 Huber, G. W. & Corma, A. Synergies between bio- and oil refineries for the production of fuels from biomass. *Angewandte Chemie-International Edition* **46**, 7184-7201 (2007).
- 31 Huber, G. W., Iborra, S. & Corma, A. Synthesis of transportation fuels from biomass: Chemistry, catalysts, and engineering. *Chemical Reviews* **106**, 4044-4098 (2006).
- 32 Maki-Arvela, P., Holmbom, B., Salmi, T. & Murzin, D. Y. Recent progress in synthesis of fine and specialty chemicals from wood and other biomass by heterogeneous catalytic processes. *Catalysis Reviews-Science and Engineering* **49**, 197-340 (2007).
- 33 Gallezot, P. Catalytic routes from renewables to fine chemicals. *Catalysis Today* **121**, 76-91 (2007).
- 34 Belgacem, M. & Gandini, A. *Monomers, Polymers and Composites from Renewable Resources*. 1.st edn, (Elsevier, UK 2008).
- 35 Mohanty, A. K., Misra, M. & Drzal, L. T. *Natural Fibers, Biopolymers and Biocomposites* (CRC Press, Boca Raton (USA) 2005).

- 36 Erhan, S. Z. *Industrial Uses of Vegetable Oils* (AOCS Press, Champaign, IL, 2005).
- 37 Gunstone, F., Harwood, J. & Dijkstra, A. *The Lipid Handbook*. third edn, (CRC Press, Boca Raton (USA) 2007).
- 38 Gandini, A. Polymers from Renewable Resources: A Challenge for the Future of Macromolecular Materials. *Macromolecules* **41**, 9491-9504 (2008).
- 39 Metzger, J. O. & Bornscheuer, U. Lipids as renewable resources: current state of chemical and biotechnological conversion and diversification. *Applied Microbiology and Biotechnology* **71**, 13-22 (2006).
- 40 USDA. Oilseeds: World Markets and trade Monthly Circular. (United States Department of Agriculture).
- 41 Gunstone, F. D. Market report. *Lipid Technology* **20** (2008).
- 42 Vilela, C., Rua, R., Silvestre, A. J. D. & Gandini, A. Polymers and copolymers from fatty acid-based monomers. *Industrial Crops and Products* **32**, 97-104 (2010).
- 43 Lu, Y. S. & Larock, R. C. Novel Polymeric Materials from Vegetable Oils and Vinyl Monomers: Preparation, Properties, and Applications. *Chemsuschem* **2**, 136-147 (2009).
- 44 Hou, C. T. Biotechnology for fats and oils: new oxygenated fatty acids. *New Biotechnology* **26**, 2-10 (2009).
- 45 Orellana-Coca, C., Tornvall, U., Adlercreutz, D., Mattiasson, B. & Hatti-Kaul, R. Chemo-enzymatic epoxidation of oleic acid and methyl oleate in solvent-free medium. *Biocatalysis and Biotransformation* **23**, 431-437 (2005).
- 46 Piazza, G. J. & Foglia, T. A. One-pot synthesis of fatty acid epoxides from triacylglycerols using enzymes present in oat seeds. *Journal of the American Oil Chemists Society* **83**, 1021-1025 (2006).
- 47 Schneider, R. D. S., Lara, L. R. S., Bitencourt, T. B., Nascimento, M. D. & Nunes, M. R. D. Chemo-Enzymatic Epoxidation of Sunflower Oil Methyl Esters. *Journal of the Brazilian Chemical Society* **20**, 1473-1477 (2009).
- 48 Yang, Y. X. *et al.* Two-Step Biocatalytic Route to Biobased Functional Polyesters from omega-Carboxy Fatty Acids and Diols. *Biomacromolecules* **11**, 259-268 (2010).
- 49 Guner, F. S., Yagci, Y. & Erciyes, A. T. Polymers from triglyceride oils. *Progress in Polymer Science* **31**, 633-670 (2006).
- 50 Xia, Y. & Larock, R. C. Vegetable oil-based polymeric materials: synthesis, properties, and applications. *Journal of Green Chemistry* **12**, 1893-1909 (2010).
- 51 Sonntag, N. O. V. Glycerolysis of Fats and Methyl esters - Status, Review and Critique *Journal of American Oil Chemists' Society* **59**, 795-902 (1982).
- 52 Meier, M. A. R., Metzger, J. O. & Schubert, U. S. Plant oil renewable resources as green alternatives in polymer science. *Chemical Society Reviews* **36**, 1788-1802 (2007).
- 53 Cai, C. S. *et al.* Studies on the kinetics of in situ epoxidation of vegetable oils. *European Journal of Lipid Science and Technology* **110**, 341-346 (2008).

- 54 Kockritz, A. & Martin, A. Oxidation of unsaturated fatty acid derivatives and vegetable oils. *European Journal of Lipid Science and Technology* **110**, 812-824 (2008).
- 55 Harry-O'kuru, R. E., Gordon, S. H. & Biswas, A. A facile synthesis of aminohydroxy triglycerides from new crop oils. *Journal of the American Oil Chemists Society* **82**, 207-212 (2005).
- 56 Petrovic, Z. S., Zlatanovic, A., Lava, C. C. & Sinadinovic-Fiser, S. Epoxidation of soybean oil in toluene with peroxyacetic and peroxyformic acids - kinetics and side reactions. *European Journal of Lipid Science and Technology* **104**, 293-299 (2002).
- 57 Bergman, S. D. & Wudl, F. Mendable polymers. *Journal of Materials Chemistry* **18**, 41-62 (2008).
- 58 Ghosh, S. K. Self-Healing Materials – Fundamentals, Design Strategies, and Applications (Wiley-VCH, Morlenbach (Germany) 2009).
- 59 Wool, R. P. Self-healing materials: a review. *Soft Matter* **4**, 400-418 (2008).
- 60 Wu, D. Y., Meure, S. & Solomon, D. Self-healing polymeric materials: A review of recent developments. *Progress in Polymer Science* **33**, 479-522 (2008).
- 61 Toohey, K. S., Sottos, N. R., Lewis, J. A., Moore, J. S. & White, S. R. Self-healing materials with microvascular networks. *Nature Materials* **6**, 581-585 (2007).
- 62 White, S. R. *et al.* Autonomic healing of polymer composites. *Nature* **409**, 794-797 (2001).
- 63 Chen, X. *et al.* A Thermally Re-mendable Cross-Linked Polymeric Material. *Science* **295**, 1698-1702 (2002).
- 64 Chen, X. X., Wudl, F., Mal, A. K., Shen, H. B. & Nutt, S. R. New thermally remendable highly cross-linked polymeric materials. *Macromolecules* **36**, 1802-1807 (2003).
- 65 Cordier, P., Tournilhac, F., Soulié-Ziakovic, C. & Leibler, L. Self-healing and thermoreversible rubber from supramolecular assembly. *Nature* **451**, 977-980 (2008).
- 66 Kessler, M. R. Self-healing: a new paradigm in materials design. *Proceedings of the Institution of Mechanical Engineers Part G-Journal of Aerospace Engineering* **221**, 479-495 (2007).
- 67 Craven, J. M. Cross-linked Thermally Reversible Polymers Produced from Condensation Polymers with Pendant Furan Groups Cross-linked with Maleimides. US Patent 3,435,003, Mar 25, 1969.
- 68 Stevens, M. P. & Jenkins, A. D. Crosslinking of Polystyrene via Pendant Maleimide Groups. *Journal of Polymer Science Part a – Polymer Chemistry* **17**, 3675-3685 (1979)
- 69 Chujo, Y., Sada, K. & Saegusa, T. A novel nonionic hydrogel from 2-methyl-2-oxazoline.4. Reversible gelation of polyoxazoline by means of Diels-Alder reaction *Macromolecules* **23**, 2636-2641 (1990).

- 70 Canary, S. A. & Stevens, M. P. Thermally Reversible Cross-Linking of Polystyrene via the Furan-Maleimide Diels-Alder reaction. *Journal of Polymer Science Part a-Polymer Chemistry* **30**, 1755-1760 (1992).
- 71 Laita, H., Boufi, S. & Gandini, A. The application of the Diels-Alder reaction to polymers bearing furan moieties .1. Reactions with maleimides. *European Polymer Journal* **33**, 1203-1211 (1997).
- 72 Gousse, C., Gandini, A. & Hodge, P. Application of the Diels-Alder reaction to polymers bearing furan moieties. 2. Diels-Alder and retro-Diels-Alder reactions involving furan rings in some styrene copolymers. *Macromolecules* **31**, 314-321 (1998).
- 73 Gheneim, R., Perez-Berumen, C. & Gandini, A. Diels-Alder reactions with novel polymeric dienes and dienophiles: Synthesis of reversibly cross-linked elastomers. *Macromolecules* **35**, 7246-7253 (2002).
- 74 Goiti, E., Heatley, F., Huglin, M. B. & Rego, J. M. Kinetic aspects of the Diels-Alder reaction between poly(styrene-co-furfuryl methacrylate) and bismaleimide. *European Polymer Journal* **40**, 1451-1460 (2004).
- 75 Goiti, E., Huglin, M. B. & Rego, J. M. Thermal breakdown by the retro Diels-Alder reaction of crosslinking in poly styrene-co-(furfuryl methacrylate). *Macromolecular Rapid Communications* **24**, 692-696 (2003).
- 76 Goiti, E., Huglin, M. B. & Rego, J. M. Some properties of networks produced by the Diels-Alder reaction between poly(styrene-co-furfuryl methacrylate) and bismaleimide. *European Polymer Journal* **40**, 219-226 (2004).
- 77 Diakoumakos, C. D. & Mikroyannidis, J. A. Polyimides derived from Diels-Alder Polymerization of Furfuryl-Substituted Maleamic Acids or from the Reaction of Bismaleamic with Bisfurfurylpyromellitic Acids. *Journal of Polymer Science Part a-Polymer Chemistry* **30**, 2559-2567 (1992).
- 78 Diakoumakos, C. D. & Mikroyannidis, J. A. Heat-Resistant Resins Derived from Cyano-Substituted Diels-Alder Polymers *European Polymer Journal* **30**, 465-472 (1994).
- 79 He, X., Sastri, V. R. & Tesoro, G. C. *Makromol. Chem. Rapid Commun.* **9** (1989).
- 80 Kuramoto, N., Hayashi, K. & Nagai, K. Thermoreversible Reaction of Diels-Alder Polymer Composed of Difurfuryladipate with Bismaleimidodiphenylmethane. *Journal of Polymer Science Part a-Polymer Chemistry* **32**, 2501-2504 (1994).
- 81 O'Dell, R. Ph.D. thesis, Lancaster University, (1990).
- 82 Tesoro, G. C. & Sastri, V. R. *Ind. Eng. Chem. Prod. Res. Dev.* **25** (1986).
- 83 Gousse, C. & Gandini, A. Diels-Alder polymerization of difurans with bismaleimides. *Polymer International* **48**, 723-731 (1999).
- 84 Gandini, A. The Application of the Diels-Alder Reaction to Polymer Syntheses Based on Furan/Maleimide Reversible Couplings. *Polímeros: Ciência e Tecnologia* **15**, 95-101 (2005).

- 85 Gotsmann, B., Duerig, U., Frommer, J. & Hawker, C. J. Exploiting chemical switching in a Diels-Alder polymer for nanoscale probe lithography and data storage. *Advanced Functional Materials* **16**, 1499-1505 (2006).
- 86 Liu, Y. L. & Chen, Y. W. Thermally reversible cross-linked polyamides with high toughness and self-repairing ability from maleimide- and furan-functionalized aromatic polyamides. *Macromolecular Chemistry and Physics* **208**, 224-232 (2007).
- 87 Liu, Y. L. & Hsieh, C. Y. Crosslinked epoxy materials exhibiting thermal remendablility and removability from multifunctional maleimide and furan compounds. *Journal of Polymer Science Part A-Polymer Chemistry* **44**, 905-913 (2006).
- 88 Liu, Y. L., Hsieh, C. Y. & Chen, Y. W. Thermally reversible cross-linked polyamides and thermo-responsive gels by means of Diels-Alder reaction. *Polymer* **47**, 2581-2586 (2006).
- 89 Szalai, M. L., McGrath, D. V., Wheeler, D. R., Zifer, T. & McElhanon, J. R. Dendrimers based on thermally reversible furan-maleimide Diels-Alder adducts. *Macromolecules* **40**, 818-823 (2007).
- 90 Yoshie, N., Watanabe, M., Araki, H. & Ishida, K. Thermo-responsive mending of polymers crosslinked by thermally reversible covalent bond: Polymers from bisfuranic terminated poly(ethylene adipate) and tris-maleimide. *Polymer Degradation and Stability* **95**, 826-829 (2010).
- 91 Zhang, Y., Broekhuis, A. A. & Picchioni, F. Thermally Self-Healing Polymeric Materials: The Next Step to Recycling Thermoset Polymers? *Macromolecules* **42**, 1906-1912 (2009).
- 92 Gandini, A. Furans as offspring of sugars and polysaccharides and progenitors of a family of remarkable polymers: a review of recent progress. *Polymer Chemistry* **1**, 245-251 (2010).
- 93 Gandini, A., Coelho, D., Gomes, M., Reis, B. & Silvestre, A. Materials from renewable resources based on furan monomers and furan chemistry: work in progress. *Journal of Materials Chemistry* **19**, 8656-8664 (2009).
- 94 Shivani, Pujala, B. & Chakraborti, A. K. Zinc(II) perchlorate hexahydrate catalyzed opening of epoxide ring by amines: applications to synthesis of (RS)/(R)-propranolols and (RS)/(R)/(S)-naftopidils. *Journal of Organic Chemistry* **72**, 3713-3722 (2007).
- 95 Pachon, L. D., Gamez, P., van Brussel, J. J. M. & Reedijk, J. Zinc-catalyzed aminolysis of epoxides. *Tetrahedron Letters* **44**, 6025-6027 (2003).
- 96 Biswas, A., Adhvaryu, A., Gordon, S. H., Erhan, S. Z. & Willett, J. L. Synthesis of diethylamine-functionalized soybean oil. *Journal of Agricultural and Food Chemistry* **53**, 9485-9490 (2005).
- 97 Tellez, G. L., Vigueras-Santiago, E., Hernandez-Lopez, S. & Bilyeu, B. Synthesis and Thermal Cross-Linking Study of Partially-Aminated Epoxidized Linseed Oil. *Journal of Designed Monomers and Polymers* **11**, 435-445 (2008).
- 98 Knothe, G. & Kenar, J. A. Determination of the fatty acid profile by H-1-NMR spectroscopy. *European Journal of Lipid Science and Technology* **106**, 88-96 (2004).



- 99 Miyake, Y., Yokomizo, K. & Matsuzaki, N. Determination of unsaturated fatty acid composition by high-resolution nuclear magnetic resonance spectroscopy. *Journal of the American Oil Chemists Society* **75**, 1091-1094 (1998).
- 100 Lee, K. W., Hailan, C., Yinhua, J., Kim, Y. W. & Chung, K. W. Modification of soybean oil for intermediates by epoxidation, alcoholysis and amidation. *Korean Journal of Chemical Engineering* **25**, 474-482 (2008).
- 101 Okieimen, F. E., Pavithran, C. & Bakare, I. O. Epoxidation and hydroxlation of rubber seed oil: one-pot multi-step reactions. *European Journal of Lipid Science and Technology* **107**, 330-336 (2005).
- 102 Biswas, A. *et al.* Synthesis of an Amine-Oleate Derivative Using an Ionic Liquid Catalyst. *Journal of Agricultural and Food Chemistry* **57**, 8136-8141 (2009).